THE MATERIALS JOINING EXPERTS
Edison Welding Institute, Inc. 1250 Arthur E. Adams Drive | Columbus, Ohio 43221-3585 | (614) 688-5000 | FAX (614) 688-5001 | www.ewi.org

July 06, 2007

PHMSA Research and Development
Attention: Frank Licari
U.S. Department of Transportation
400 Seventh St., S.W.
Washington, D.C. 20590

EWI Project No. 47960GTH, "Optimizing Weld Integrity for X80 and X100 Linepipe" – Final Report

Dear Mr. Licari:

Enclosed is EWI's report for the above referenced project. Please feel free to contact me at (614) 688-5057, if you have any questions or comments regarding this project.

Sincerely,

Susan R. Fiore

Susan R. Fiore
Senior Engineer
Engineering, NDE and Materials

Enclosure

REPORT

July 06, 2007
Final Report
EWI Project No. 47960GTH

Optimizing Weld Integrity for X80 and X100 Linepipe

Submitted to:

U.S. Department of Transportation
Washington, D.C.

EWI®

MATERIALS JOINING TECHNOLOGY

Final Report

Project No. 47960GTH

on

Optimizing Weld Integrity for X80 and X100 Linepipe

to

U.S. Department of Transportation
Washington, DC

July 06, 2007

Susan R. Fiore
EWI
1250 Arthur E. Adams Drive
Columbus, OH 43221

Page

Table of Contents

Page

Tables

Figures

Page

Page

1.0 Introduction

This project was funded by the US Department of Transportation (Office of Pipeline Safety) under Contract Number DTRS56-04-T-0011. It was supported by several organizations through cost sharing. The project team consisted of Miller/Hobart, BP, CANMET, TransCanada Pipelines, EWI Microalloying and EWI.

The trend to higher strength pipelines has resulted in the development and use of high-strength, microalloyed, thermo-mechanically processed steels. Welding of these high-strength steels poses a range of challenges due to their sensitivity to variations in heat input, preheat, and interpass temperatures. These challenges require close control of the welding process. A substantial amount of development has been completed to characterize the properties of X80 and X100 welds made under specific conditions. These programs have confirmed that weld metal can readily match the X80 and X100 pipe using commercially available welding consumables in combination with carefully developed welding procedures. However, the move towards higher strength steels also comes at a time when design practices are evolving, and there is greater focus on overmatching criteria for pipeline girth welds to ensure that weld metals overmatch the actual pipe material properties rather than specified minimum yield strength (SMYS) of the material. This has led to a minimum weld metal yield strength requirement of almost 100 ksi for X80 pipe, and 120 ksi for X100 pipe, while still maintaining high toughness and crack tip opening displacement (CTOD) properties. As a result X80 pipe is welded with X100 grade consumables and X100 pipe is welded with X120 grade consumables.

Extensive tests have been performed on commercially available X100 and X120 grade welding consumables, but they tend to provide either low tensile properties or very high tensile properties in combination with low toughness. All the consumables are very susceptible to minor variations in cooling rate. Weld metals tested under very minor changes in cooling rate have shown a +/- 15% variation in yield strength, which can lead to either girth weld undermatching or very high-strength, low-ductility girth welds. Therefore, there is a need to optimize weld metal chemistry for weld tensile properties higher than 100 ksi to produce consumables that are more tolerant of field welding process variations.

The proposed project will review the current status of X80 and X100 pipeline welding technology and examine the trend towards overmatching weld metals. A best practice guide will be developed for X80 welding based on existing commercially available welding technology as well as the development of optimized welding consumables and welding procedures for X100 pipelines.

Although the current experimental approach of making full-scale welds with a range of filler metals and process conditions is time consuming and expensive, it has produced a valuable body of data that can be used for further analysis. The project used the available data as initial input and applied a modeling approach to determine the influence of weld metal chemistry on physical properties and assess the optimum weld metal chemistry for the required balance of metallurgical properties when strength levels over 100 ksi are necessary. This project provided a better understanding of the factors that control strength and toughness in high-strength girth welds, and enabled high-integrity girth welds to be more reliably and economically achieved.

2.0 Objectives

The major objectives of this program were to:

- Provide a better understanding of the factors that control strength and toughness in high-strength girth welds.
- Develop optimized welding consumables and welding procedures for high-strength pipelines.
- Develop best practice guidelines for welding of high-strength pipelines.
- Disseminate best practice information to the pipeline industry.
- Enable high-integrity girth welds to be more reliably and economically achieved in high-strength pipelines.

The goal of the strain-based design for X80 and X100 pipe is shown graphically in Figure 1 and Figure 2. The goal for CVN toughness was a minimum or 50J at -10°C.

3.0 Technical Approach

The project aimed to develop optimized weld metal chemistries for higher strength pipelines in order to ensure an optimum balance of strength, ductility and toughness with tolerance to process variations and resistance to hydrogen cracking. The project was performed in the following tasks:

(1) Review of X80 and X100 pipeline welding and a review of the case for overmatching

(2) Development of Best Practice Welding Guidelines for X80 Pipelines

(3) Development of Optimized Welding Consumables and Procedures for X100 Pipelines

3.1 Review of X80 and X100 Pipeline Welding

A number of articles covering welding of various-strength pipelines were reviewed. The completed review was submitted previously and information about it is provided in Appendix A.

3.2 Best Practice Welding Guidelines for X80 Pipelines

The Best Practices Welding Guide was developed primarily from the experiences and lessons learned from the production of the Cheyenne Plains pipeline as well as several Canadian pipeline projects. The completed report was submitted previously and information about it appears in Appendix B.

3.3 Development of Optimized Welding Consumables and Procedures for X100 Pipelines

As discussed previously, there has been a tremendous amount of research centered on developing welding consumables that will meet the requirements for overmatching X100 grade pipelines. Much of the work has been performed on a trial and error basis which has a dramatic effect on the cost of development. The approach taken during this program was to use previous research as a baseline to develop computer models that could be used to predict the cooling rate of the welding process, which in turn could aid in the prediction of the mechanical properties of the completed weld.

3.3.1 Two-Dimensional Finite Element Analysis

To determine the cooling rate for a given welding procedure and its dependence on welding parameters, finite element analysis was utilized. Under a previous program funded by Pipeline Research Council, Inc., EWI established a two-dimensional model to analyze the thermal, metallurgical, and mechanical processes in welding.[1] The model was based on the fact that heat transfer in a workpiece occurs mainly in the cross section perpendicular to welding direction. By neglecting the heat flux out of the cross sectional plane, a two-dimensional model was conceived to analyze the welding process. Compared to its three-dimensional full-scale counterpart, the two-dimensional analysis offers much higher computational efficiency in characterizing the fundamental physics of welding.

The two-dimensional model was implemented using ABAQUS commercial finite element software.[2] The cooling time predicted by the two-dimensional model was compared against that measured in welding. Good agreement was observed between the two.[1] The most recent version of the two-dimensional welding analysis is named E-Weld Predictor,[3] and it further packages the ABAQUS calculation with a Microsoft Excel-based Graphics User Interface (GUI) that enables users to launch welding analysis through the GUI. Figure 3 shows the input page of the E-Weld Predictor. Details of E-Weld Predictor can be found in Reference [3].

In the two-dimensional welding analysis, the temperature dependence of the material's thermal properties is taken into account. Table 1 lists the thermal conductivity and specific heat of X100 at different temperatures. The other material properties required by the thermal analysis are also listed with Table 1.

3.3.2 Neural Network Model

Weld metal mechanical properties depend on a large number of variables ranging from the weight percent of alloying elements in the welding consumable to details of the welding process such as weld groove geometry, heat input, pre-heating, and bead geometry and dimensions. Such a large number of variables makes it prohibitive to model the impact of each of them. Therefore, the method of Artificial Neural Network (ANN) was utilized to optimize the welding of X100.

An ANN, more commonly referred to as an Neural Network (NN), imitates the information processing paradigm in the human brain. Like the human brain, an NN is a collection of massively interconnected cells that are arranged in a way that each cell derives its input from one or more other cells. Under this structure, input to an NN is distributed throughout the network, so that an output is in the form of one or more activated cells. When implemented in a computer, an NN can acquire, store, update, and utilize experiential knowledge. It is a powerful data modeling tool that is capable of capturing and representing complex input-output relationships.

A NN is configured for a specific application. In the current project, the weight percentages of alloying elements and the cooling time from 800°C to 400°C are the inputs to the NN models. The yield strength (YS) and ultimate tensile strength (UTS) are the outputs of the NN models. As a modeling strategy, the cooling time is used as input to the NN models instead of various welding parameters because it affects the microstructure, and thus, the material properties of the weld metal. Different welding parameters can lead to the same cooling time, therefore using cooling time as a variable helps reduce the number of inputs needed for the NN models. The reduced number of inputs also helps in building more accurate NN models for the same number of data points. Ultimately, the desired cooling time from 800°C to 400°C will have to be delivered by a combination of welding parameters including travel speed, heat input, weld preparation, bead geometry, etc. – these relationships were established by EWI using the aforementioned two-dimensional finite element model.

3.3.3 Training and Testing of Neural Network

NN models have been created to predict YS and UTS of the weld metal in X100 pipe based upon data provided by Cranfield University,[4, 5] CANMET Materials Technology Laboratory (CANMET-MTL),[6] BP and a literature survey conducted by EWI.[7] The NN models for

predicting CTOD and Charpy V-notch (CVN) toughness values could not be created because the number of data points available was not sufficient.

The data from the above sources cover the welding of X100 using more than 40 consumables having different weight percentages of 16 alloying elements. Since some data sources only report cooling time for selected welding passes, the two-dimensional finite element model was used to replicate the cooling times which were not available to form a complete data set for training the NN models.

The NN predictions were tested against the data used to train it, as well as other data. The maximum error in the predictions for both YS and UTS was found to be about 50 MPa, which is equivalent to a maximum error of about ±6%. This level of error is within the typical scatter range for weld metal tensile testing, indicating that the NN model is a valid prediction tool for this system.

3.3.4 Determination of Optimal Welding of X100

As described earlier, a variety of trial weld-metal compositions were used as input to predict the YS and UTS from the NN models. The aim of this set of NN predictions was to determine eight metal-cored filler-wire compositions that could be used for single-wire multi-pass welding of X100 pipe, and ones that were expected to deliver the target levels of YS and UTS. Given the inherent experimental error in test data that forms the basis of the NN models, numerical/regression error in the predicted levels of the YS/UTS, and the assumed levels of dilution/recovery of the alloying elements, it was considered prudent to pick a range of compositions. The compositions were picked based on the requirements specified for YS and YS/UTS ratio for the expected range of cooling times. For this case, the minimum YS requirement is 820 MPa and the maximum YS/UTS ratio requirement is 0.94 for the expected range of cooling times from 3.5 seconds to 7 seconds.

The team was asked to provide suggested weld metal chemistries, which were fed into the Neural Network model in order to determine the likelihood of meeting the design criteria. Based on the mechanical property predictions, eight experimental target chemistries were chosen for production as metal-cored electrodes by the Hobart Brothers Company (Miller/Hobart). The eight chemistries selected are shown in Table 2. Both the target and actual metal cored wire chemistries (as measured from a chemical analysis weld pad) are shown in Table 2. The corresponding predictions for the YS and YS/UTS ratio are shown in Figure 4 and Figure 5. It should be noted that several of the chemistries have YS/UTS ratios that are greater than 1. This is because some of the chemistries were out of the range of the data used to produce the model.

Testing of the eight metal-cored electrodes was done by making welds in 914-mm (36-in.) diameter X100 pipe with a wall thickness of 19 mm (0.75 in.). All welding was done at CRC

Evans. The joint was prepared using the standard CRC Evans joint preparation, with a 5° bevel and a 52° offset angle. The backside angle was 37.5° with an offset distance of 0.100-in. The land and the backside bevel depth were each 0.050-in. A schematic of the joint is shown in Figure 6. The root pass weld was made using an ER70S-G filler wire. The pipe was rolled in order to minimize positional effects with the electrode held at the 1 o'clock position, as shown in Figure 7. Welding with the experimental electrodes was done in quadrants such that each electrode was used to complete one quarter of the pipe girth weld (see Figure 8). Thermocouples were attached along side the weld, and additional thermocouples were plunged into the welds during welding as shown in Figure 9 and Figure 10, respectively. This allowed the complete cooling profiles of the welds to be documented.

Following the completion of welding, the welded sections were removed from the pipe and inspected visually and radiographically. They were then sent to CANMET-MTL for mechanical testing, and chemical and metallographic analysis. The results are summarized in Section 4.0.

4.0 Results of Optimized Consumable Development Effort (Task 3)

As stated previously, thermocouple measurements were taken adjacent to the welds, and additional measurements were taken during welding by plunging thermocouples into the molten weld metal. Information about the complete results of both the welding and the thermocouple measurements are given in Appendix C.

4.1 Mechanical Property Test Results

The layout of the mechanical test specimens that were machined and tested is shown in Figure 11. Round bar tensiles, strip tensiles and Charpy V-notch specimens were taken from each weld section. The round bar tensiles were taken in two depths within the weld metal, closer to the I.D. and closer to the O.D. Schematic diagrams showing the location of the various samples within the weld metal are shown in Figure 12 through Figure 14. Because the welding was done in quadrants, as described previously, the first four wires were used to complete one girth weld, and the second four wires were used to complete a second girth weld in another location. The two girth welds were labeled "A" and "B", respectively. Consequently, the weld made with Chemistry 1 was produced in Pipe Section A, so its weld designation is A1. Likewise, the weld made with Chemistry 5 was produced in Pipe Section B, so its weld designation is B5, etc.

4.1.1 Round Bar Tensile Results

Results of the round bar tensile testing are summarized in Table 3. They are also shown graphically in Figure 15 through Figure 17. The yield strength was measured both at 0.2% offset and 0.5% total strain. It was noted that the yield strengths were significantly higher for

samples that were taken closer to the I.D. than those near the O.D. There was not a similar variation in tensile strength levels.

Stress-strain curves for each of the round bar tensile tests are shown in Figure 18 through Figure 25. The difference in the shapes of the I.D. and O.D. curves can be seen quite clearly, as can the differences in the yield strength levels. Some of the welds, such as A3 and B5, showed very distinct upper and lower yield points for the I.D. samples (see Figure 20 and Figure 22, respectively). Weld B8, on the other hand, showed very similar shapes for both the I.D. and O.D. samples (see Figure 25).

Table 4 shows the results of chemical analyses taken from the actual pipe welds. The analyses, which were done by CANMET-MTL, were taken at three locations within the weld metal. The pipe was also analyzed, and that analysis is included in Table 4. Those elements highlighted in blue in Table 4 indicate the primary variants for the given electrode composition. Chemistry 5 represents the “control” chemistry.

For the most part, the chemistry did not vary with the depth of sampling. The nickel tended to vary the most, although generally, it was lower in the root area than at the cap, which would not explain the higher yield strength levels that were noted closer to the root. The variation in the nickel content with depth may be a result of dilution, since the pipe is significantly lower in nickel than most of the electrodes, and dilution would be expected to be greatest close to the weld root.

The welds were also analyzed for oxygen contents. Those results are shown in Table 5. For the most part, the oxygen and nitrogen contents in the weld metal were typical of what is found in welds produced with metal core welding. While there were some small differences in nitrogen content between the I.D. and O.D. samples (up to about 35 ppm), in most, but not all, cases the O.D sample that had the higher reading. The variation in oxygen content from the I.D. to the O.D. ranged up to about 60 ppm, or roughly 10%. In the case of oxygen it was generally, but again not always, the I.D. sample that had the higher reading. These variations are likely within the experimental error of the analysis and are not significant.

Weld metal sections were also sent to Hobart for chemical analysis. The results of those analyses are shown in Table 6. The weld chemical analysis pad test results are included for reference. In general, the agreement between the Hobart results and CANMET-MTL results was good. The one exception tended to be nickel. In general, the Hobart nickel analyses were higher than those performed by CANMET-MTL. The nickel levels in the pipewelds also tended to be higher than the levels in the chemical analysis pads. Throughout the testing, nickel showed the greatest degree of variability, both within the individual labs and lab-to-lab. The cause of the variability was not clear.

The weld metal carbon equivalents were calculated for all of the welds. These are summarized in Table 7. Three different carbon equivalent formulas were used in the calculations, as indicated, and were performed on both the CANMET-MTL and Hobart analyses. In general, the agreement was fair between the two facilities, with the carbon equivalents typically being somewhat higher for the Hobart results, due primarily to the differences in nickel results discussed previously. Not surprisingly, the A4 welds, which had the highest strength levels, also had the highest carbon equivalent levels.

4.1.2 Strip Tensile Test Results

The results for the strip tensile tests are provided in Table 8 , and summarized in Table 9. They are also presented graphically in Figure 26. Figure 27 and Figure 28 show comparisons of the strip and round bar tensile results for Chemistries 1-4 and 5-8, respectively. It can be seen that the strip tensile yield strengths tend to fall between the I.D. and O.D. yield strengths measured for the round bar tensile samples. This is as would be expected, since the strip tensile samples are full thickness and contain material from all depths of the weld metal.

Stress-strain curves were also generated for each of the strip tensile tests. These are shown in Figure 29 through Figure 36. For comparison purposes, the strip tensile stress-strain curves were also plotted along with those for the round bar tensiles, as well as, those for the pipe material. The pipe tensile tests were taken longitudinally, parallel to the pipe axis. The graphs are shown in Figure 37 through Figure 44. Again, the behavior of the strip tensile samples falls between that of the I.D. round bar tensile samples and the O.D. round bar tensile samples. The O.D. round bar tensile behavior was also most similar to that of the pipe material.

4.1.3 CVN Test Results

The CVN test results are summarized in Table 10. Initially, three impact specimens from each set were broken at -40°C. Because the results were generally very good at -40°C, the decision was made to break the additional three samples at -60°C. Overall, the results were quite good, especially for Chemistries 1-5. In fact, only Chemistry 8 had results that were below 50J at -40°C. *(Note that the goal was a minimum of 50J at -10°C, which Chemistry 8, in all likelihood, would have met easily)*.

The results are also shown graphically in Figure 45 through Figure 48. Figure 45 shows the CVN energy for each of the welds at -40° and -60°C. Similarly, Figure 46 shows the data for the fracture appearance. Figure 47 and Figure 48 show the CVN energy and the % shear plotted together for -40°C and -60°C, respectively. Finally, the fracture surfaces themselves are shown in Figure 49 through Figure 64.

4.1.4 Micro-Hardness Test Results

Micro-hardness traverses are summarized in Table 11, and shown graphically in Figure 65 through Figure 72. Traverses were taken across the cap and through the midsection of the welds. There were high hardness readings noted in the base material of Welds A1 and A3. These were due to the indents being taken along the segregation line at the mid-thickness of the pipe.

The majority of the weld metals seemed to fall around 300 to 350 Vicker's Hardness Number. Compositions 1-4 may have been marginally harder than Compositions 5-8, which was in general agreement with the UTS results. Overall, the differences were relatively minor.

4.2 Metallographic Analysis

Macrographs of each of the weld cross-sections are shown in Figure 73 through Figure 80. Photo-micrographs were taken at both EWI and CANMET-MTL. Some of them are shown in Figure 81 through Figure 96. An effort was made to take the photomicrographs at different locations in the weld metal in order to determine if there were significant differences in the microstructures that would explain the variations in properties. The micrographs taken at EWI were generally taken near the I.D. (approximately in the first to second fill pass), and the O.D. (approximately at the boundary between the last fill pass and the capping pass). Micrographs taken at CANMET-MTL were taken from the capping pass and the last fill pass.

In general, the differences in the various locations were not dramatic, the typical difference being in the amount of grain boundary ferrite that may have been present. There was not a great deal of variation among the different weld metals either. The one dramatic exception was Weld B8, which was significantly different from the others. It appears that the B8 microstructure was, to a large degree, composed of martensite-austenite-carbide (M-A-C) constituent, which seems counter-intuitive since it was significantly lower in carbon than the other weld metals. In all likelihood, the microstructure was actually a bainitic ferrite lath structure.

A number of the other weld metals appeared to have some of the M-A-C constituent present in the cap area where there was no reheating (see Sample B6, Figure 92). Sample B7 had a very extensive network of grain boundary ferrite (see Figure 93). There was also a fair amount of grain boundary ferrite present in samples B5 and B6 (see Figure 89 and Figure 91, respectively), although not as much as in B7. As was expected, Sample A4 had the most martensite in its microstructure (Figure 87 and Figure 88). This is the electrode that also provided the highest yielded strength and had the most alloying.

5.0 Discussion of Results

The results of the mechanical property testing of the eight experimental metal-cored electrodes indicate that it is possible to formulate a weld metal chemistry that is capable of meeting the design requirements for X100 pipe. A number of the weld metals exhibited yield strengths that exceeded the 820 MPa minimum requirement when the measurements were taken close to the I.D. of the pipe. Chemistry 4 also exceeded the 820 MPa yield strength goal in the full strip tensile specimen. Chemistries 2, 3 and 6 did not meet the 820 MPa goal, but did exceed 800 MPa.

In addition to meeting or approaching the target yield strength level, most of the electrodes exceeded the target toughness levels. While there was not sufficient material to perform CTOD testing, the results of the CVN testing were much better than expected, with all but one of the chemistries exceeding 50J at -40°C. The toughness results at -60°C were also quite good, with six of the eight chemistries exceeding 50J.

It was noted that the yield strength was consistently higher closer to the I.D. than at the O.D. This trend has been observed previously in a number of cases. It is not entirely clear why this difference exists. There was no significant difference in the chemistry, including oxygen and nitrogen, between the two locations. There also did not appear to be significant differences in the weld microstructures between locations closer to the I.D. and those close to the O.D. One possible explanation for the strength difference was that there were differences in heat input, especially if the weld travel speed was increased in order to fill the joint effectively. There also may have been differences in the level of refinement/reheating because of the wider weave which is typically used higher in the weld joint.

6.0 Conclusions

1. Finite element analysis along with neural network modeling is an effective design tool for developing weld metal compositions.
2. Several of the experimental weld metal compositions exhibited yield strengths that exceeded the goal of 820 MPa when the samples were taken near the ID of the pipe.
3. Composition 4 also exhibited yield strengths that exceeded 820 MPa in full thickness strip tensile samples.
4. Compositions 2, 3 and 6 had yield strengths that exceeded 800 MPa in full thickness strip tensile samples.
5. All of the compositions had yield to tensile strength ratios that fell below 0.94 for the full thickness strip tensile specimens.
6. The weld metal yield strength measured close to the ID of the pipe was significantly higher than that measured close to the OD of the pipe.

7. The minor differences in weld metal chemistry could not explain the differences in the yield strengths at the two locations.
8. Differences in heat input and/or weld bead morphology may have contributed to the strength variations.
9. Seven of the eight compositions had toughness that exceeded 50 J at -40°C, and six of the eight had toughness that exceeded 50 J at -60°C.

7.0 Recommendations for Future Work

While a great deal of information has been gathered from the work done under this program, there is still more that can be learned. Crack tip opening displacement (CTOD) is an important design criterion which is commonly used in the pipeline industry. Future work should include CTOD testing, especially of the most promising compositions, such as composition 4. Additional testing should be done on this composition to determine test repeatability. Wide plate tensile testing should be performed in order to fully characterize the strain distributions in large pipe sections. Finally, composition 4 should also be used as a baseline chemistry for further refinements and improvements in properties.

8.0 References

[1] Jung, G., Khurana, S., Boring, M., and Fiore, S**., "**A Weld Metal Cooling Rate Prediction of Narrow Groove Pipeline Girth Welds – A Finite-Element Modeling Approach," Edison Welding Institute, Columbus, Ohio, EWI Project No. 47452CAP, 2005.

[2] ABAQUS, Inc., "Analysis User's Manual," Version 6.4, 2003.

[3] Zhang, W., Gan, W., Zhang, P., Khurana, S., Babu, S. S., "E-Weld Predictor User Manual," Edison Welding Institute, Columbus, Ohio, 2007.

[4] Hudson, M., "Welding of X100 Linepipe," Thesis, Cranfield University, United Kingdom, 2004.

[5] Husain, I.K., Blackman, S.A., "Mechanized P-GMAW for X100 Steels, Effect of Heat Input and Interpass Temperature on Mechanical Properties," Cranfield University, United Kingdom, 2005.

[6] Gianetto, J.A., Bowker, J.T., Dorling, D.V., Horsley, D., "Structure and Properties of X80 and X100 Pipeline Girth Welds," Proceeding of International Pipeline Conference, 2004.

[7] Johnson, M., "Evaluation of Welding Consumables and Processes for X100 Linepipe Steel," Edison Welding Institute, Columbus, Ohio, EWI Project No. 42144CAP/42636IRD, 2003.

Table 1. Material Properties for Two-Dimensional Welding Analysis

Temperature °C	Thermal Conductivity W/mm °C	Specific Heat J/kg °C
21	0.05234	450
320	0.04123	
580		780
600	0.03547	
643	0.03491	
740		1110
760		990
820		1000
831	0.02712	
840		600
1440	0.03487	700
3000	0.15	

Other Material Properties Required by Thermal Analysis:
Density = 7.85 g/cm^3
Latent heat = 256.7 kJ/kg
Solidus Temperature = 1440°C
Liquidus Temperature = 1500°C

Table 2. Eight Experimental Metal-cored Wire Chemistries

		C	Mn	Si	Ni	Mo	Cr	Ti
Chem 1	Aim	0.09	1.65	0.50	0.85	0.65	0.05	0.025
	Actual	0.062	1.71	0.54	0.92	0.675	0.06	0.04
Chem 2	Aim	0.09	1.65	0.50	0.85	0.8	0.05	0.025
	Actual	0.069	1.74	0.52	0.89	0.830	0.06	0.04
Chem 3	Aim	0.09	1.65	0.50	1.50	0.42	0.05	0.025
	Actual	0.064	1.70	0.52	1.50	0.419	0.06	0.04
Chem 4	Aim	0.09	1.65	0.50	0.85	0.65	0.35	0.025
	Actual	0.066	1.69	0.53	0.88	0.658	0.35	0.04
Chem 5	Aim	0.09	1.65	0.50	0.85	0.42	0.05	0.025
	Actual	0.065	1.73	0.53	0.88	0.412	0.06	0.04
Chem 6	Aim	0.05	1.65	0.35	1.50	0.65	0.05	0.025
	Actual	0.033	1.71	0.38	1.53	0.711	0.06	0.03
Chem 7	Aim	0.05	1.65	0.50	1.20	0.2	0.20	0.025
	Actual	0.035	1.71	0.53	1.27	0.207	0.22	0.03
Chem 8	Aim	0.03	1.40	0.35	2.70	0.5	0.05	0.025
	Actual	0.019	1.54	0.36	2.80	0.524	0.06	0.03

Table 3. Summary of Round Bar Tensile Results

Specimen ID	YS(0.2%) MPa	YS(0.5%) MPa	UTS MPa	El %	RA %	Uniform Strain %
A1-R1-OD	731	716	883	21.8	57.8	9.5
A1-R1-ID	835	830	876	18.9	58.7	5.8
A1-R2-OD	751	733	895	20.5	55.1	8.6
A1-R2-ID	852	837	896	21.4	58	7.1
A2-R1-OD	748	723	926	22.6	63.1	9.7
A2-R1-ID	866	846	907	12.7	62.4	6.8
A2-R2-OD	732	715	914	21.9	63.7	8.4
A2-R2-ID	874	867	911	12.2	63.7	6.1
A3-R1-OD	743	714	823	1.6	100	1.9
A3-R1-ID	855	850	879	19.8	64	6.8
A3-R2-OD	744	725	913	19	57.1	7.7
A3-R2-ID	871	853	898	19.6	61.3	6.5
A4-R1-OD	772	749	933	9.4	57.5	8.2
A4-R1-ID	916	894	945	16.3	61.1	4.6
A4-R2-OD	782	751	951	20.4	61.1	8.1
A4-R2-ID	919	897	943	18	61.4	5.7
B5-R1-OD	679	664	841	19.4	61.6	9.4
B5-R1-ID	804	823	835	21	60.6	7.0
B5-R2-OD	678	666	854	10.7	63.7	6.9
B5-R2-ID	807	830	837	20.3	68.3	10.2
B6-R1-OD	753	735	877	19.5	59.9	7.8
B6-R1-ID	831	813	877	8.7	57.9	5.1
B6-R2-OD	767	737	913	19.1	59.5	8.1
B6-R2-ID	858	833	899	17.1	59.1	5.3
B7-R1-OD	705	695	831	14.6	55.9	6.5
B7-R1-ID	795	805	820	20.5	63.6	7.2
B7-R2-OD	700	692	827	23.2	60.4	9.9
B7-R2-ID	788	803	812	18.9	61.4	6.5
B8-R1-OD	725	705	837	18.8	58.4	5.9
B8-R1-ID	769	752	817	15.3	60.9	5.1
B8-R2-OD	710	689	827	17	57.1	5.6
B8-R2-ID	787	764	842	8.1	56.3	5.3

Table 4. Chemical Analyses taken from Cap Area (C), Mid-thickness (M) and Root Area (R) of Pipe Welds Made Using Eight Experimental Metal-cored Electrodes

MC Wire	WM ID	Element %																
		C	Mn	Si	S	P	Ni	Cr	Mo	Cu	Al	Nb	V	Ti	B	Sn	Zr	Ca
MC-001	X100-C001-C	**0.080**	**1.80**	0.45	0.006	0.009	**0.80**	0.065	**0.57**	0.12	0.011	0.005	0.0054	0.042	<.0005	0.004	<.005	<.002
	X100-C001-M	**0.082**	**1.80**	0.46	0.005	0.008	**0.81**	0.068	**0.58**	0.11	0.013	0.005	0.0056	0.050	<.0005	0.004	<.005	<.002
	X100-C001-R	**0.080**	**1.80**	0.45	0.005	0.008	**0.74**	0.066	**0.57**	0.10	0.012	0.006	0.0055	0.050	<.0005	0.004	<.005	<.002
MC-002	X100-C002-C	0.082	1.80	0.45	0.005	0.008	0.98	0.063	**0.71**	0.070	0.014	0.005	0.0055	0.046	<.0005	0.002	<.005	<.002
	X100-C002-M	0.081	1.80	0.48	0.005	0.008	0.81	0.061	**0.71**	0.073	0.013	0.005	0.0057	0.048	<.0005	0.002	<.005	<.002
	X100-C002-R	0.080	1.80	0.45	0.005	0.008	0.95	0.066	**0.68**	0.084	0.016	0.006	0.0056	0.046	<.0005	0.002	<.005	<.002
MC-003	X100-C003-C	0.078	1.80	0.47	0.005	0.009	**1.30**	0.062	0.39	0.10	0.014	0.004	0.0053	0.048	<.0005	0.003	<.005	<.002
	X100-C003-M	0.083	1.80	0.48	0.005	0.008	**1.32**	0.065	0.38	0.14	0.011	0.005	0.0053	0.046	<.0005	0.004	<.005	<.002
	X100-C003-R	0.082	1.80	0.41	0.005	0.008	**1.22**	0.062	0.36	0.12	0.011	0.006	0.0051	0.042	<.0005	0.003	<.005	<.002
MC-004	X100-C004-C	0.077	1.80	0.46	0.005	0.009	0.74	**0.35**	**0.58**	0.093	0.009	0.005	0.0053	0.045	<.0005	0.003	<.005	<.002
	X100-C004-M	0.081	1.80	0.49	0.006	0.008	0.74	**0.35**	**0.57**	0.078	0.008	0.005	0.0053	0.050	<.0005	0.003	<.005	<.002
	X100-C004-R	0.082	1.80	0.46	0.005	0.008	0.73	**0.33**	**0.56**	0.094	0.008	0.006	0.0054	0.050	<.0005	0.004	<.005	<.002
MC-005	X100-C005-C	**0.078**	**1.76**	**0.46**	0.005	0.009	**1.09**	**0.074**	**0.36**	0.170	0.013	0.007	0.0050	**0.049**	<.0005	0.002	<.005	<.002
	X100-C005-M	**0.077**	**1.76**	**0.47**	0.005	0.009	**1.03**	**0.077**	**0.36**	0.077	0.013	0.006	0.0050	**0.051**	<.0005	0.002	<.005	<.002
	X100-C005-R	**0.078**	**1.77**	**0.43**	0.005	0.009	**0.98**	**0.066**	**0.36**	0.084	0.013	0.007	0.0050	**0.046**	<.0005	0.002	<.005	<.002
MC-006	X100-C006-C	**0.054**	1.84	**0.33**	0.005	0.010	**1.43**	0.062	**0.64**	0.083	0.011	0.007	0.0055	0.044	<.0005	0.002	<.005	<.002
	X100-C006-M	**0.055**	1.89	**0.33**	0.005	0.010	**1.39**	0.059	**0.62**	0.068	0.012	0.005	0.0055	0.042	<.0005	0.002	<.005	<.002
	X100-C006-R	**0.056**	1.87	**0.32**	0.005	0.010	**1.34**	0.056	**0.61**	0.078	0.013	0.007	0.0057	0.050	<.0005	0.002	<.005	<.002
MC-007	X100-C007-C	**0.062**	1.80	0.47	0.005	0.011	**1.79**	**0.26**	**0.20**	0.093	0.015	0.006	0.0050	0.050	<.0005	0.002	<.005	<.002
	X100-C007-M	**0.060**	1.80	0.49	0.005	0.010	**1.43**	**0.25**	**0.20**	0.074	0.015	0.005	0.0050	0.054	<.0005	0.002	<.005	<.002
	X100-C007-R	**0.055**	1.80	0.46	0.005	0.010	**1.05**	**0.21**	**0.19**	0.083	0.014	0.007	0.0050	0.051	<.0005	0.002	<.005	<.002
MC-008	X100-C008-C	**0.040**	1.60	0.34	0.006	0.010	**2.44**	**0.064**	**0.50**	0.120	0.012	0.005	0.0050	0.042	<.0005	0.002	<.005	<.002
	X100-C008-M	**0.041**	1.60	0.32	0.005	0.010	**2.28**	**0.058**	**0.48**	0.073	0.012	0.006	0.0050	0.038	<.0005	0.002	<.005	<.002
	X100-C008-R	**0.046**	1.60	0.33	0.006	0.010	**2.42**	**0.071**	**0.47**	0.078	0.013	0.006	0.0050	0.046	<.0005	0.002	<.005	<.002
Pipe	X100-C002-BM	0.065	1.80	0.08	<.002	0.007	0.51	0.027	0.26	0.30	0.028	0.030	0.0044	0.011	<.0005	0.002	<.005	<.002
	X100-C003-BM	0.064	1.80	0.08	<.002	0.006	0.51	0.028	0.26	0.31	0.029	0.030	0.0045	0.011	<.0005	0.002	<.005	<.002
	X100-C005-BM	0.064	1.80	0.08	<.002	0.007	0.51	0.027	0.26	0.30	0.037	0.031	0.0044	0.011	<.0005	0.002	<.005	<.002

Table 5. Weld Metal Oxygen and Nitrogen Analyses Performed by CANMET-MTL

Pipe Weld	Sample Identification	Oxygen Analysis	Oxygen Average	Nitrogen Analysis	Nitrogen Average
A1	A1-R1-OD	0.0591, 0.0585, 0.0587, 0.0582	0.0586	0.0046, 0.0051, 0.0056, 0.0047	0.0050
	A1-R1-ID	0.0553, 0.0642, 0.0556, 0.0606, 0.0588	0.0589	0.0033, 0.0037, 0 .0035, 0.0035, 0.0035	0.0035
A2	A2-R1-OD	0.0537, 0.0380, 0.0537, 0.0510, 0.0468	0.0486	0.0068, 0.0071, 0.0070, 0.0071, 0.0069	0.0069
	A2-R1-ID	0.0540, 0.0581, 0.0564, 0.0584, 0.0496	0.0553	0.0046, 0.0046, 0.0046, 0.0048, 0.0043	0.0046
A3	A3-R1-OD	0.0523, 0.0515, 0.0454, 0.0532, 0.0524	0.0510	0.0033, 0.0033, 0.0034, 0.0035, 0.0035	0.0034
	A3-R1-ID	0.0584, 0.0574, 0.0617, 0.0562, 0.0557	0.0579	0.0041, 0.0042, 0.0040, 0.0039, 0.0040	0.0040
A4	A4-R1-OD	0.0482, 0.0516, 0.0480, 0.0556, 0.0546	0.0516	0.0064, 0.0068, 0.0065, 0.0068, 0.0064	0.0066
	A4-R1-ID	0.0587, 0.0594, 0.0454, 0.0597	0.0558	0.0062, 0.0059, 0.0060, 0.0058	0.0060
B5	B5-R1-OD	0.0528, 0.0493, 0.0472, 0.0543, 0.0542	0.0516	0.0081, 0.0080, 0.0083, 0.0079, 0.0081	0.0081
	B5-R1-ID	0.0549, 0.0457, 0.0368, 0.0557	0.0483	0.0051, 0.0050, 0.0045, 0.0050	0.0049
B6	B6-R1-OD	0.0618, 0.0628, 0.0640, 0.0569	0.0614	0.0083, 0.0092, 0.0089, 0.0088	0.0087
	B6-R1-ID	0.0698, 0.0608, 0.0540, 0.0592, 0.0686	0.0625	0.0052, 0.0054, 0.0049, 0.0049, 0.0054	0.0052
B7	B7-R1-OD	0.0549, 0.0611, 0.0642, 0.0620, 0.0609	0.0606	0.0065, 0.0070, 0.0063, 0.0065, 0.0069	0.0066
	B7-R1-ID	0.0677, 0.0623, 0.0650, 0.0614	0.0641	0.0054, 0.0055, 0.0059, 0.0057	0.0056
B8	B8-R1-OD	0.0637, 0.0664, 0.0694, 0.0676, 0.0661	0.0666	0.0043, 0.0043, 0.0045, 0.0043, 0.0042	0.0043
	B8-R1-ID	0.0742, 0.0760, 0.0610, 0.0688, 0.0773	0.0715	0.0063, 0.0063, 0.0063, 0.0063, 0.0064	0.0063

Table 6. Pipe Weld Chemical Analysis Data Provided by Hobart

ID	Element (%)																	
	C	Mn	P	S	Si	Cu	Cr	V	Ni	Mo	Al	Ti	Nb	Co	B	Sn	Pb	Zr
Chem. 1	0.062	1.71			0.54	0.03	0.06		0.92	0.68		0.04						
1c Pipe Weld	0.080	1.76	0.012	0.012	0.47	0.21	0.06	0.002	1.02	0.59	0.014	0.04	0.009	0.016	0.0001	0.005	0.0004	0.003
Pipe Chem.	0.062	1.85	0.007	0.005	0.10	0.32	0.02	0.002	0.54	0.30	0.040	0.01	0.034	0.014				
Chem. 2	0.069	1.74			0.52	0.03	0.06		0.89	0.83		0.04						
2c Pipe Weld	0.079	1.81	0.011	0.011	0.50	0.09	0.06	0.002	0.99	0.72	0.014	0.04	0.009	0.015	0.0001	0.005	0.0005	0.002
Pipe Chem.	0.061	1.85	0.007	0.006	0.10	0.32	0.02	0.003	0.52	0.30	0.041	0.01	0.034	0.020				
Chem. 3	0.064	1.70			0.52	0.03	0.06		1.50	0.42		0.04						
3c Pipe Weld	0.080	1.76	0.012	0.012	0.48	0.09	0.05	0.002	1.39	0.40	0.012	0.04	0.009	0.013	0.0003	0.005	0.0003	0.003
Pipe Chem.	0.062	1.85	0.007	0.005	0.10	0.32	0.02	0.002	0.54	0.30	0.040	0.01	0.034	0.014				
Chem. 4	0.066	1.69			0.53	0.03	0.35		0.88	0.66		0.04						
4c Pipe Weld	0.080	1.78	0.011	0.011	0.51	0.08	0.33	0.002	0.88	0.60	0.013	0.04	0.009	0.012	0.0001	0.005	0.0003	0.003
Pipe Chem.	0.062	1.85	0.007	0.005	0.10	0.32	0.02	0.002	0.54	0.30	0.040	0.01	0.034	0.014				
Chem. 5	0.065	1.73			0.53	0.04	0.06		0.88	0.41		0.04						
5c Pipe Weld	0.074	1.76	0.010	0.012	0.48	0.94	0.07	0.003	1.26	0.40	0.014	0.04	0.011	0.009	0.0003	0.005	0.0006	0.003
Pipe Chem.	0.062	1.87	0.007	0.004	0.10	0.33	0.02	0.001	0.54	0.30	0.040	0.01	0.034	0.012				
Chem. 6	0.033	1.71			0.38	0.04	0.06		1.53	0.71		0.03						
6c Pipe Weld	0.057	1.86	0.012	0.014	0.39	0.08	0.07	0.003	1.58	0.66	0.013	0.04	0.009	0.012	0.0001	0.005	0.0007	0.002
Pipe Chem.	0.062	1.85	0.007	0.005	0.10	0.32	0.02	0.002	0.54	0.30	0.040	0.01	0.034	0.014				
Chem. 7	0.035	1.71			0.53	0.04	0.22		1.27	0.27		0.03						
7c Pipe Weld	0.061	1.83	0.012	0.013	0.51	0.08	0.24	0.003	1.88	0.24	0.016	0.05	0.011	0.009	0.0001	0.005	0.0003	0.004
Pipe Chem.	0.062	1.85	0.007	0.005	0.10	0.32	0.02	0.002	0.54	0.30	0.040	0.01	0.034	0.014				
Chem. 8	0.019	1.54			0.36	0.03	0.06		2.80	0.52		0.03						
8c Pipe Weld	0.040	1.66	0.012	0.013	0.37	0.08	0.07	0.003	2.74	0.54	0.015	0.04	0.010	0.010	0.0001	0.005	0.0003	0.003
Pipe Chem.	0.063	1.84	0.008	0.007	0.10	0.31	0.02	0.001	0.55	0.29	0.039	0.01	0.033	0.011				

Table 7. Carbon Equivalent Values Based on CANMET-MTL and Hobart Chemical Analyses

MC Wire	WM ID		CE_{IIW}	Pcm	CEN
MC-001	X100-C001-M	CANMET-MTL	0.574	0.249	0.376
	1c Pipe Weld	Hobart	0.586	0.254	0.378
MC-002	X100-C002-M	CANMET-MTL	0.595	0.255	0.387
	2c Pipe Weld	Hobart	0.609	0.259	0.391
MC-003	X100-C003-M	CANMET-MTL	0.570	0.247	0.371
	3c Pipe Weld	Hobart	0.563	0.241	0.362
MC-004	X100-C004-M	CANMET-MTL	0.621	0.260	0.403
	4c Pipe Weld	Hobart	0.627	0.261	0.404
MC-005	X100-C005-M	CANMET-MTL	0.533	0.230	0.341
	5c Pipe Weld	Hobart	0.608	0.276	0.379
MC-006	X100-C006-M	CANMET-MTL	0.604	0.232	0.344
	6c Pipe Weld	Hobart	0.623	0.241	0.357
MC-007	X100-C007-M	CANMET-MTL	0.551	0.220	0.325
	7c Pipe Weld	Hobart	0.592	0.233	0.345
MC-008	X100-C008-M	CANMET-MTL	0.573	0.209	0.306
	8c Pipe Weld	Hobart	0.626	0.224	0.330
Pipe	**ID**				
	X100-C002-BM	CANMET-MTL	0.477	0.200	0.292

Note:

$$CE_{IIW} = C + \frac{Mn}{6} + \frac{Cu + Ni}{15} + \frac{Cr + Mo + V}{5}$$

$$P_{CM} = C + \frac{Si}{30} + \frac{Mn + Cu + Cr}{20} + \frac{Ni}{60} + \frac{Mo}{15} + \frac{V}{10} + 5B$$

$$CEN = C + A(C)\left(\frac{Si}{24} + \frac{Mn}{6} + \frac{Cu}{15} + \frac{Ni}{20} + \frac{Cr + Mo + Nb + V}{5} + 5B\right)$$

where $A(C) = 0.75 + 0.25\tanh[20(C - 0.12)]$

Table 8. Full Strip Tensile Results

Specimen #	W (mm)	t (mm)	YS (0.2%) MPa	YS (0.5%) MPa	UTS MPa	El (%)	RA (%)	Uniform Strain (%)
A1-S2	12.68	4.75	787	779	866	22.4	49.6	7.3
A1-S3	12.68	4.76	793	786	872	21.8	51.1	7.1
A1-S4	12.68	4.74	808	798	893	23.4	46.9	7.6
A1-Strip			**796**	**788**	**877**	**23**	**49**	**7.3**
A2-S2	12.68	4.76	805	795	892	22.2	45.1	7.7
A2-S3	12.67	4.75	807	792	906	23.2	47.1	7.9
A2-S4	12.67	4.74	819	803	911	21.4	48.6	7.2
A2-Strip			**810**	**797**	**903**	**22**	**47**	**7.6**
A3-S2	12.66	4.74	782	771	873	22.9	47.5	7.5
A3-S3	12.66	4.74	801	786	894	20.0	NA	7.6
A3-S4	12.66	4.74	853	832	943	22.9	46.3	7.5
A3-Strip			**812**	**796**	**903**	**22**	**47**	**7.5**
A4-S2	12.69	4.75	836	814	936	21.0	47.2	7.2
A4-S3	12.69	4.75	853	833	944	22.5	46.8	7.9
A4-S4	12.68	4.76	851	817	953	20.3	45.0	7.1
A4-Strip			**847**	**821**	**945**	**21**	**46**	**7.4**
B5-S2	12.68	4.77	728	727	815	24.3	50.2	8.4
B5-S3	12.68	4.78	733	733	818	24.3	53.9	8.9
B5-Strip			**730**	**730**	**816**	**24**	**52**	**8.7**
B6-S2	12.70	4.76	798	779	873	20.0	47.7	6.5
B6-S4	12.68	4.78	806	782	895	21.3	44.7	6.2
B6-Strip			**802**	**781**	**884**	**21**	**46**	**6.4**
B7-S2	12.69	4.76	721	715	803	23.4	51.9	7.9
B7-S3	12.67	4.75	730	724	805	21.4	42.3	7.7
B7-Strip			**725**	**719**	**804**	**22**	**47**	**7.8**
B8-S2	12.67	4.75	748	735	828	19.1	47.3	5.5
B8-S3	12.67	4.75	729	718	817	19.5	45.7	5.4
B8-S4	12.67	4.75	751	733	836	18.6	41.1	5.6
B8-Strip			**743**	**728**	**827**	**19**	**45**	**5.5**

Table 9. Summary of Full Strip Tensile Results

Specimen	YS (0.2%) MPa	YS (0.5%) MPa	UTS MPa	El (%)	RA (%)	Uniform Strain (%)
A1-Strip	796	788	877	23	49	7.3
A2-Strip	810	797	903	22	47	7.6
A3-Strip	812	796	903	22	47	7.5
A4-Strip	847	821	945	21	46	7.4
B5-Strip	730	730	816	24	52	8.7
B6-Strip	802	781	884	21	46	6.4
B7-Strip	725	719	804	22	47	7.8
B8-Strip	743	728	827	19	45	5.5

Table 10. Results of CVN Testing

Specimen Description No.	Test Temperature (°C)	Absorbed Energy (J)	Appearance % shear	Average (J)	Average (%)
A1-1	-40	95.5	99	92	95
A1-2	-40	93.0	98		
A1-3	-40	87.0	89		
A1-4	-60	73.5	75	81	81
A1-5	-60	85.5	85		
A1-6	-60	83.0	82		
A2-1	-40	85.0	80	86	86
A2-2	-40	83.0	98		
A2-3	-40	90.0	81		
A2-4	-60	70.5	66	71	65
A2-5	-60	68.0	59		
A2-6	-60	75.0	70		
A3-1	-40	82.5	92	91	93
A3-2	-40	96.0	92		
A3-3	-40	94.5	96		
A3-4	-60	70.0	69	80	77
A3-5	-60	87.0	82		
A3-6	-60	81.5	80		
A4-1	-40	80.5	69	95	81
A4-2	-40	93.0	75		
A4-3	-40	112.0	99		
A4-4	-60	70.0	70	68	63
A4-5	-60	61.0	62		
A4-6	-60	72.0	56		

Table 10. Results of CVN Testing (continued)

Specimen Description No.	Test Temperature (°C)	Absorbed Energy (J)	Appearance % shear	Average (J)	Average (%)
B5-1	-40	93.0	75	88	74
B5-2	-40	82.5	72		
B5-3	-40	87.0	75		
B5-4	-60	68.0	55	72	54
B5-5	-60	76.0	55		
B5-6	-60	72.0	52		
B6-1	-40	60.0	70	57	66
B6-2	-40	49.0	59		
B6-3	-40	62.0	69		
B6-4	-60	47.5	59	47	56
B6-5	-60	46.0	55		
B6-6	-60	47.0	55		
B7-1	-40	73.5	70	76	73
B7-2	-40	77.0	75		
B7-3	-40	78.0	75		
B7-4	-60	70.5	62	65	59
B7-5	-60	68.0	59		
B7-6	-60	56.0	55		
B8-1	-40	42.0	55	48	55
B8-2	-40	58.0	62		
B8-3	-40	44.0	47		
B8-4	-60	38.0	39	39	38
B8-5	-60	36.0	35		
B8-6	-60	42.5	40		

Table 11. Summary of Microhardness Results

WM ID	Microhardness, VHN, 300 g		
	Through-thickness excluding root	Subsurface cap pass cross-weld traverse	Mid-thickness cross-weld traverse
A1	(276-417) **324**	(305-341) **305**	(288-417) **327**
A2	(291-325) **306**	(291-319) **302**	(272-334) **311**
A3	(292-383) **330**	(307-371) **353**	(298-344) **321**
A4	(299-385) **329**	(313-369) **332**	(293-321) **312**
B5	(264-298) **280**	(260-287) **277**	(272-304) **285**
B6	(268-327) **297**	(282-307) **292**	(284-327) **304**
B7	(248-298) **271**	(268-284) **277**	(258-292) **278**
B8	(257-316) **286**	(275-324) **302**	(277-310) **293**

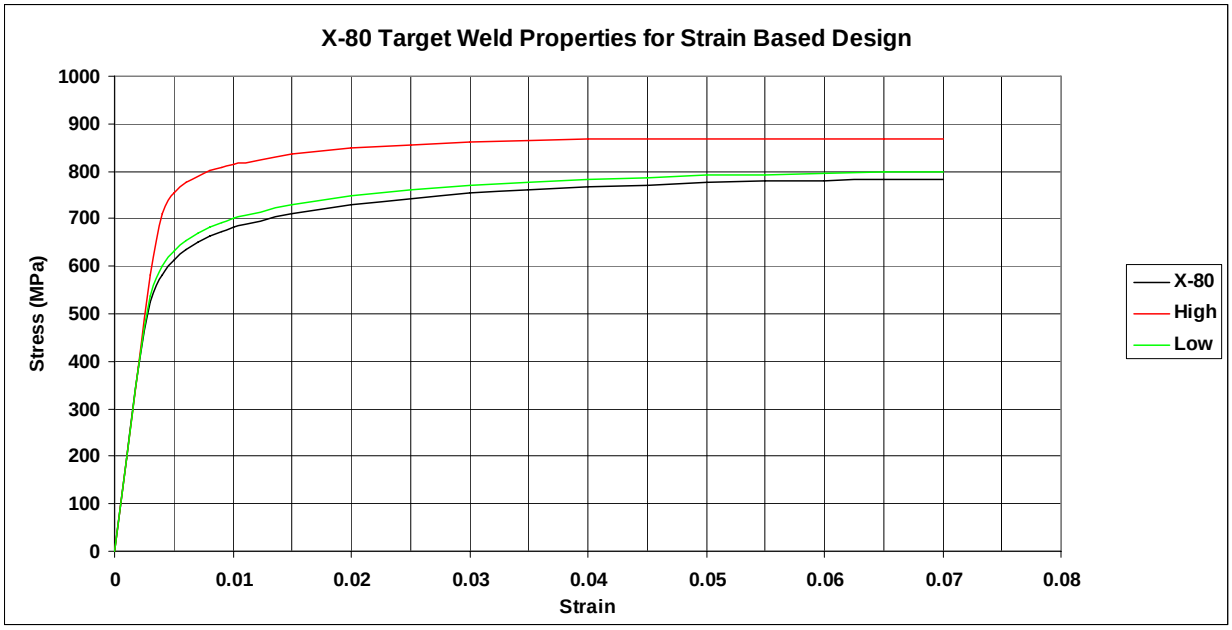

Figure 1. Theoretical Stress Strain Curve for Optimized X80 Weld Metal

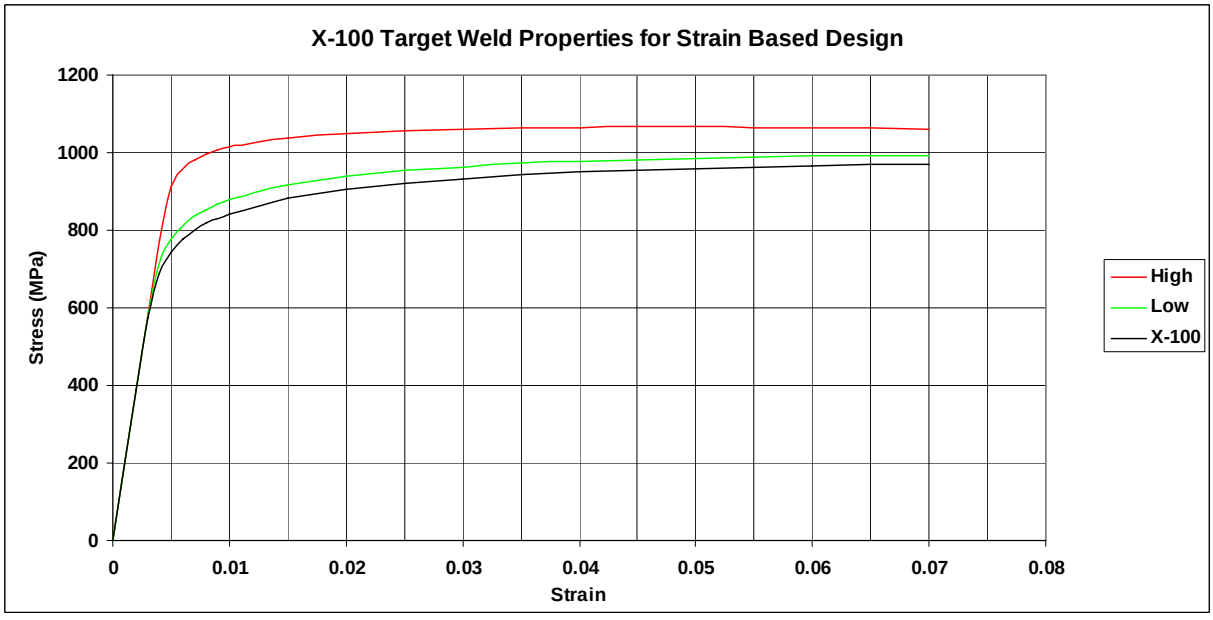

Figure 2. Theoretical Stress Strain Curve for Optimized X100 Weld Metal

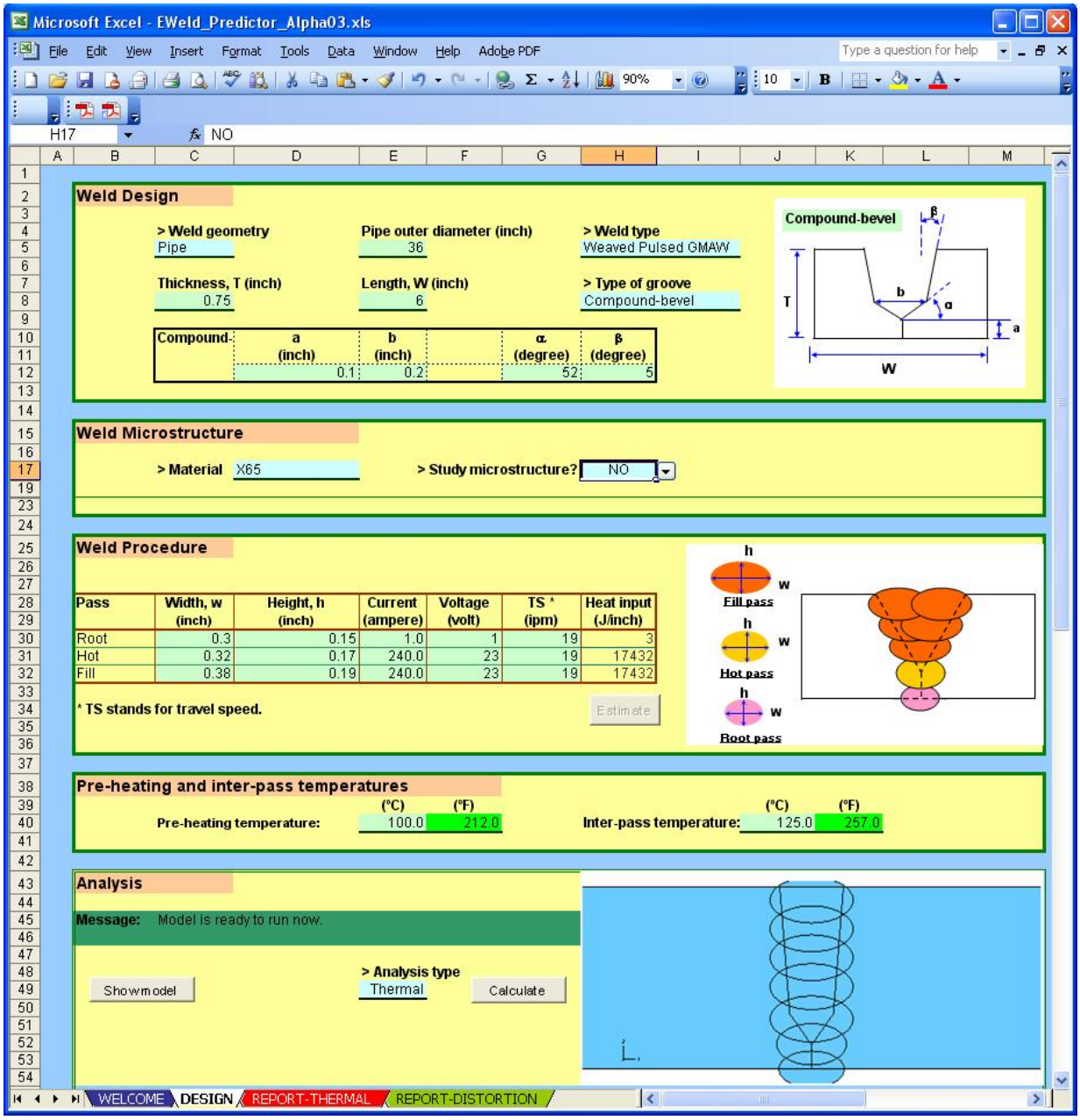

Figure 3. Input Page from E-Weld Predictor

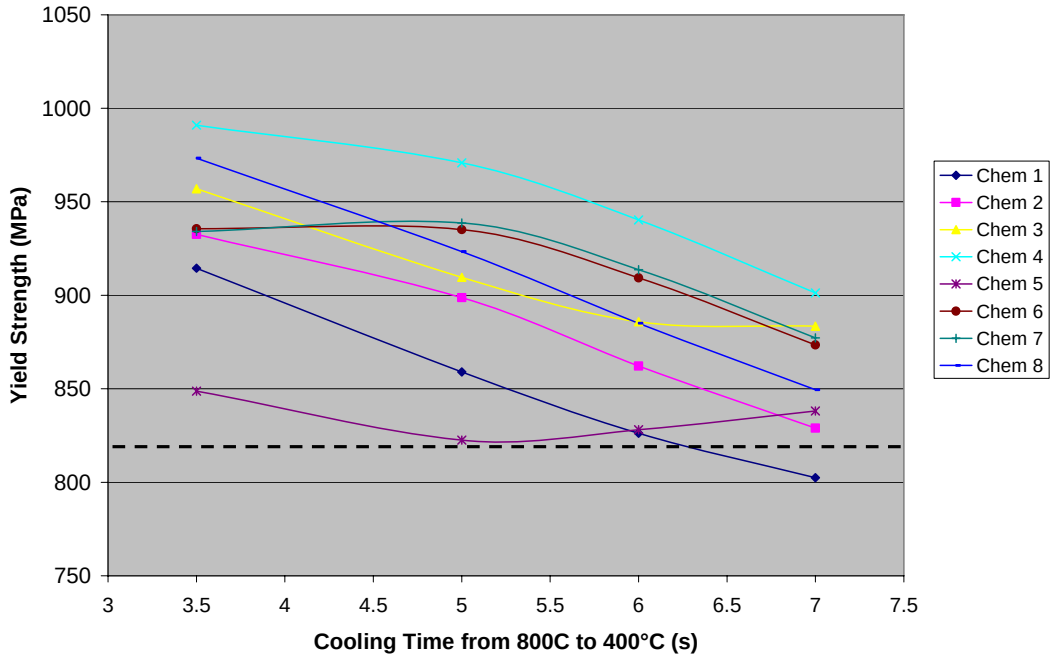

Figure 4. Plot of Predicted Yield Strength vs. Cooling Time for Eight Experimental Electrode Chemistries

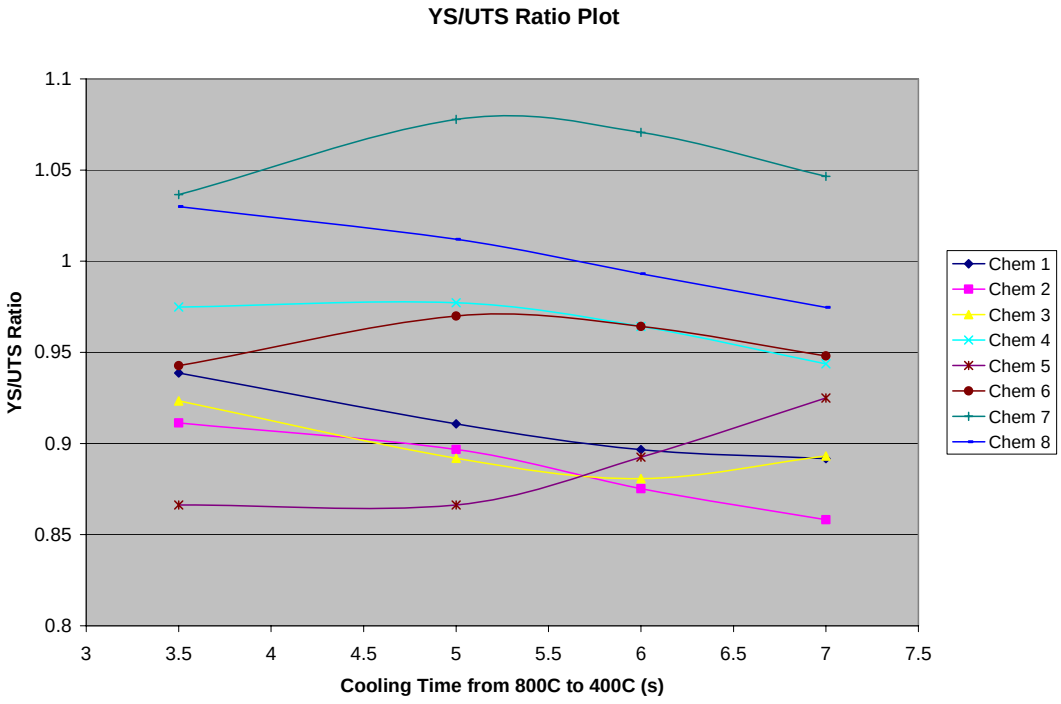

Figure 5. Plot of Predicted YS/UTS Ratio vs. Cooling Time for Eight Experimental Electrode Chemistries

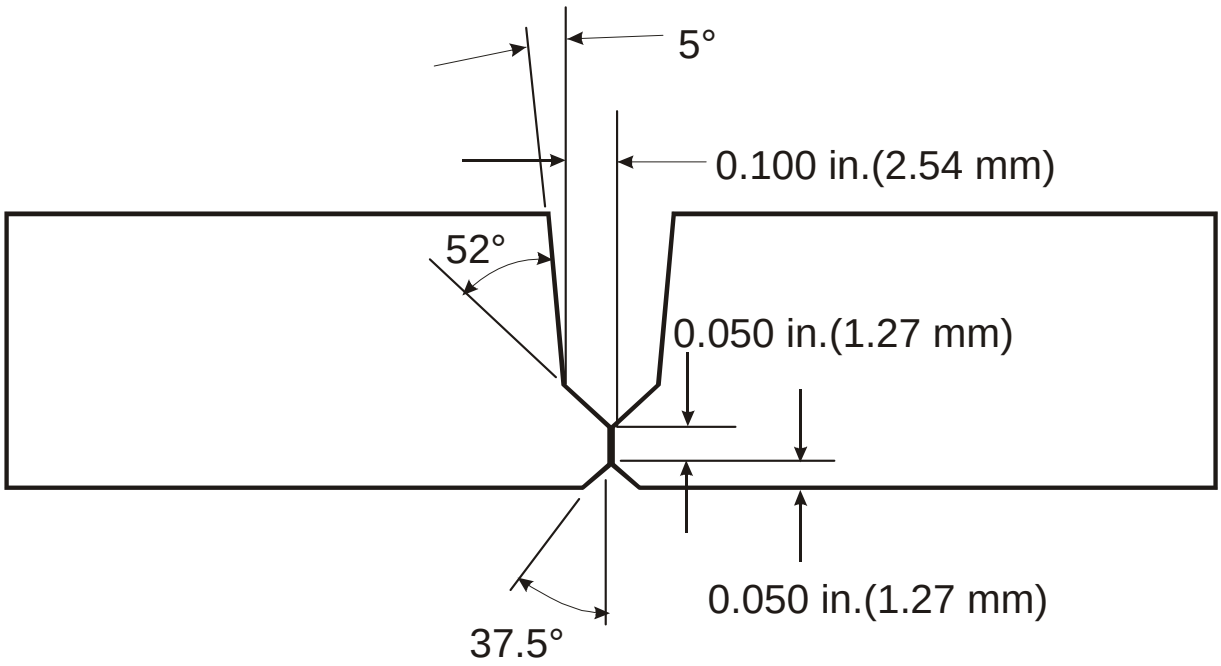

Figure 6. Schematic Diagram of Joint Prep for Pipe Welds Produced with Eight Experimental Metal-cored Electrodes

Figure 7. Set-up of Welding Head in One o'clock Position

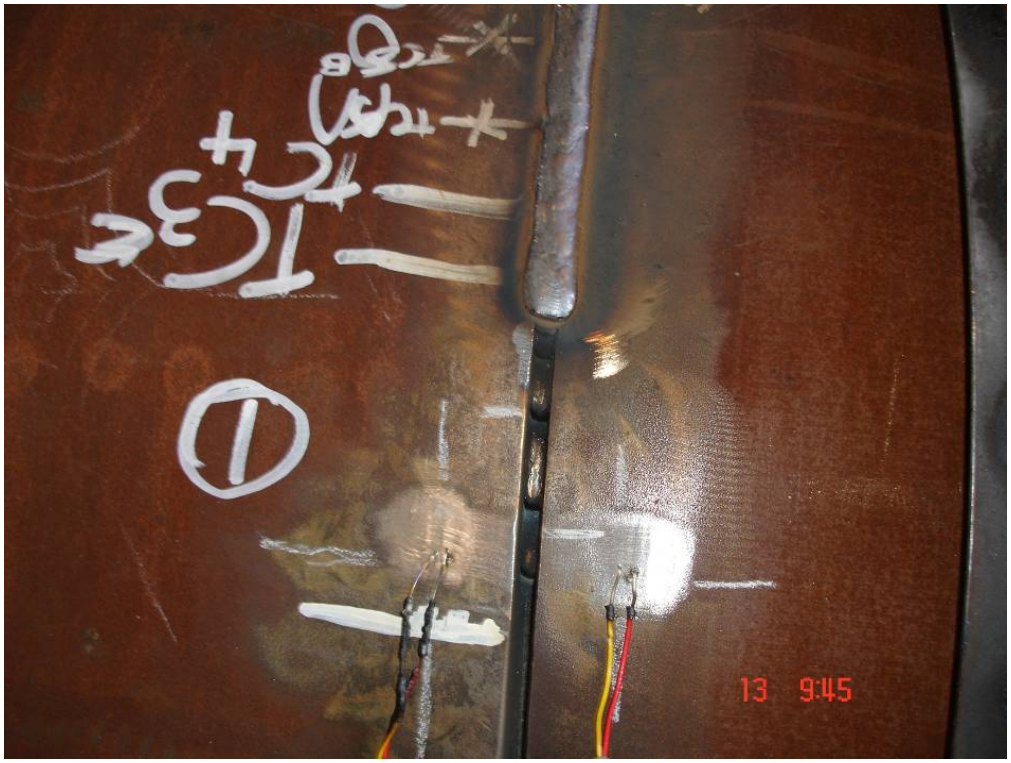

Figure 8. Pipe Section with One-quarter Weld Completed

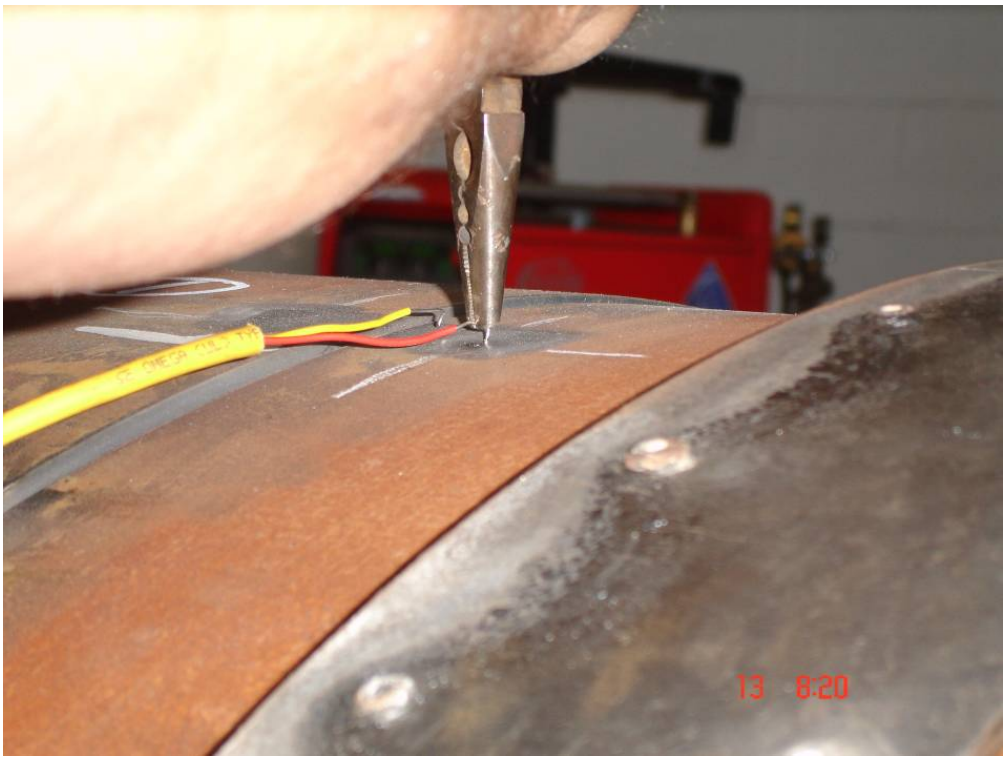

Figure 9. Attachment of Thermocouples Prior to Welding

Figure 10. Plunging of Thermocouples during Welding

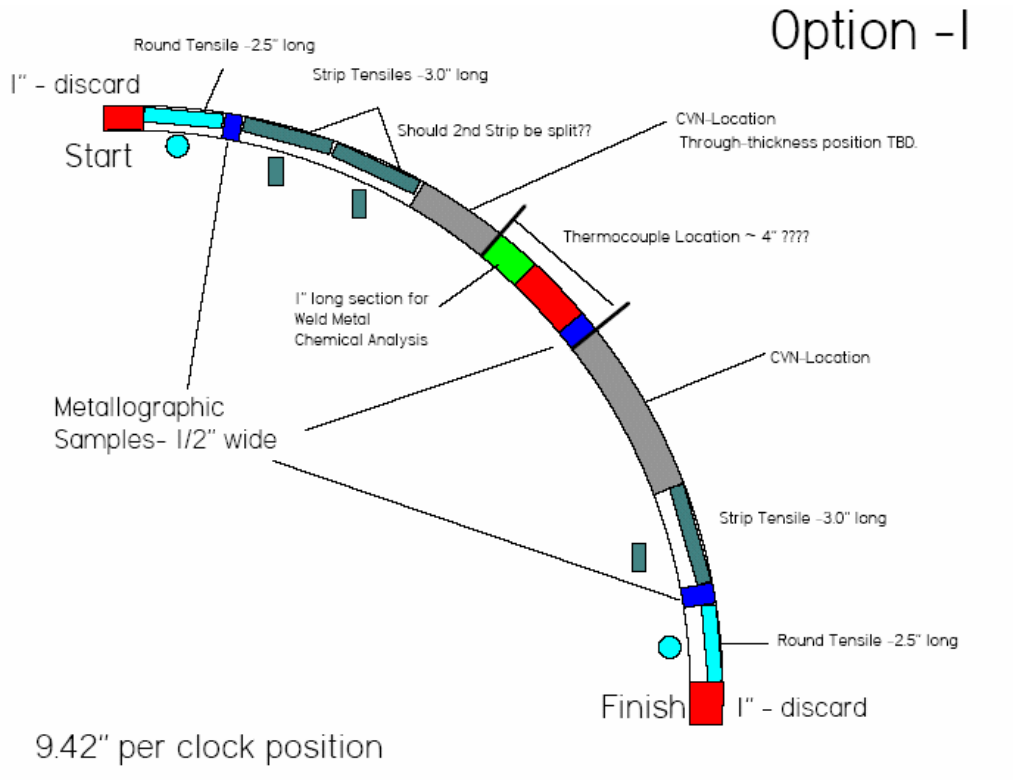

Figure 11. Schematic Showing Location of Mechanical Test Samples

Experimental X100 Metal Cored Girth Welds
NPS36 - 0.750" WT

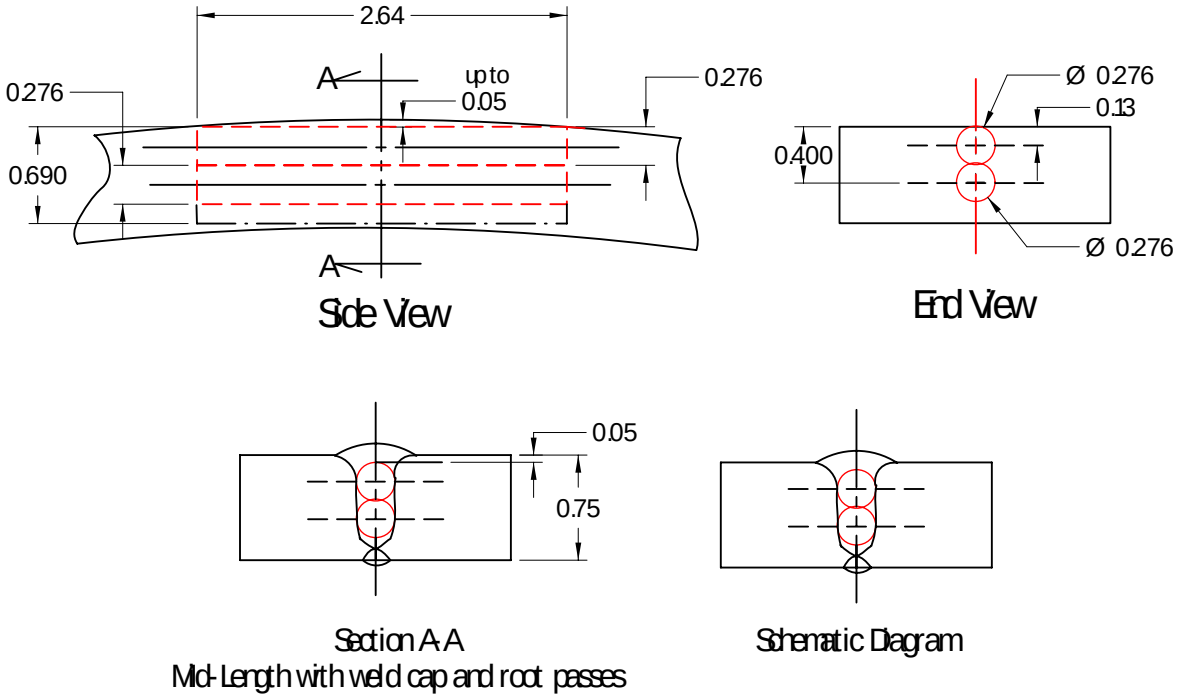

Figure 12. Schematic Showing Weld Cross-sections and Locations of Round Bar Tensiles

Experimental X100 Metal Cored Girth Welds
NPS36 - 0.750" WT

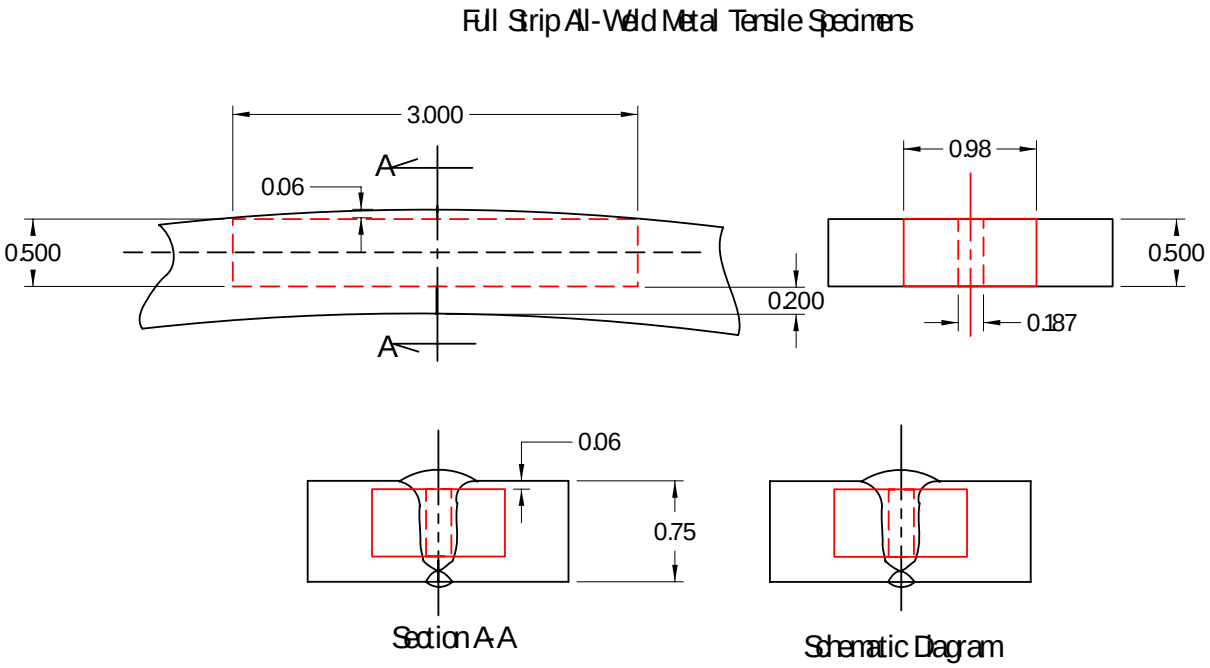

Figure 13. Schematic Showing Weld Cross-sections and Locations of Strip Tensiles

Experimental X100 Metal Cored Girth Welds
NPS36 - 0.750" WT

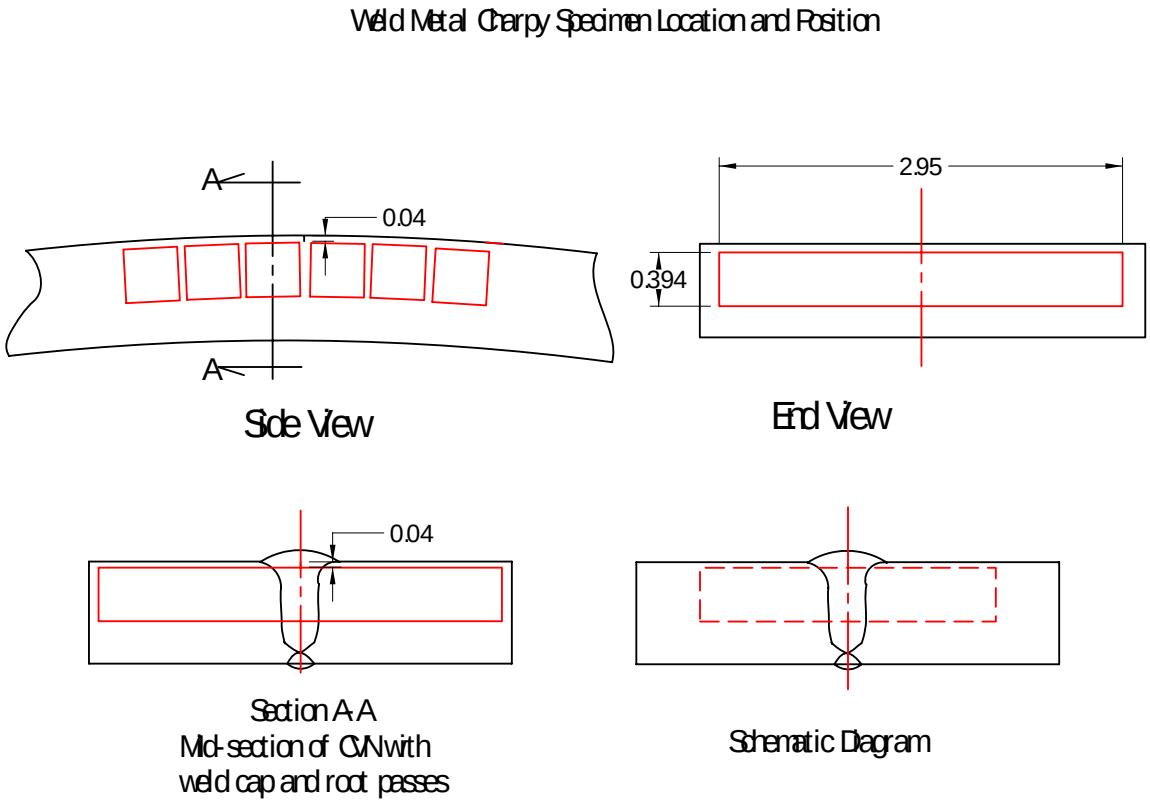

Figure 14. Schematic Showing Weld Cross-sections and Locations of Charpy V-Notch Specimens

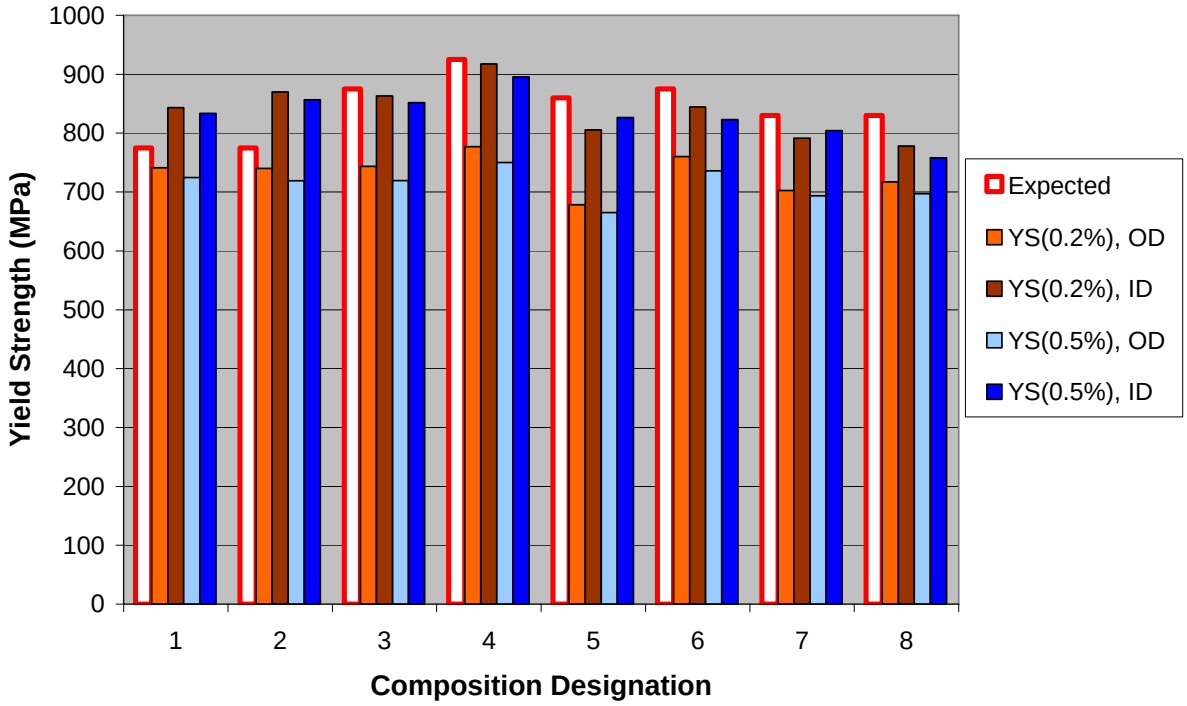

Figure 15. Summary of Average Yield Strengths for Various Chemical Compositions

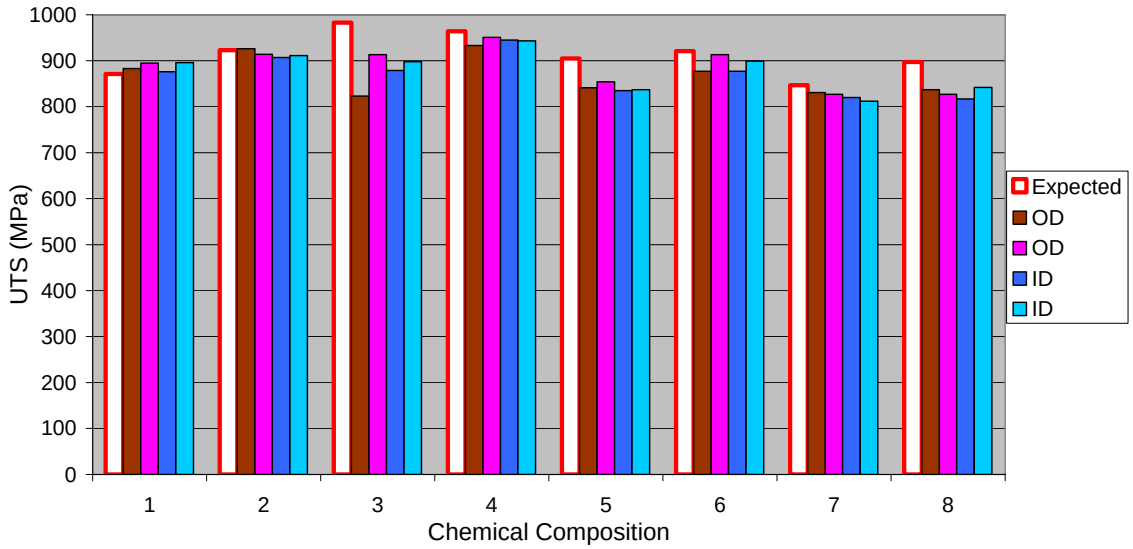

Figure 16. Summary of Ultimate Tensile Strength Results for Various Chemical Compositions

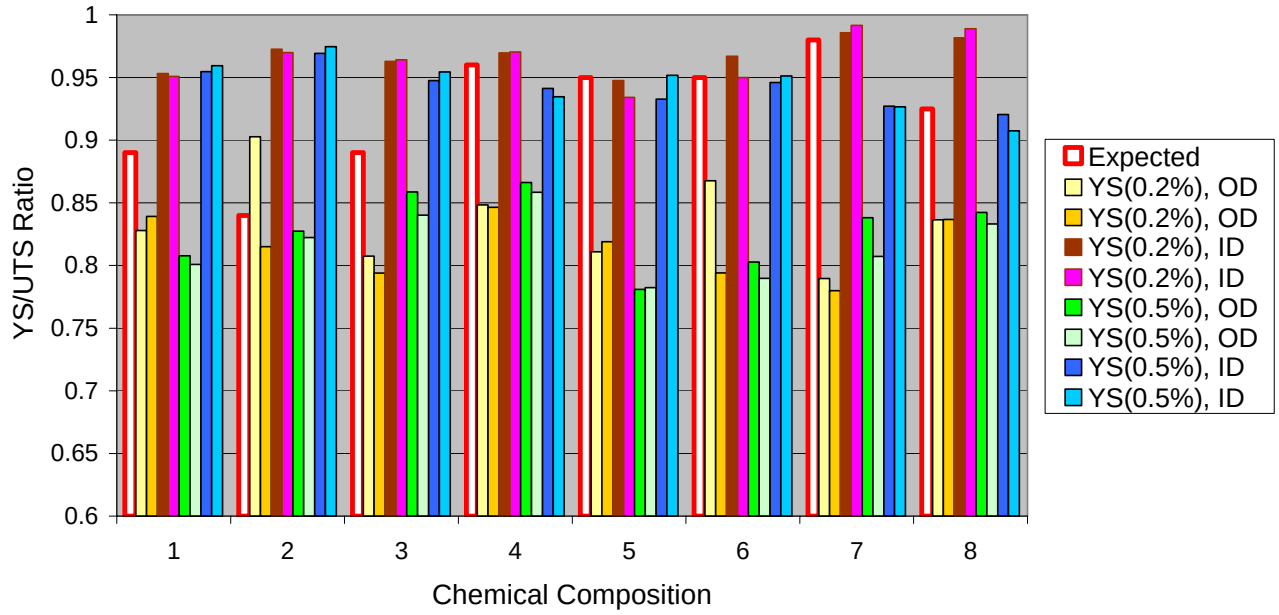

Figure 17. Summary of YS/UTS Ratio Results for Various Chemical Compositions

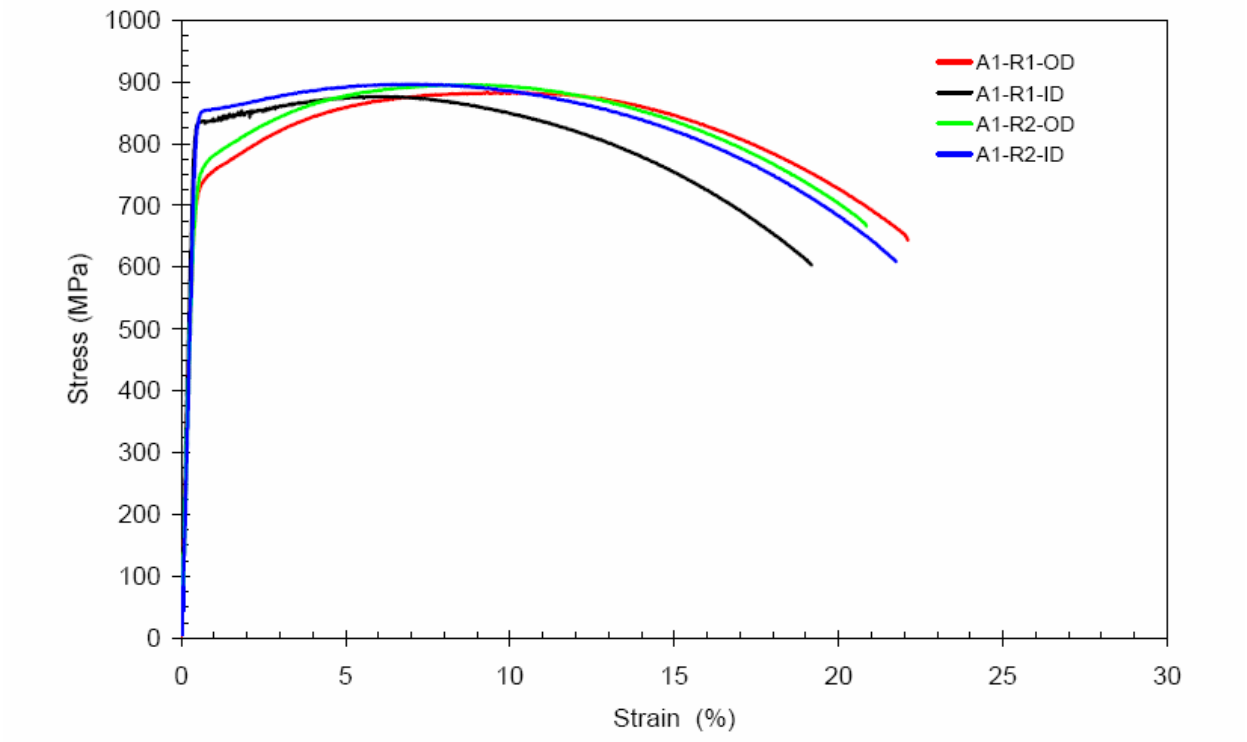

Figure 18. Stress vs. Strain for Chemistry 1 Round Bar Tensile Samples

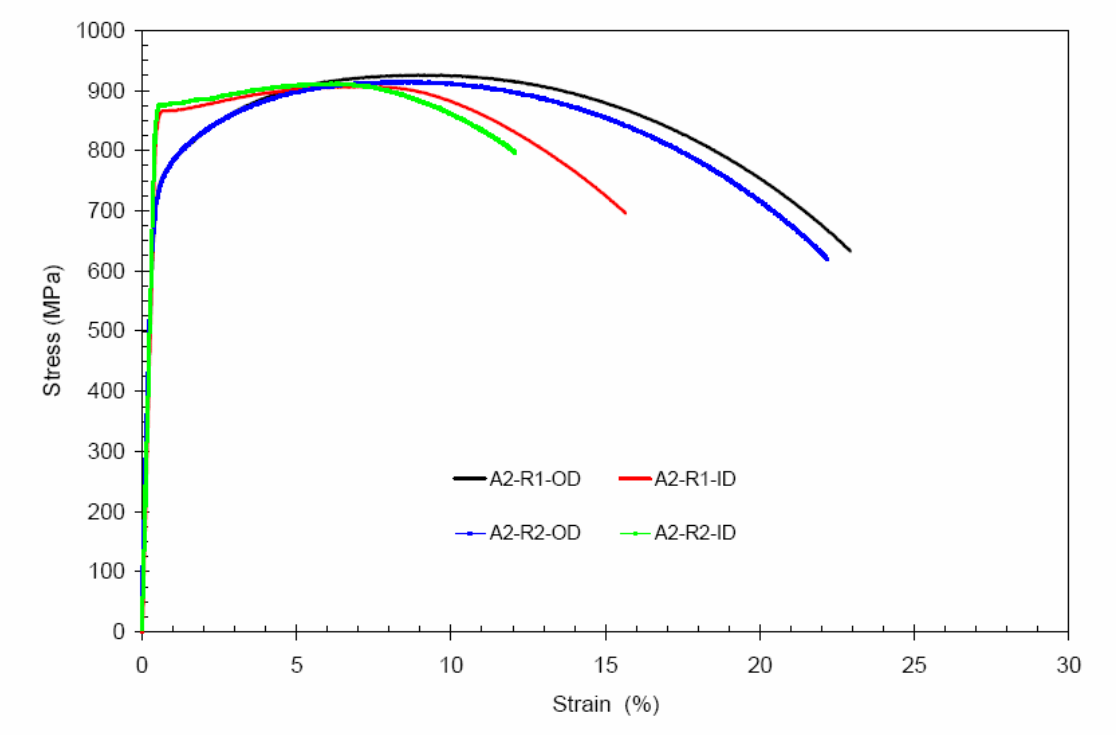

Figure 19. Stress vs. Strain for Chemistry 2 Round Bar Tensile Samples

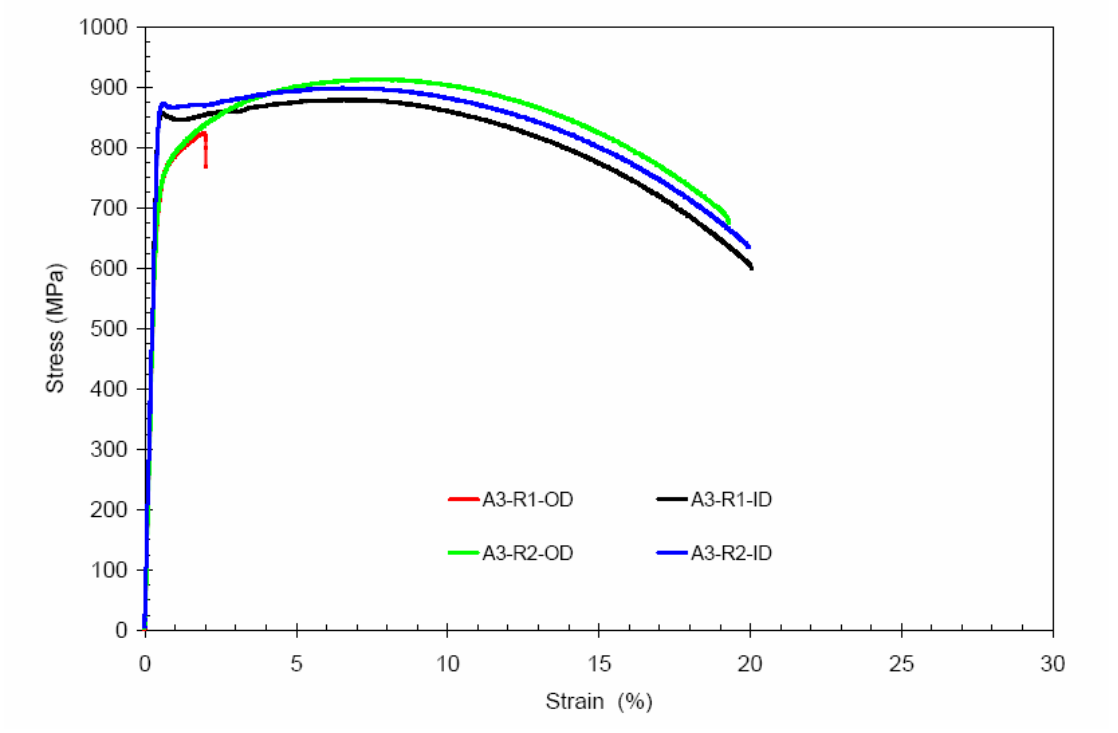

Figure 20. Stress vs. Strain for Chemistry 3 Round Bar Tensile Samples
(*Note:* Sample A3-R1-OD broke outside of gage area.)

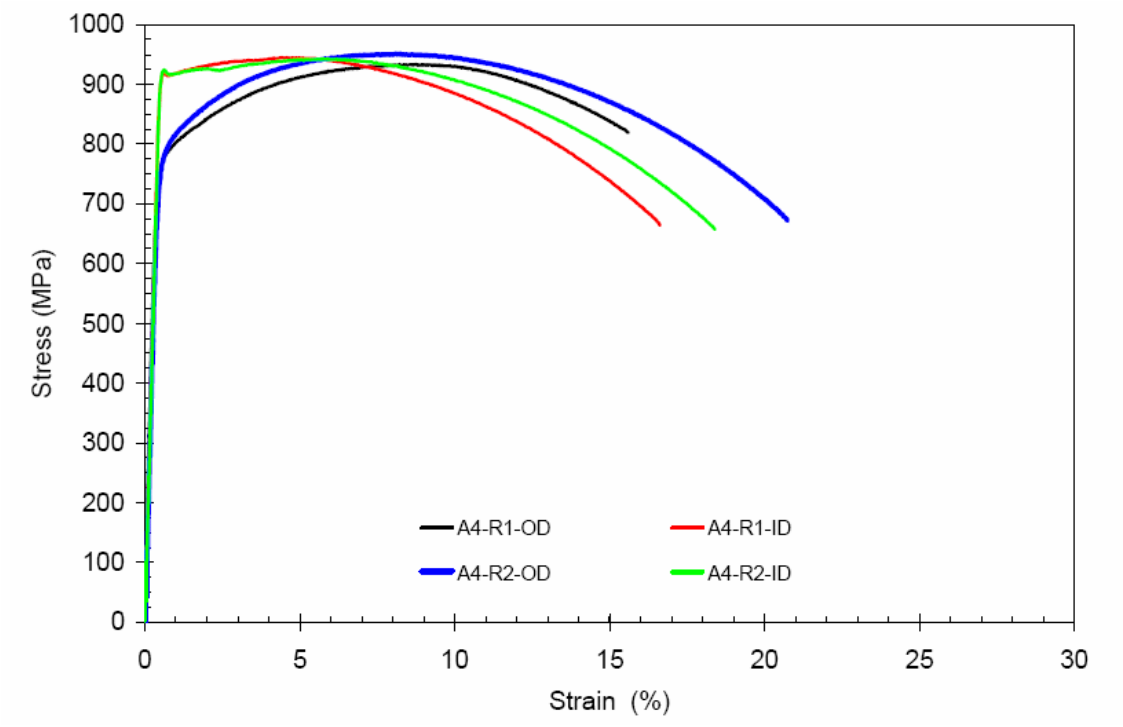

Figure 21. Stress vs. Strain for Chemistry 4 Round Bar Tensile Samples

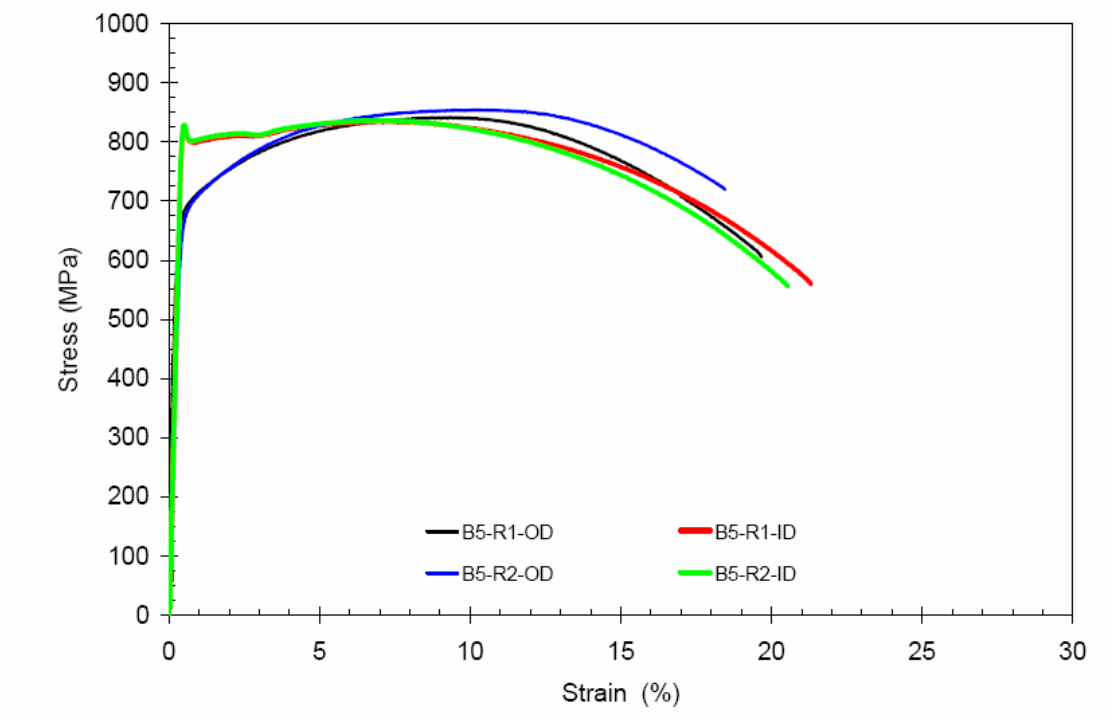

Figure 22. Stress vs. Strain for Chemistry 5 Round Bar Tensile Samples

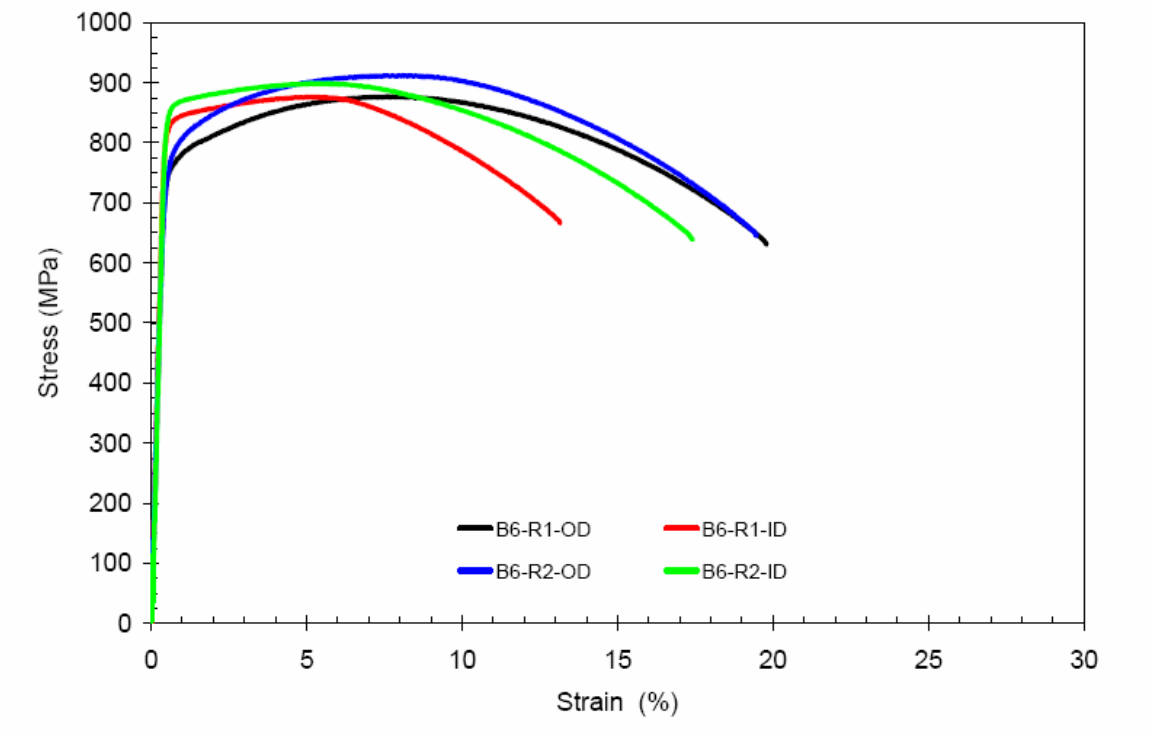

Figure 23. Stress vs. Strain for Chemistry 6 Round Bar Tensile Samples

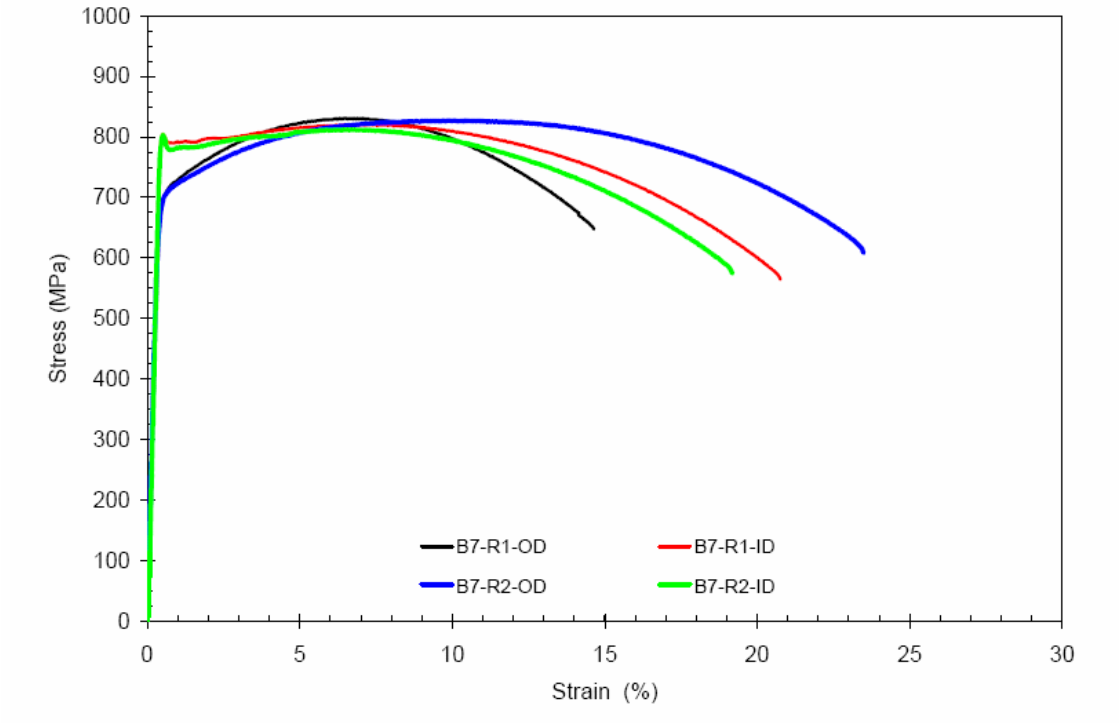

Figure 24. Stress vs. Strain for Chemistry 7 Round Bar Tensile Samples

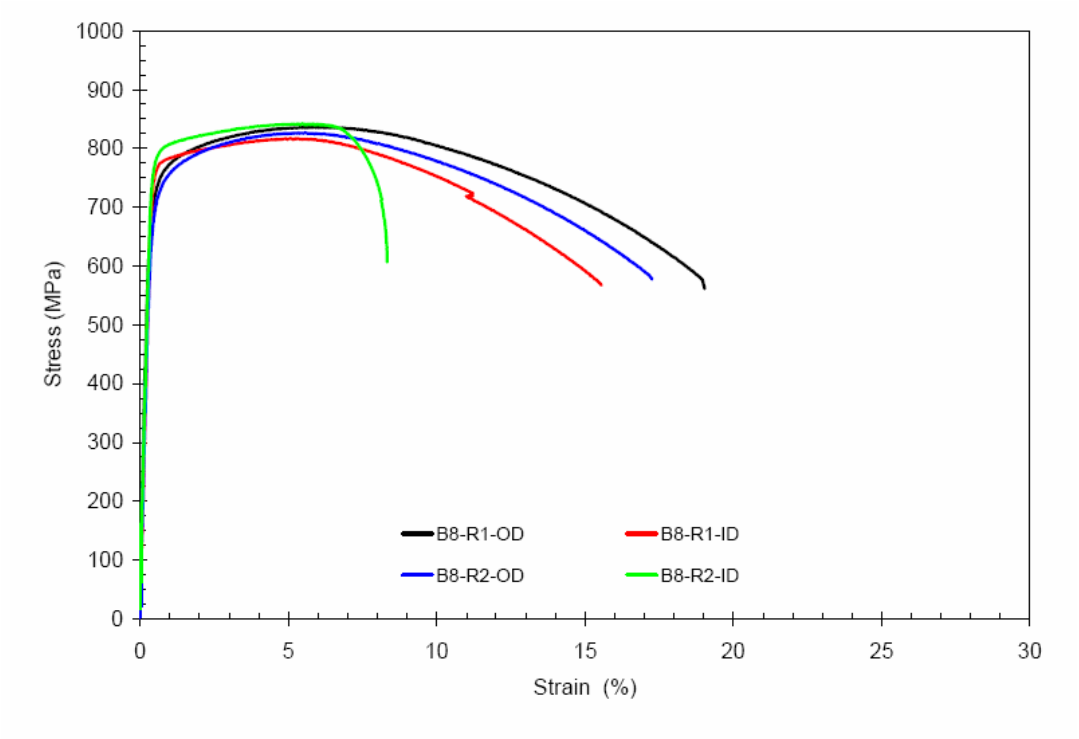

Figure 25. Stress vs. Strain for Chemistry 8 Round Bar Tensile Samples

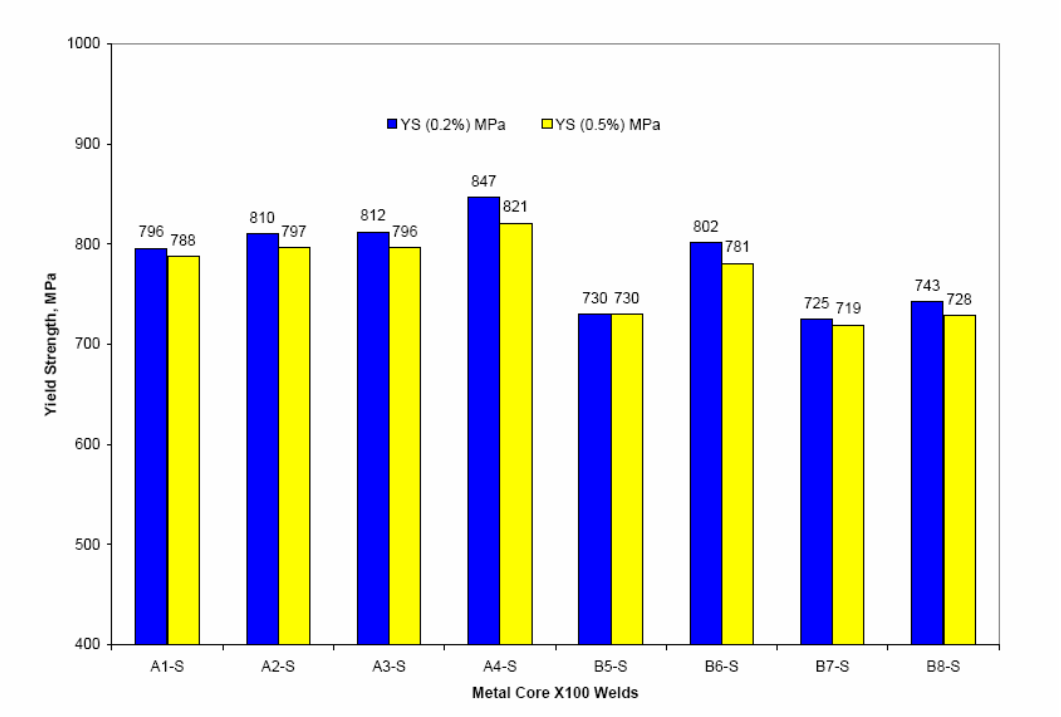

Figure 26. Summary of Strip Tensile Test Results

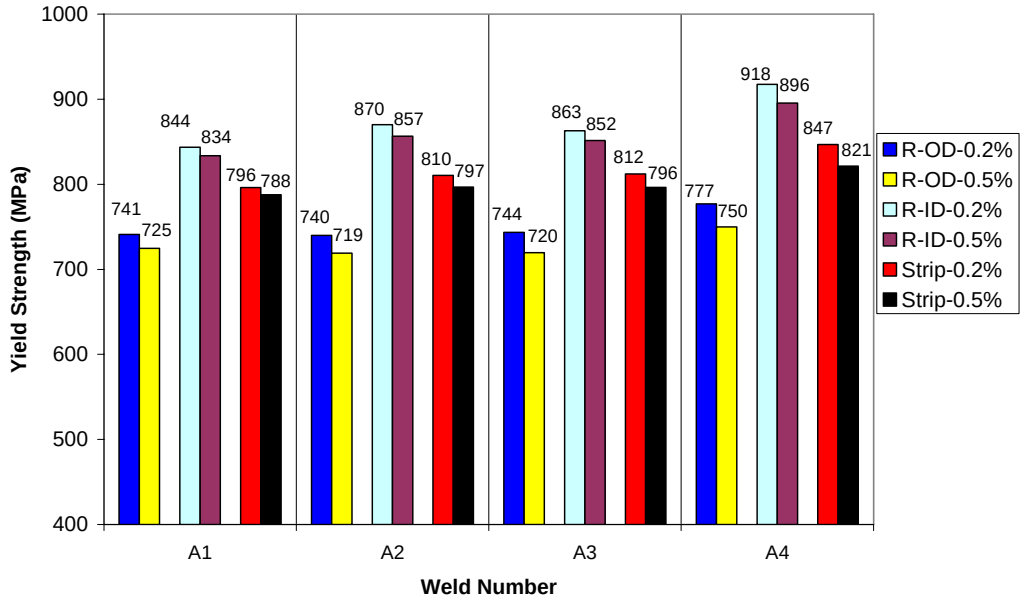

Figure 27. Comparison of Round vs. Strip Tensile Results, Chemistry 1-4

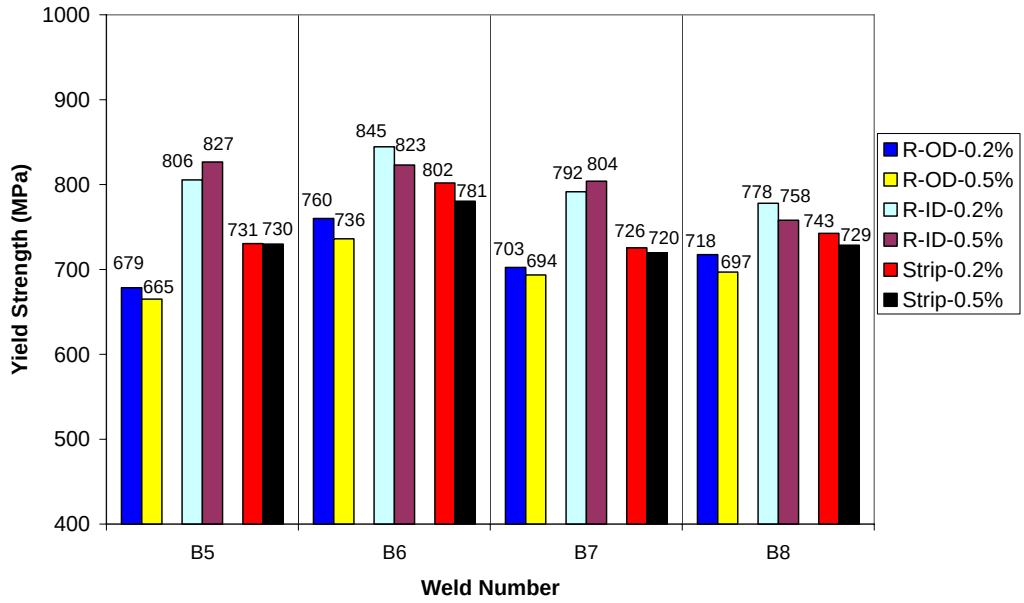

Figure 28. Comparison of Round vs. Strip Tensile Results, Chemistry 5-8

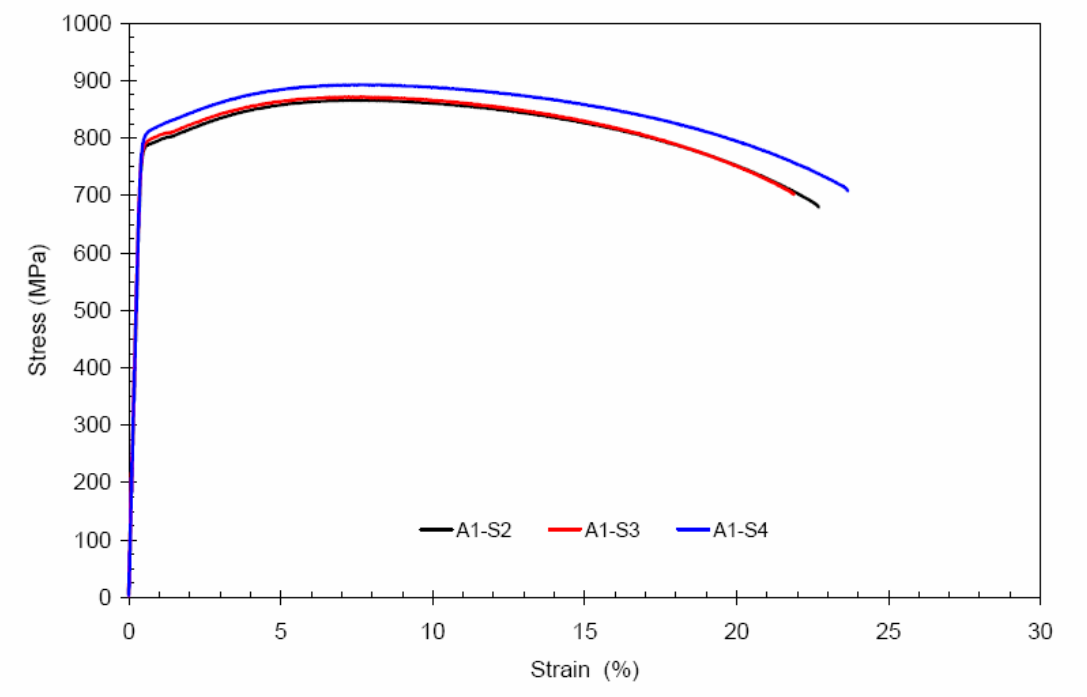

Figure 29. Stress vs. Strain for Chemistry 1 Strip Tensile Samples

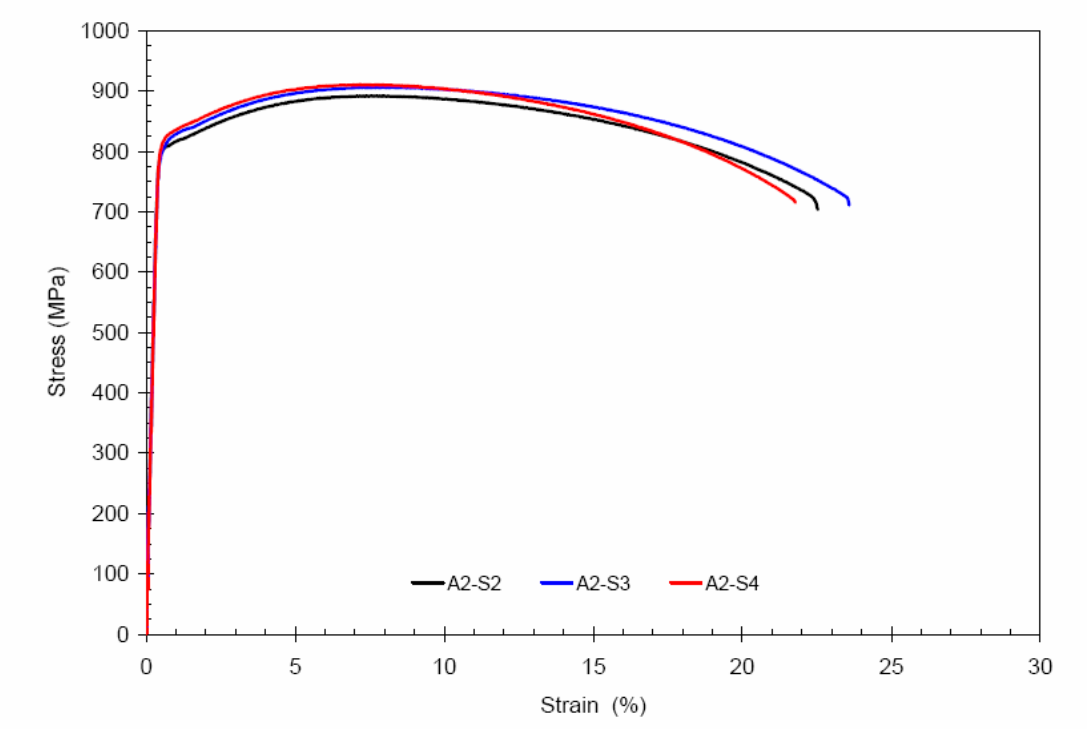

Figure 30. Stress vs. Strain for Chemistry 2 Strip Tensile Samples

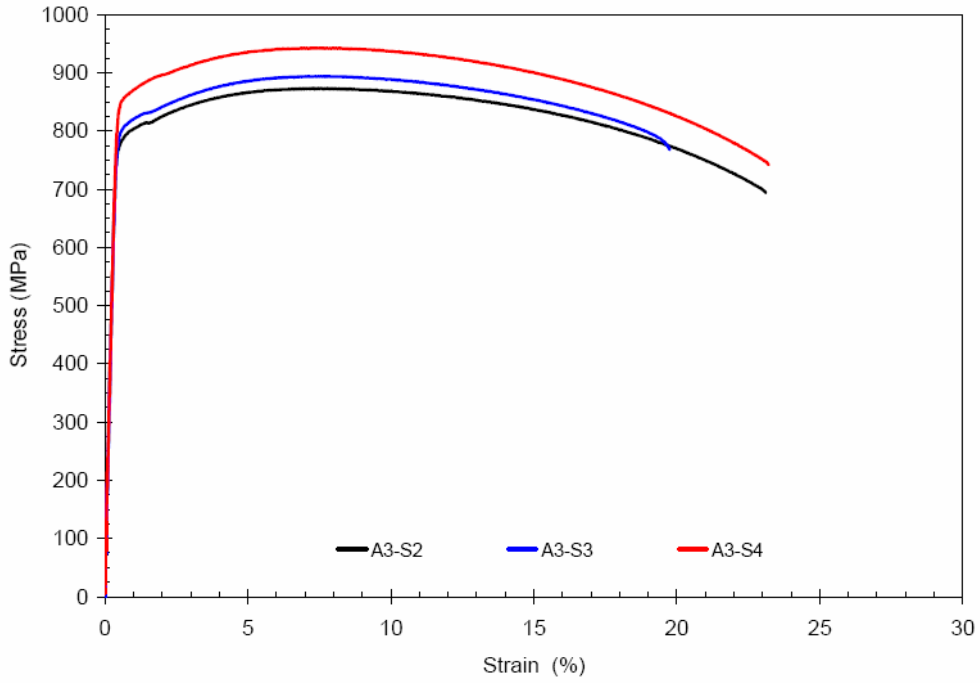

Figure 31. Stress vs. Strain for Chemistry 3 Strip Tensile Samples

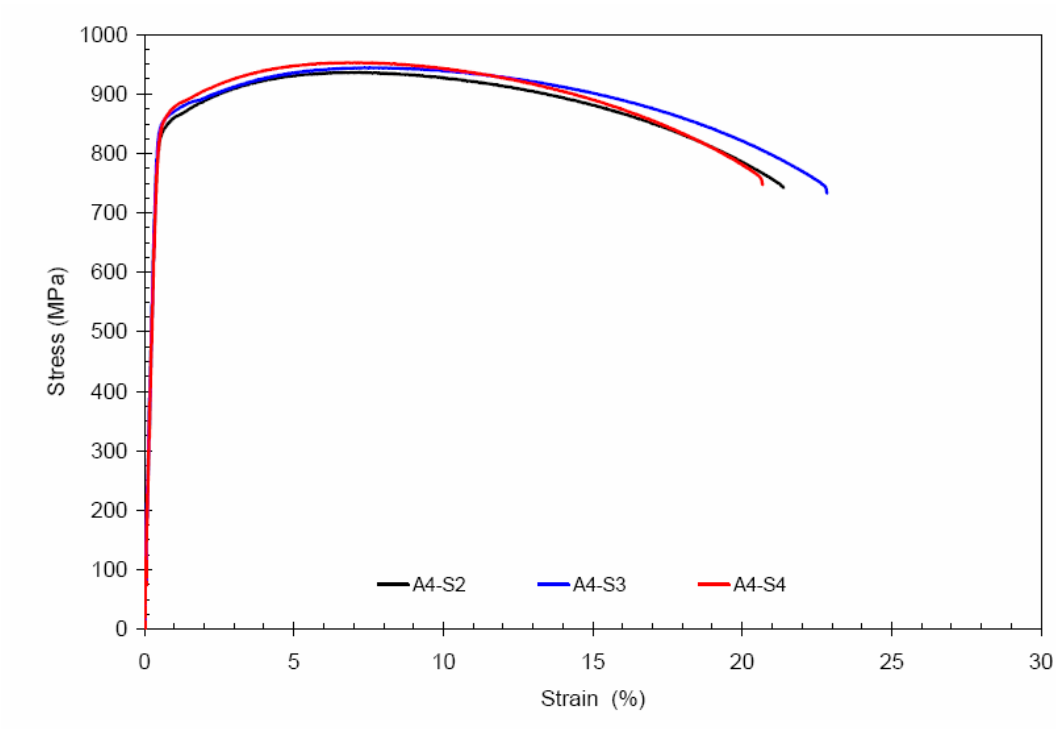

Figure 32. Stress vs. Strain for Chemistry 4 Strip Tensile Samples

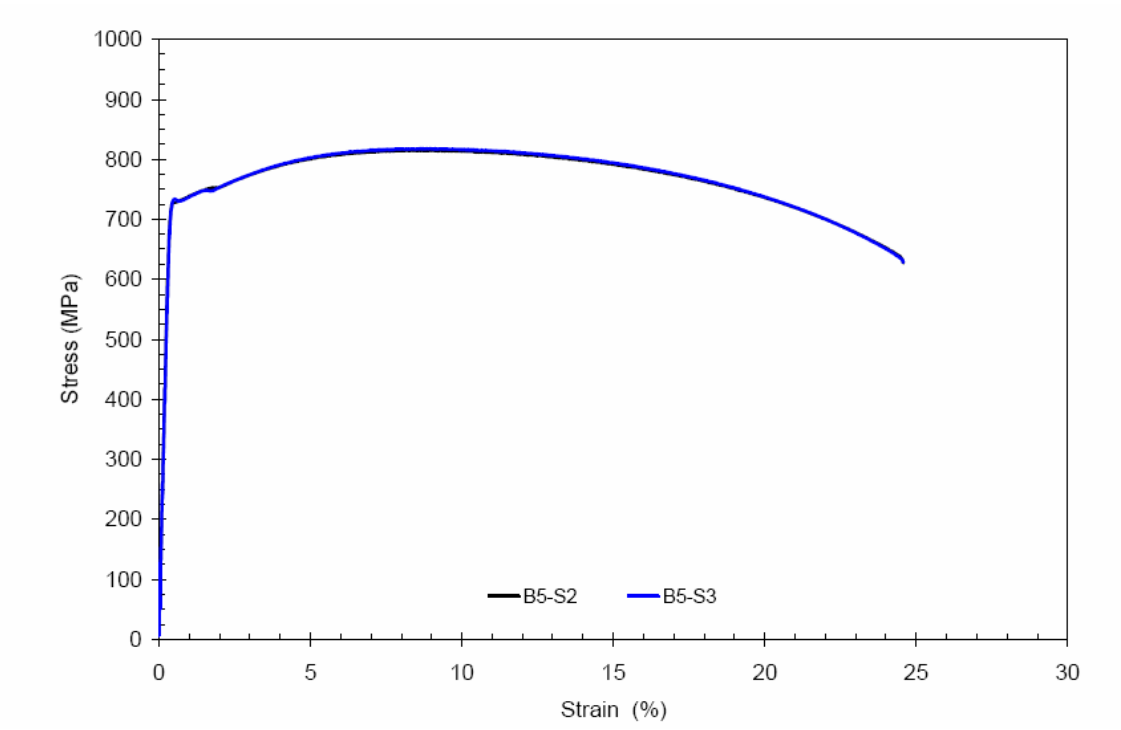

Figure 33. Stress vs. Strain for Chemistry 5 Strip Tensile Samples

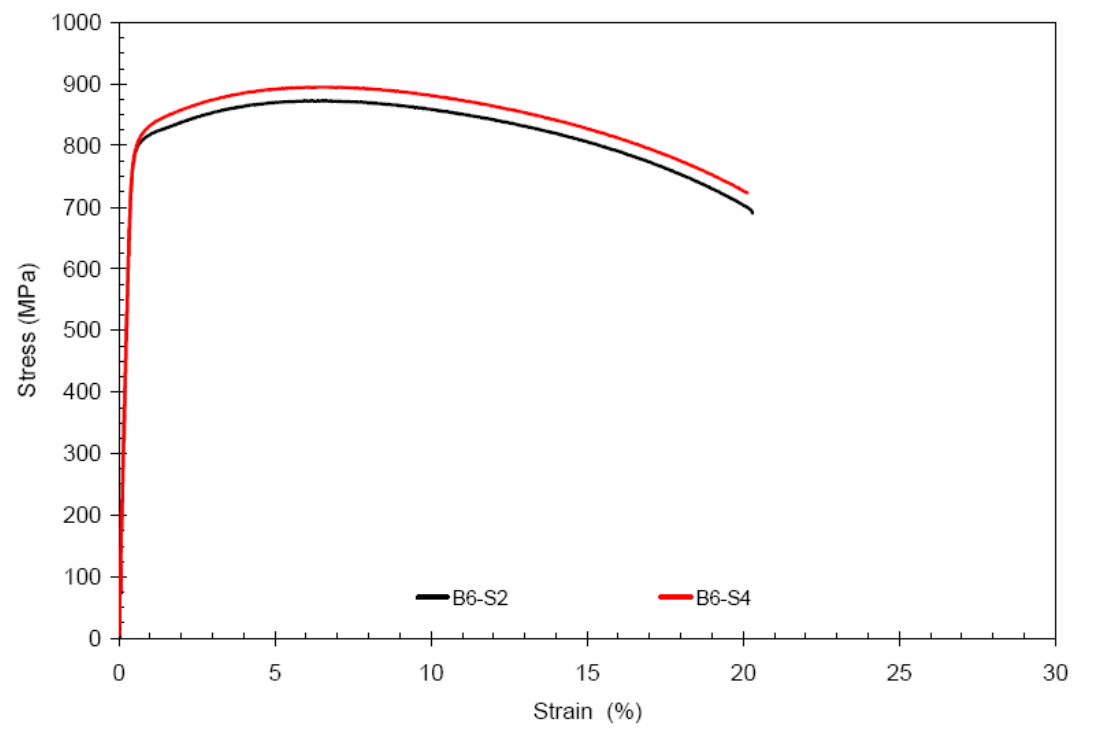

Figure 34. Stress vs. Strain for Chemistry 6 Strip Tensile Samples

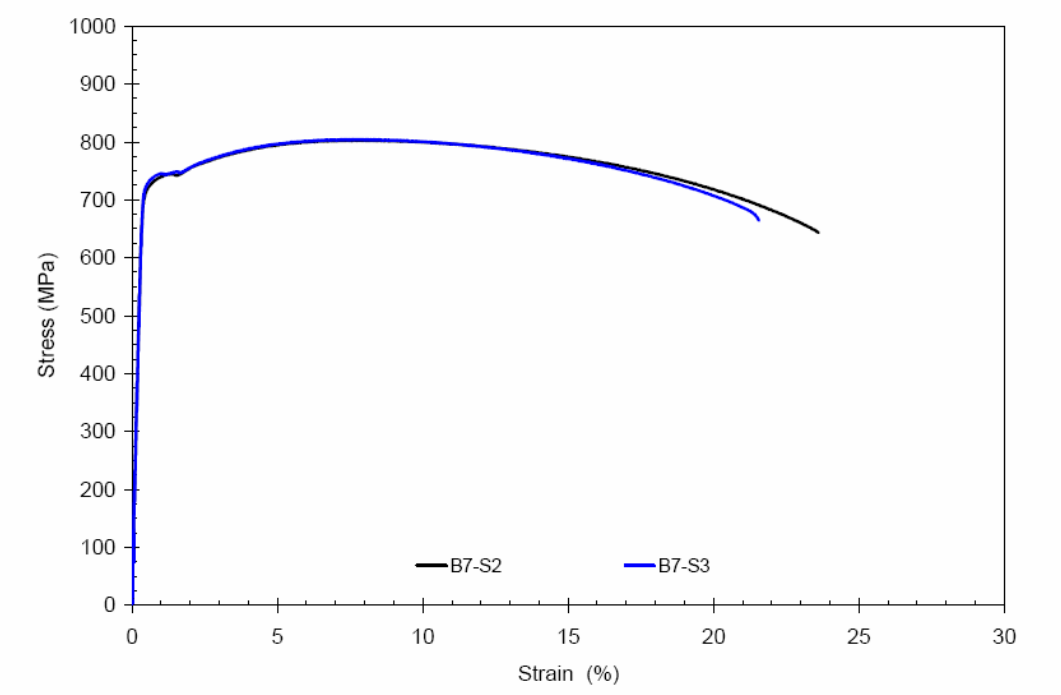

Figure 35. Stress vs. Strain for Chemistry 7 Strip Tensile Samples

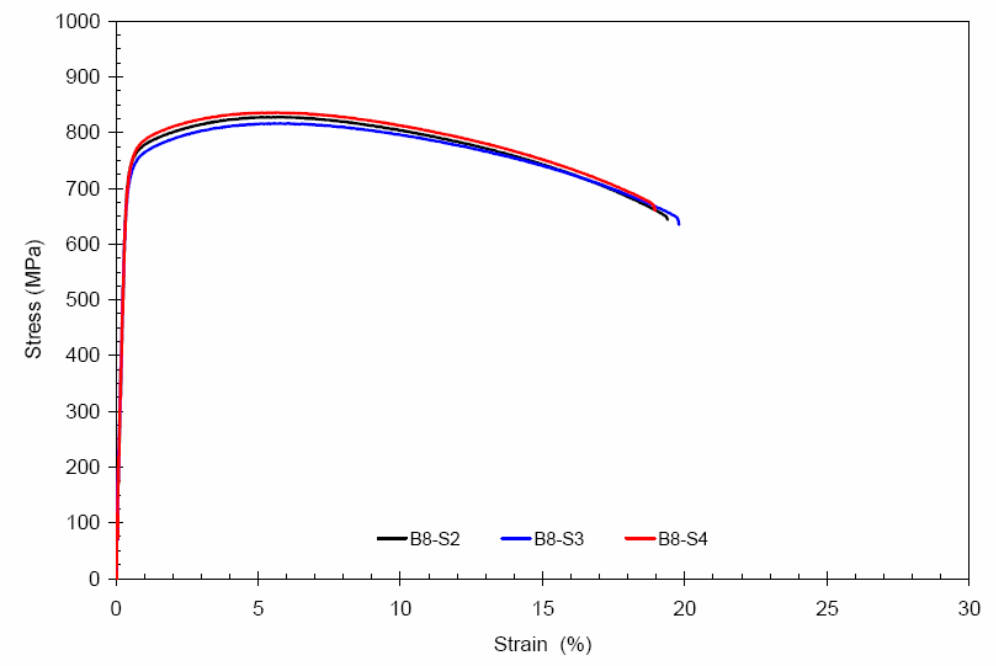

Figure 36. Stress vs. Strain for Chemistry 8 Strip Tensile Samples

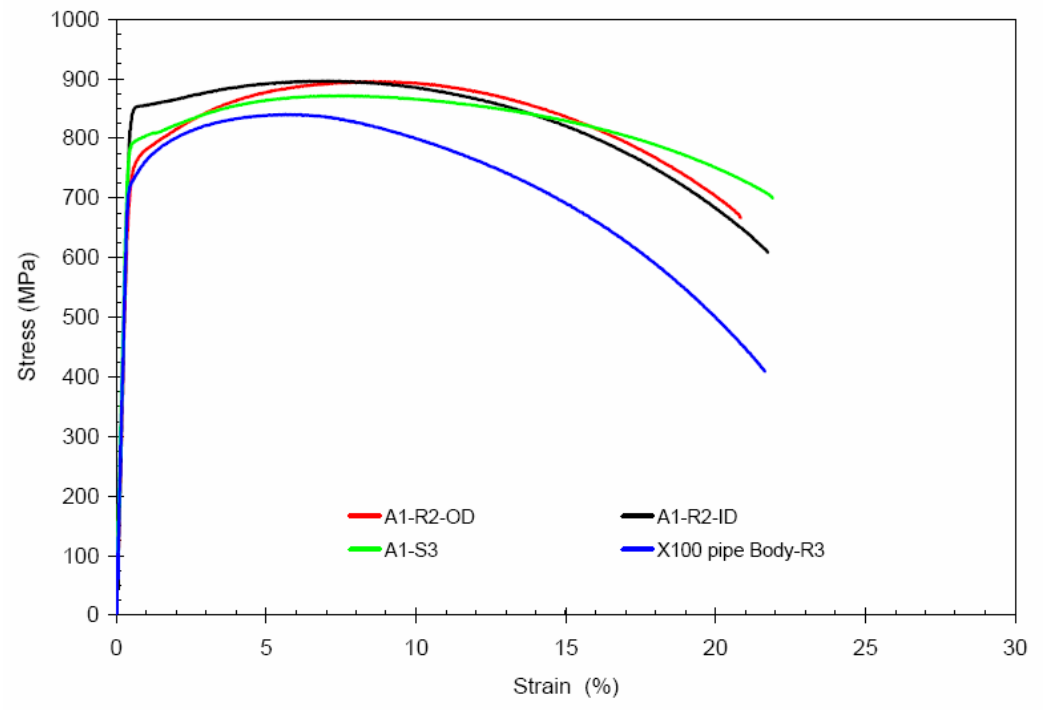

Figure 37. Comparison of Stress/Strain Behavior for Strip vs. Round Tensile Samples, Chemistry 1

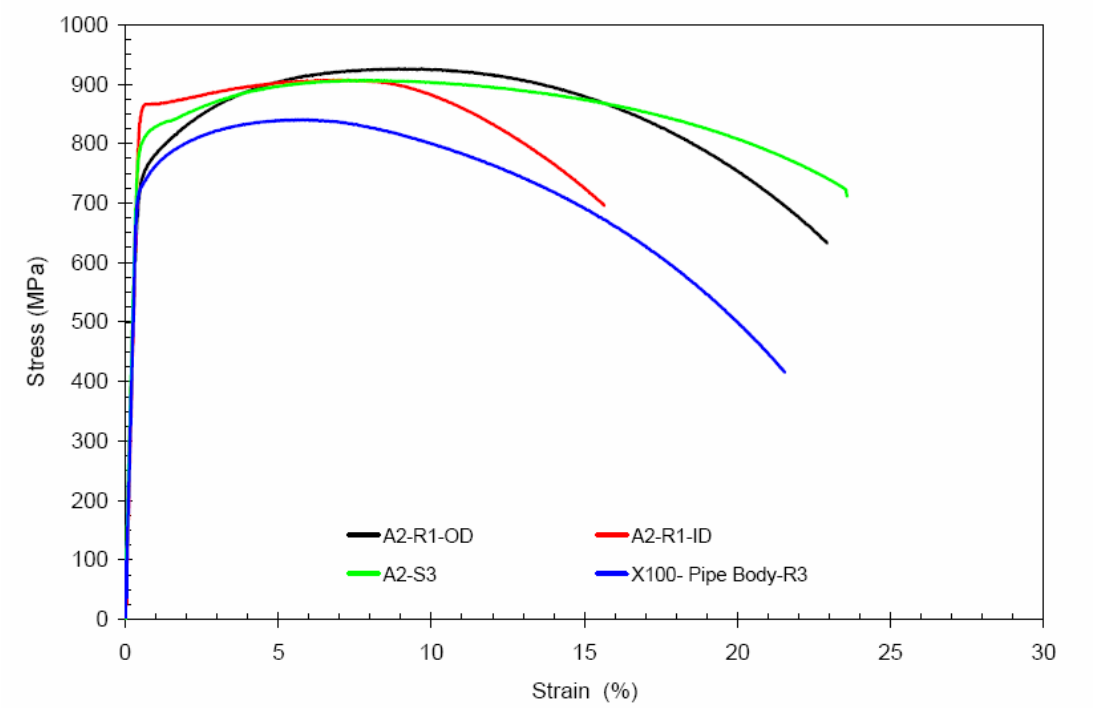

Figure 38. Comparison of Stress/Strain Behavior for Strip vs. Round Tensile Samples, Chemistry 2

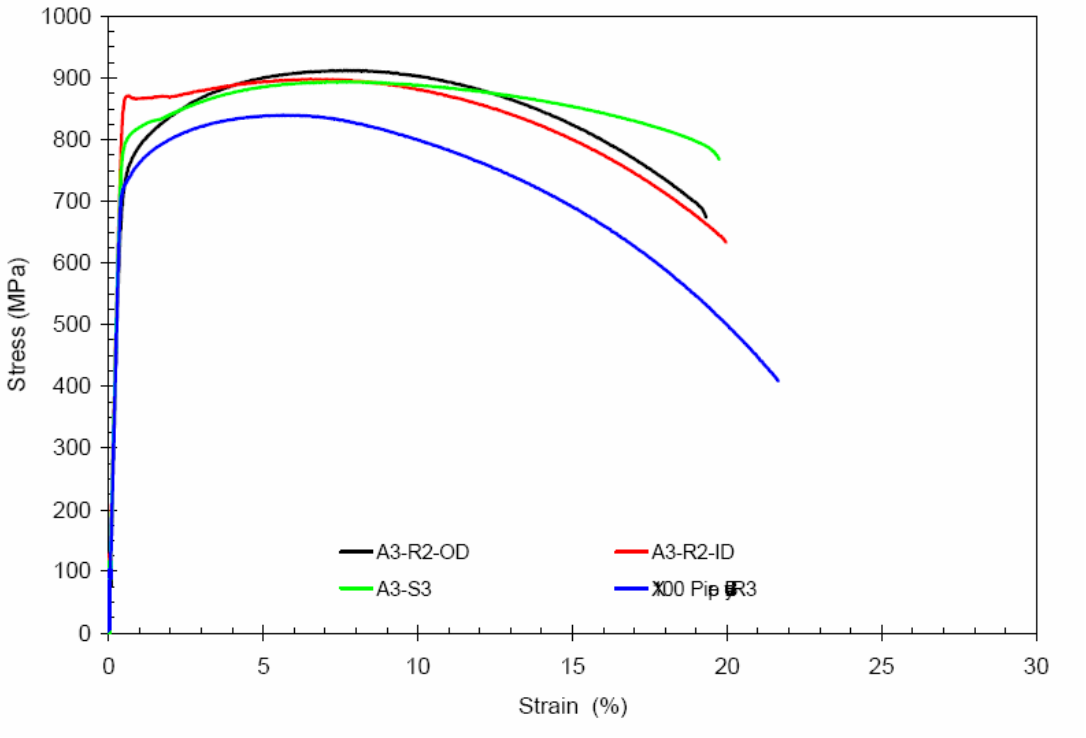

Figure 39. Comparison of Stress/Strain Behavior for Strip vs. Round Tensile Samples, Chemistry 3

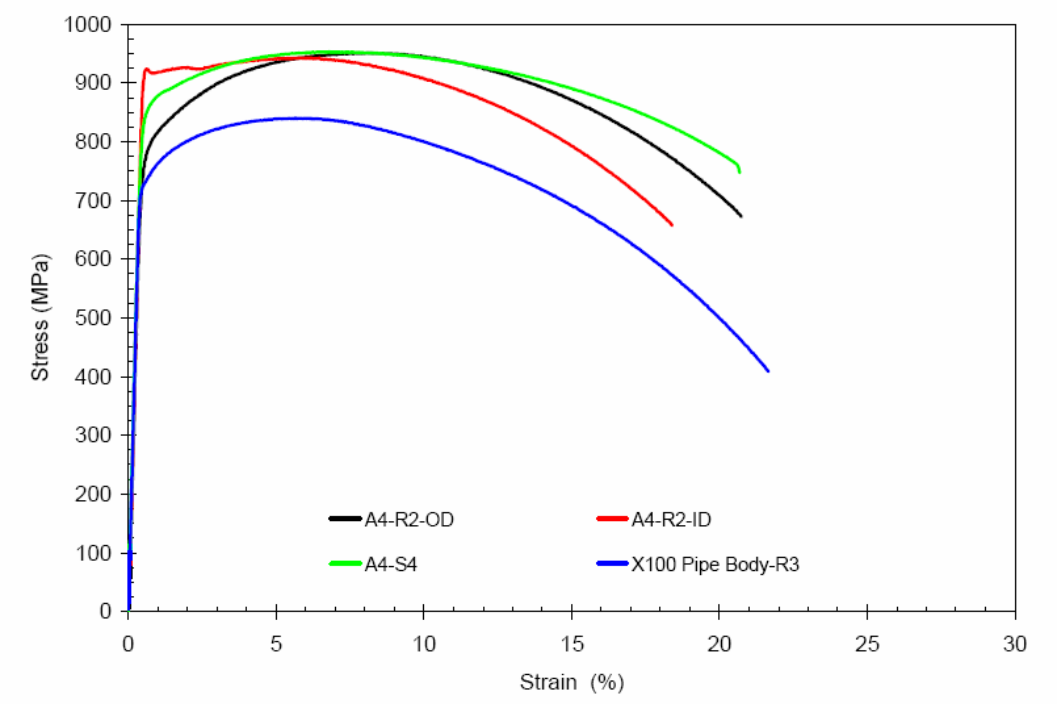

Figure 40. Comparison of Stress/Strain Behavior for Strip vs. Round Tensile Samples, Chemistry 4

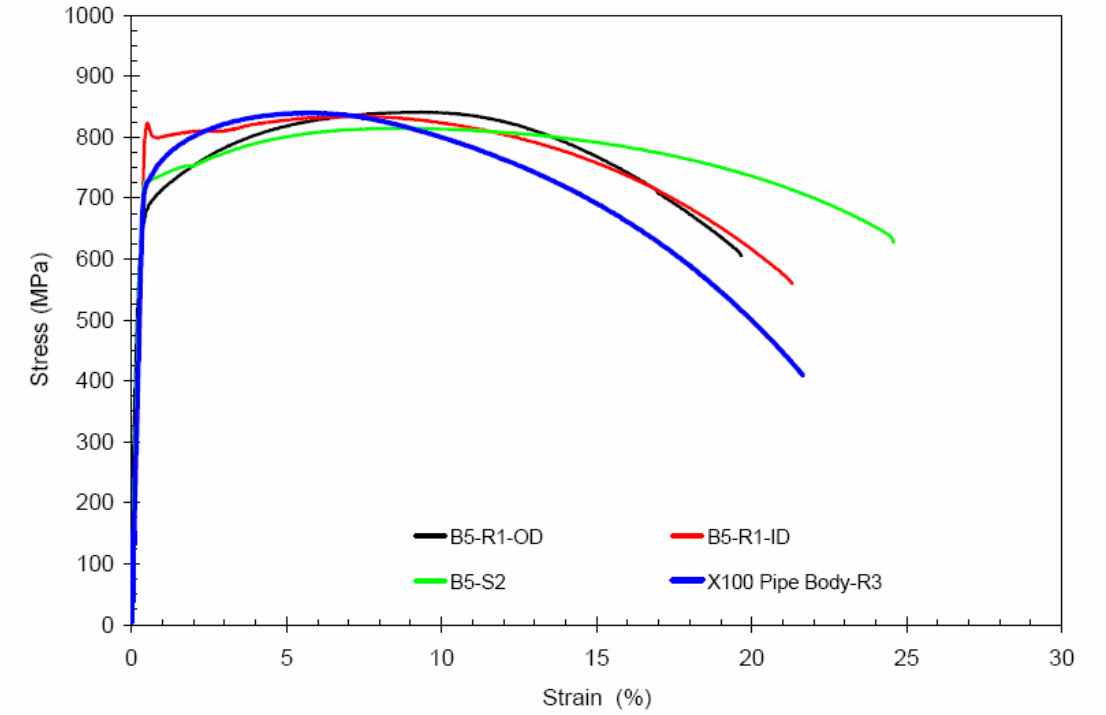

Figure 41. Comparison of Stress/Strain Behavior for Strip vs. Round Tensile Samples, Chemistry 5

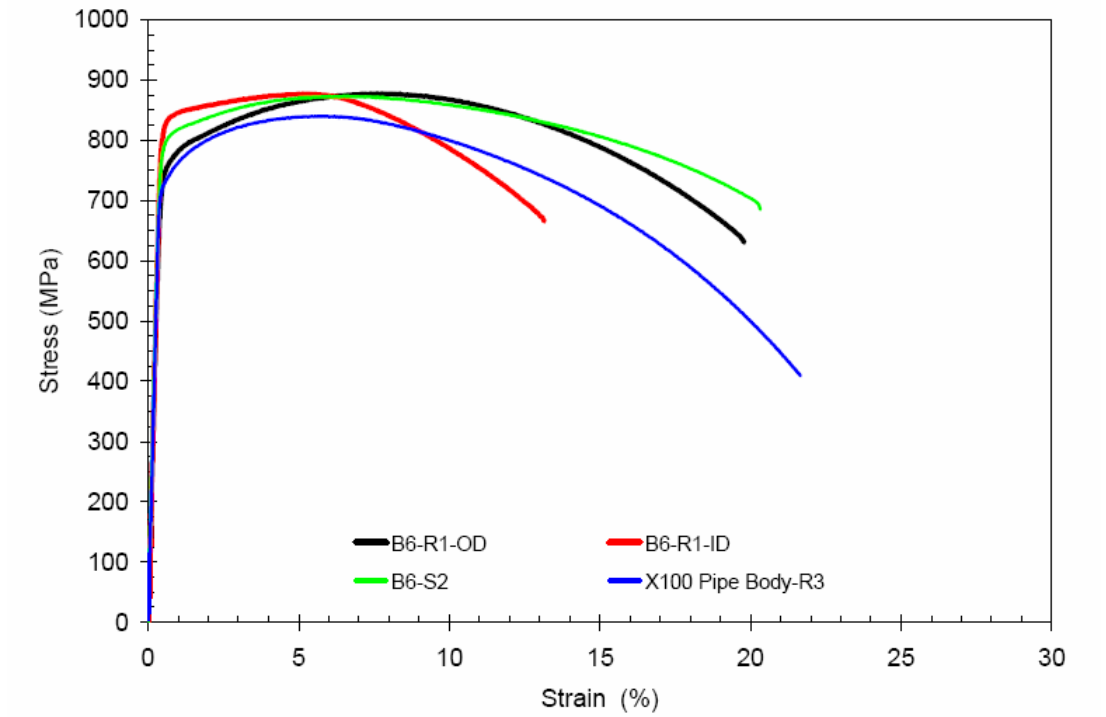

Figure 42. Comparison of Stress/Strain Behavior for Strip vs. Round Tensile Samples, Chemistry 6

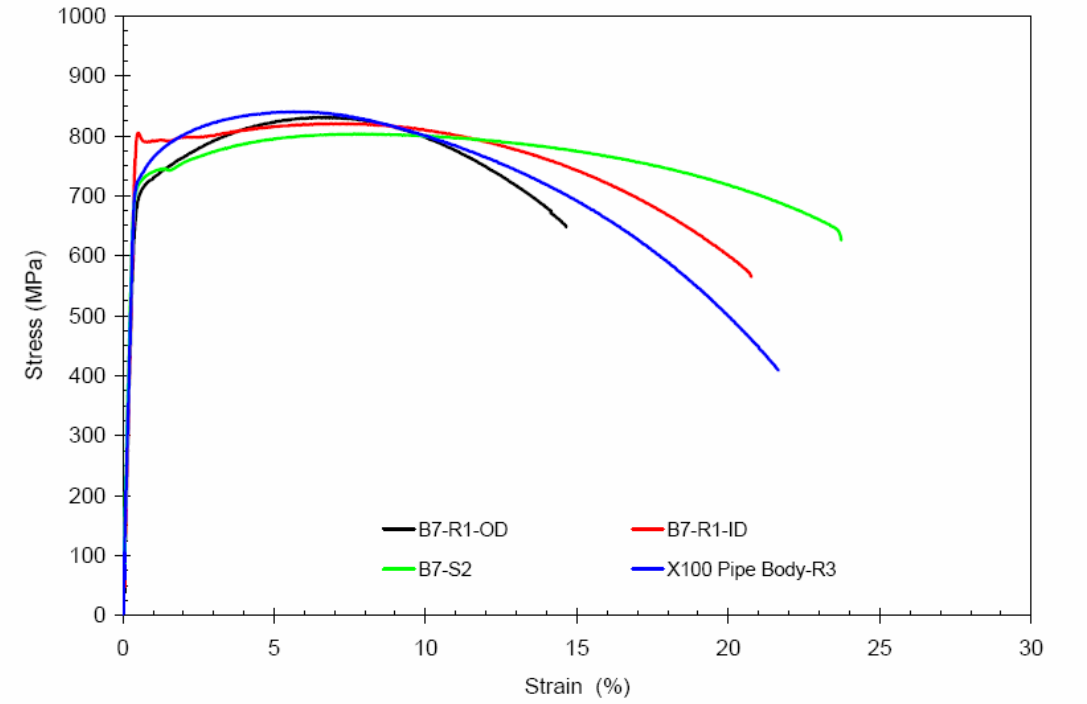

Figure 43. Comparison of Stress/Strain Behavior for Strip vs. Round Tensile Samples, Chemistry 7

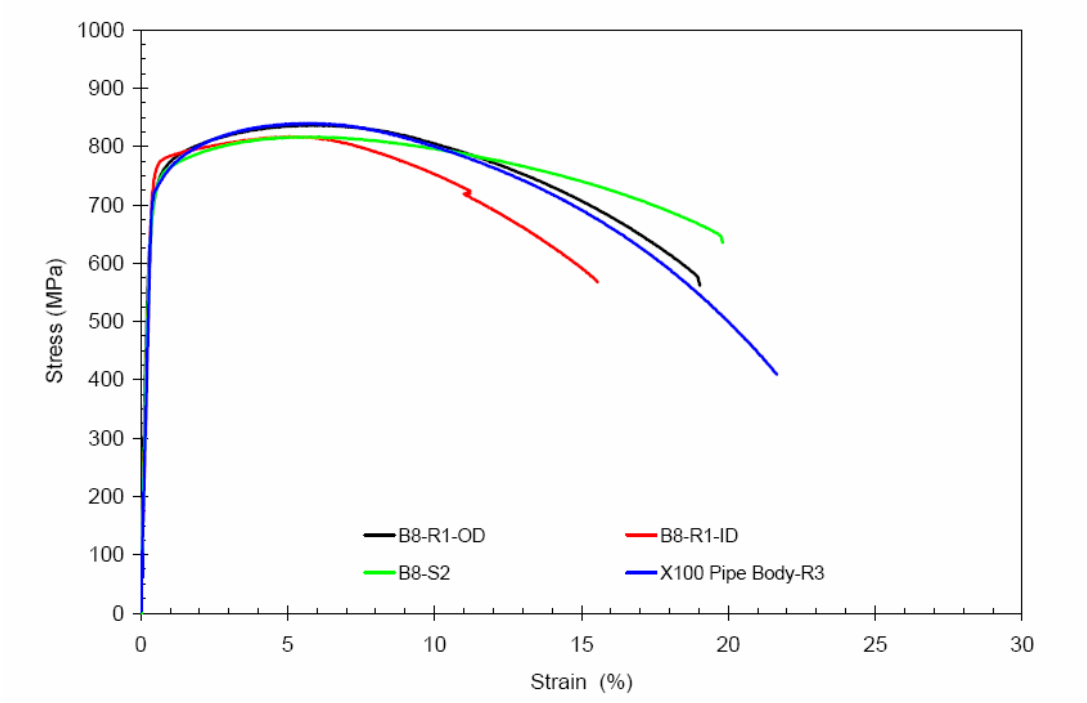

Figure 44. Comparison of Stress/Strain Behavior for Strip vs. Round Tensile Samples, Chemistry 8

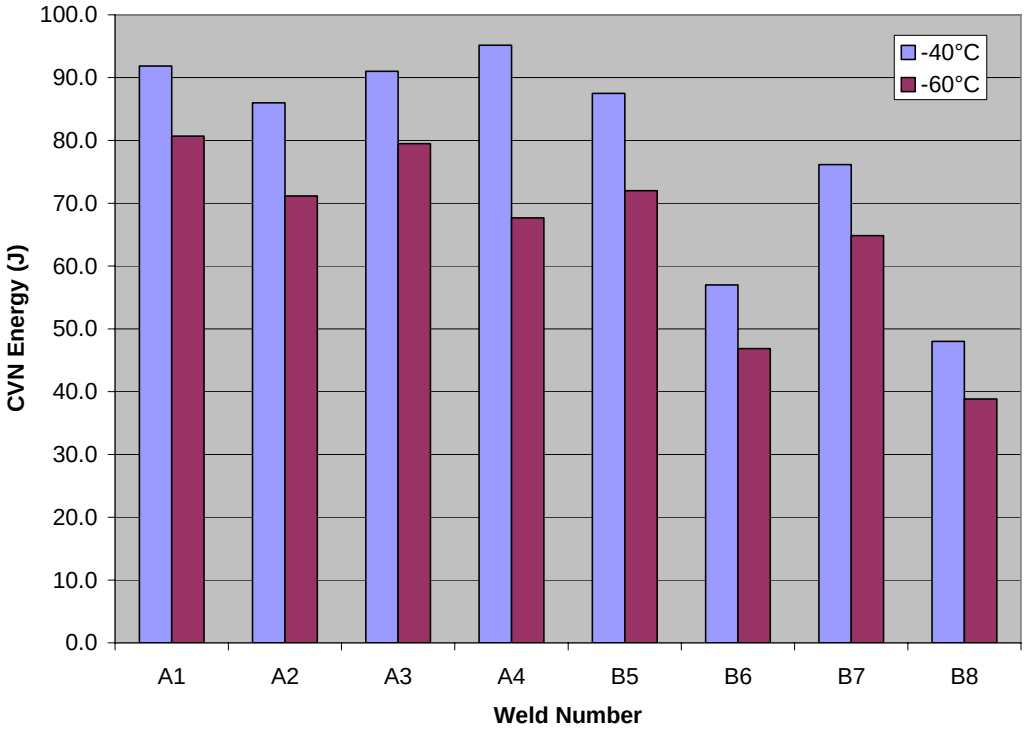

Figure 45. Summary of CVN Energy Data

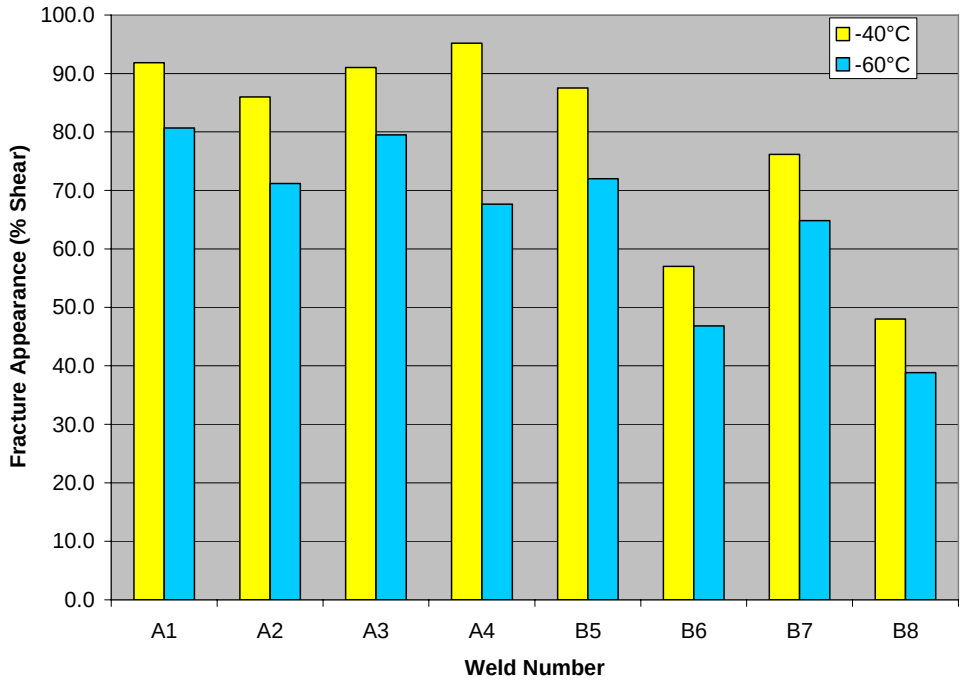

Figure 46. Summary of CVN Fracture Appearance Data

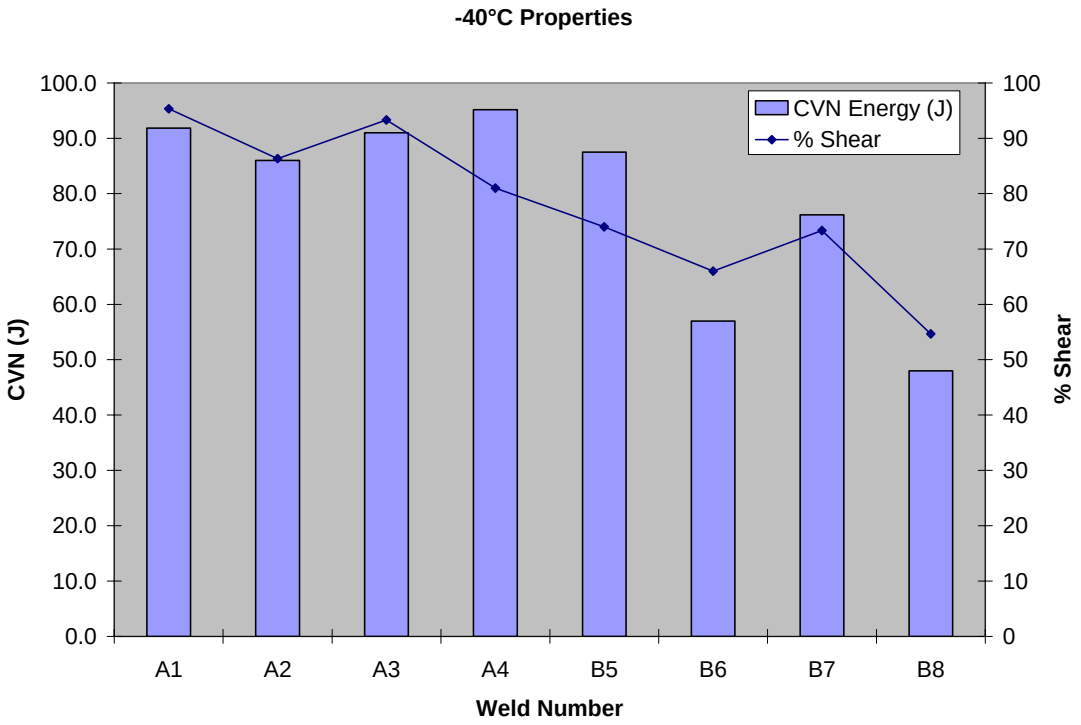

Figure 47. CVN Properties at -40°C

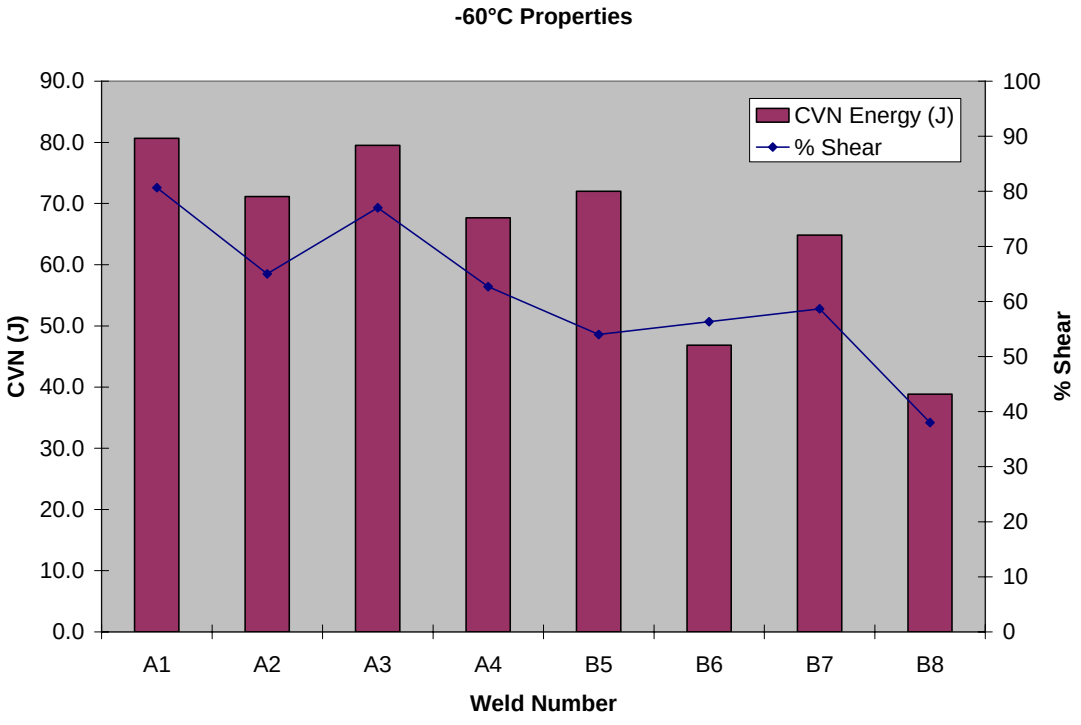

Figure 48. CVN Properties at -60°C

Figure 49. Samples A1-1, A1-2 and A1-3, tested at -40°C

Figure 50. Samples A1-4, A1-5 and A1-6, Tested at -60°C

Figure 51. Samples A2-1, A2-2 and A2-3, Tested at -40°C

Figure 52. Samples A2-4, A2-5 and A2-6, Tested at -60°C

Figure 53. Samples A3-1, A3-2 and A3-3, Tested at -40°C

Figure 54. Samples A3-4, A3-5 and A3-6, Tested at -60°C

Figure 55. Samples A4-1, A4-2 and A4-3, Tested at -40°C

Figure 56. Samples A4-4, A4-5 and A4-6, Tested at -60°C

Figure 57. Samples B5-1, B5-2 and B5-3, Tested at -40°C

Figure 58. Samples B5-4, B5-5 and B5-6, tested at -60°C

Figure 59. Samples B6-1, B6-2 and B6-3, Tested at -40°C

Figure 60. Samples B6-4, B6-5 and B6-6, Tested at -60°C

Figure 61. Samples B7-1, B7-2 and B7-3, Tested at -40°C

Figure 62. Samples B7-4, B7-5 and B7-6, Tested at -60°C

Figure 63. Samples B8-1, B8-2 and B8-3, Tested at -40°C

Figure 64. Samples B8-4, B8-5 and B8-6, Tested at -60°C

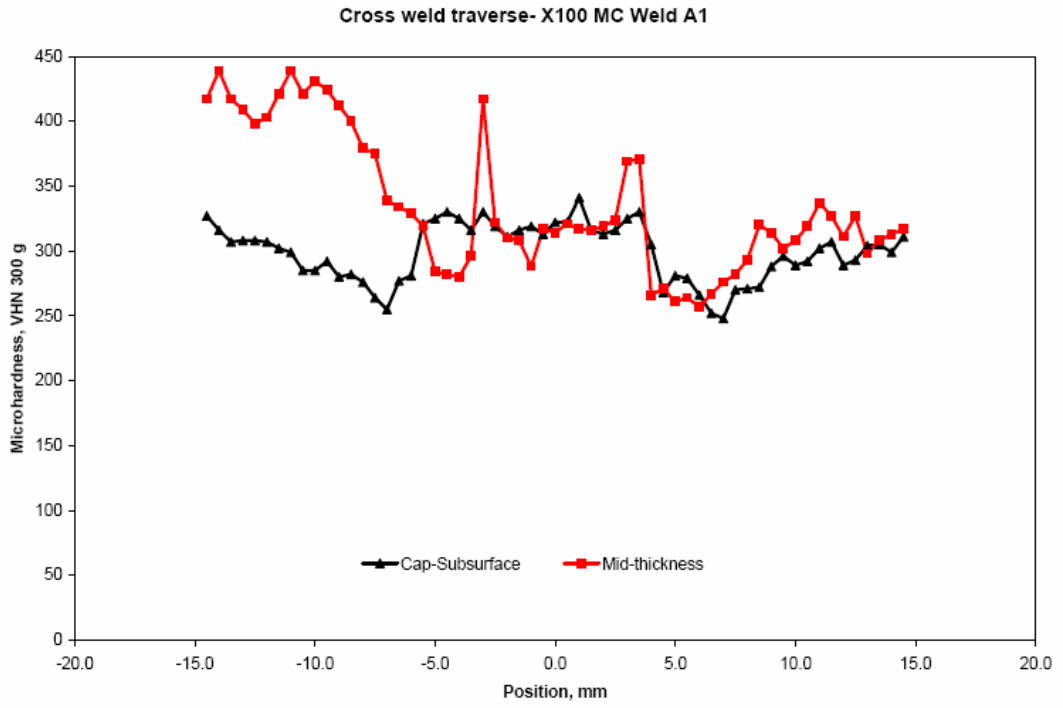

Figure 65. Microhardness Traverse, Weld A1

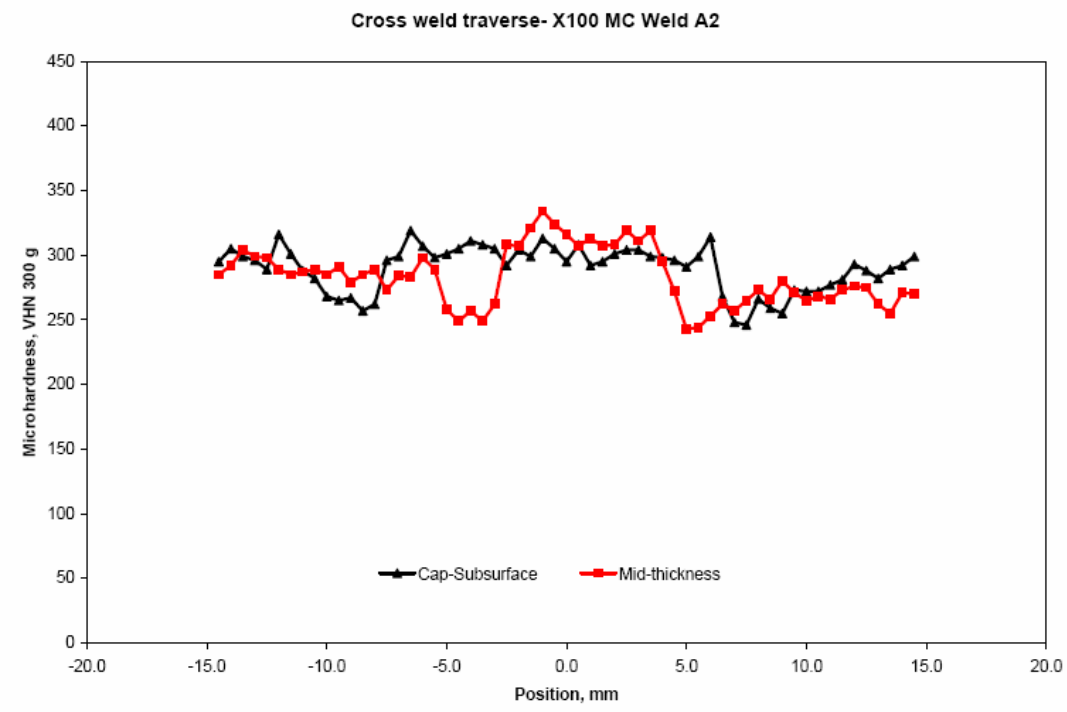

Figure 66. Microhardness Traverse, Weld A2

Figure 67. Microhardness Traverse, Weld A3

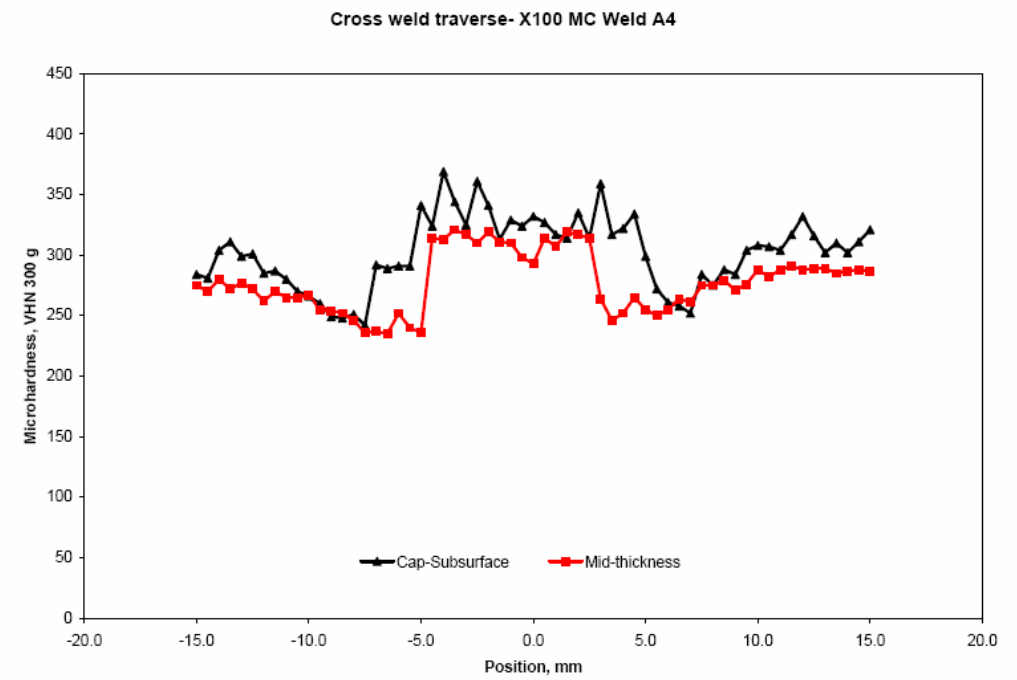

Figure 68. Microhardness Traverse, Weld A4

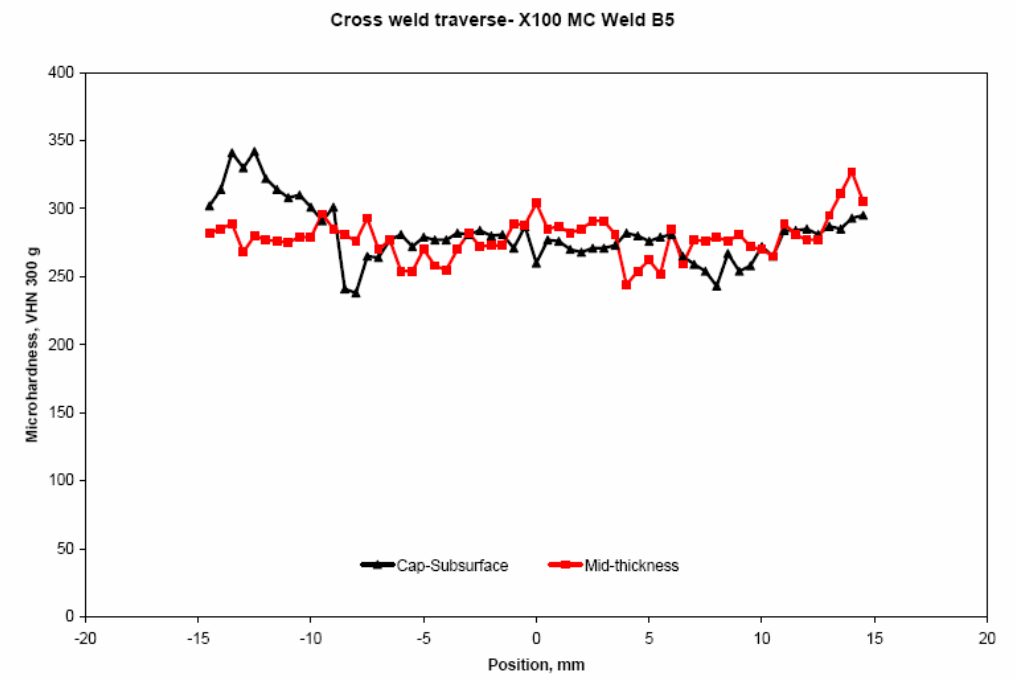

Figure 69. Microhardness Traverse, Weld B5

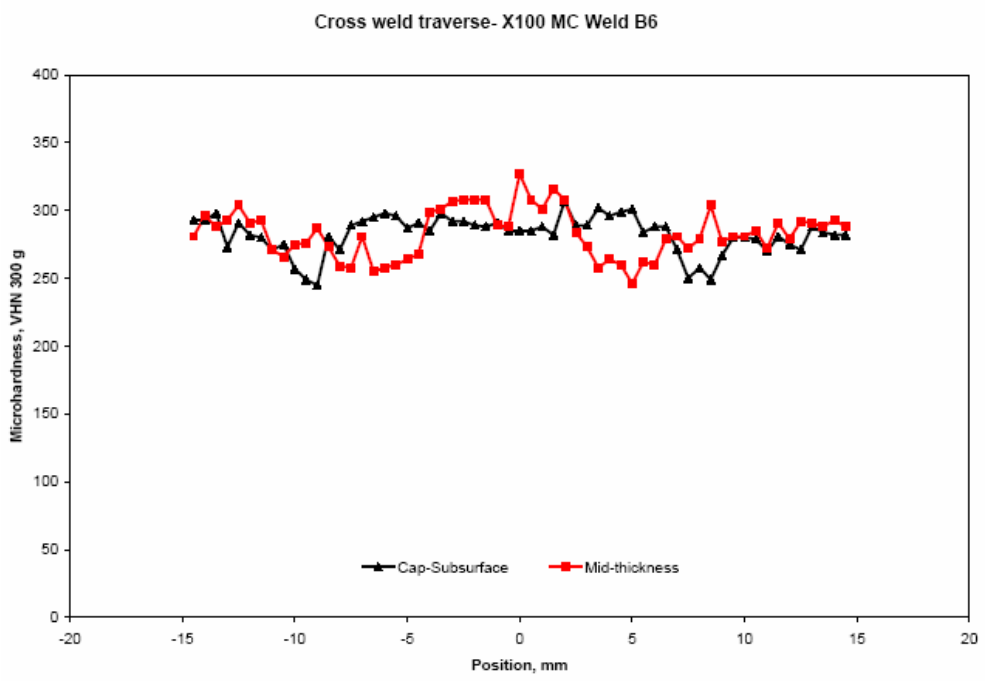

Figure 70. Microhardness Traverse, Weld B6

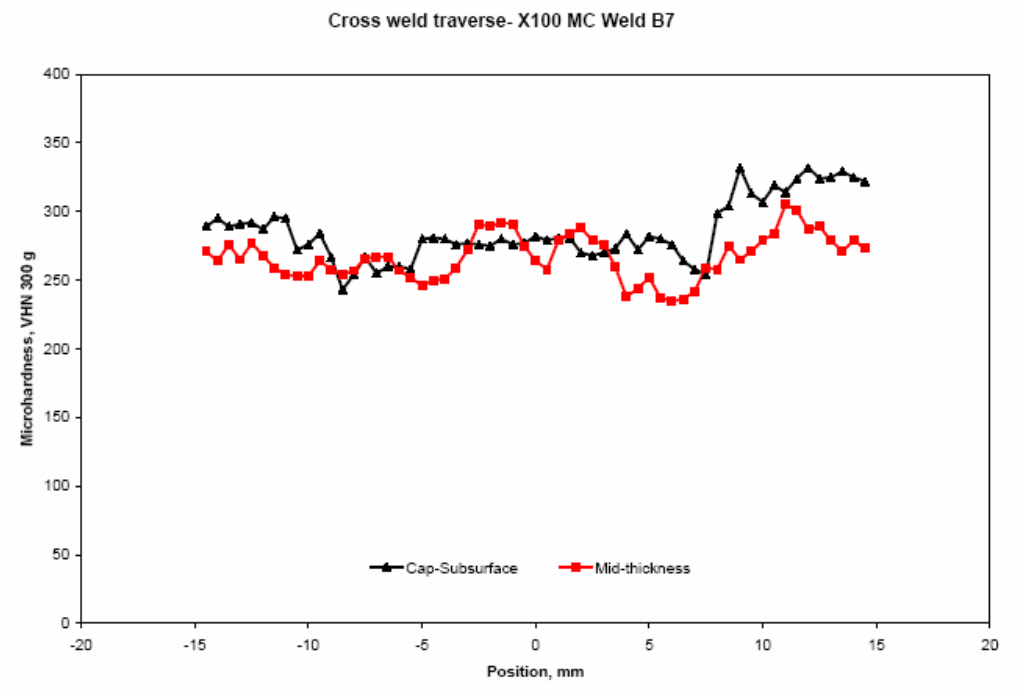

Figure 71. Microhardness Traverse, Weld B7

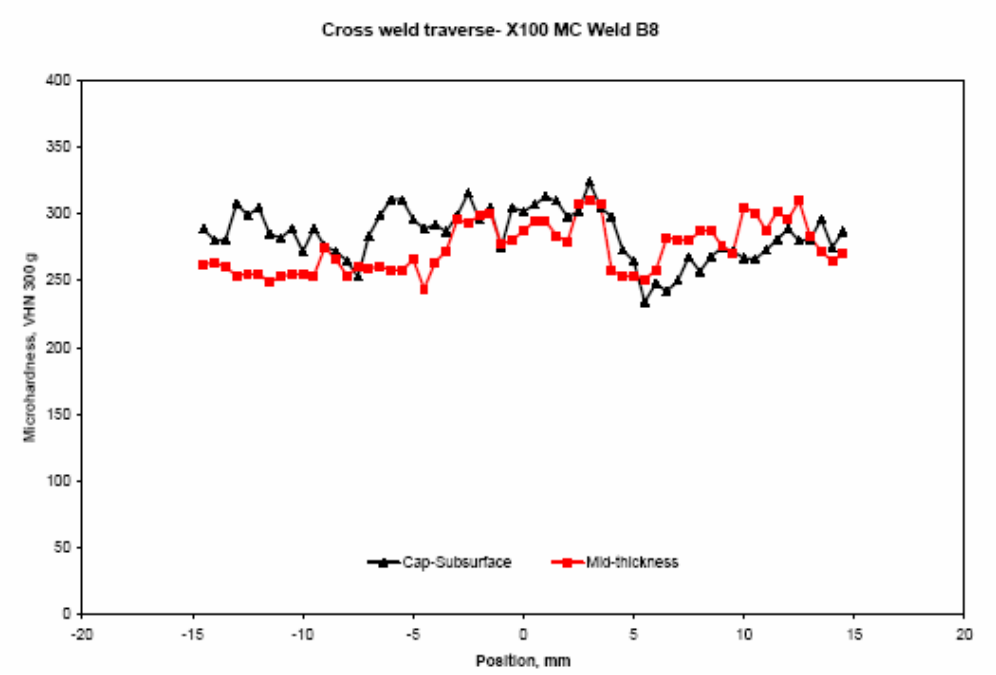

Figure 72. Microhardness Traverse, Weld B8

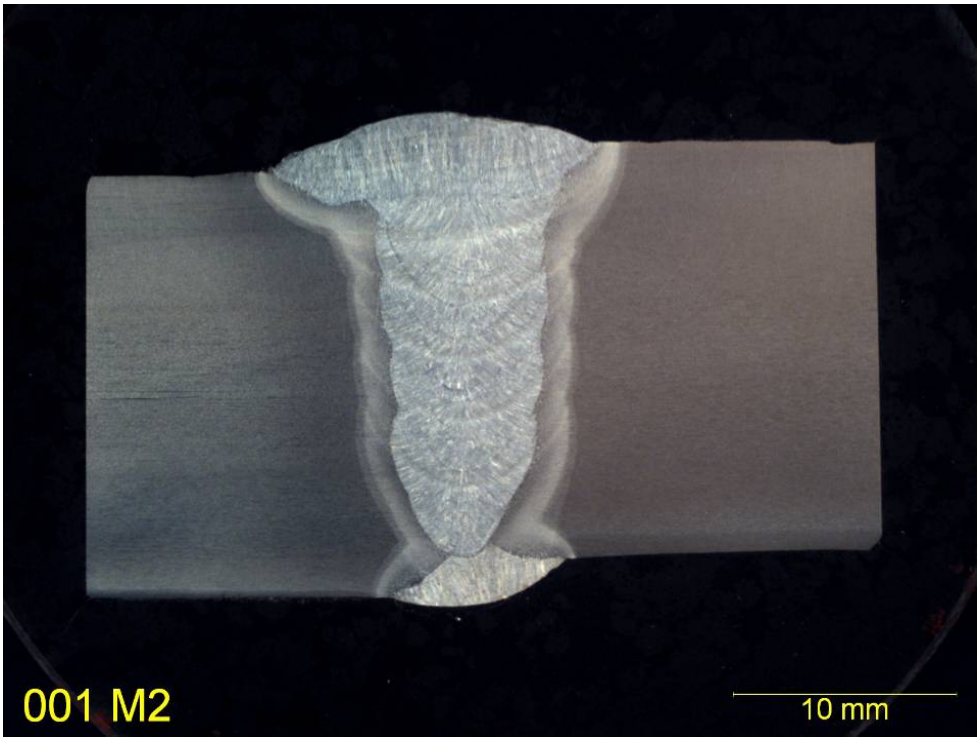

Figure 73. Photo-macrograph Showing Cross-section of Weld A1

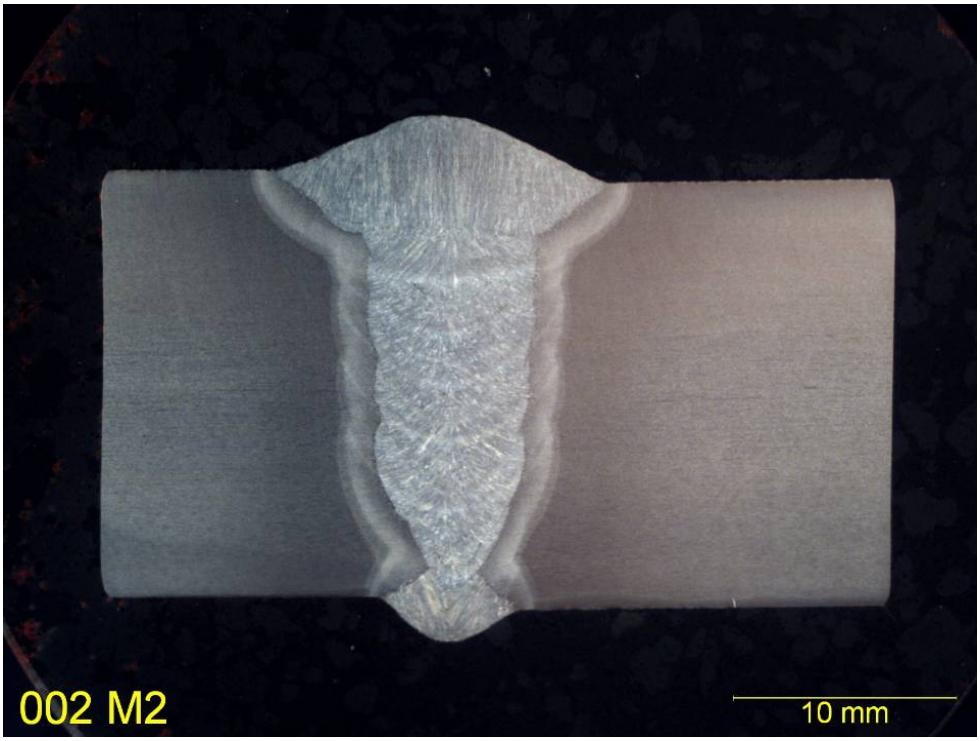

Figure 74. Photo-macrograph Showing Cross-section of Weld A2

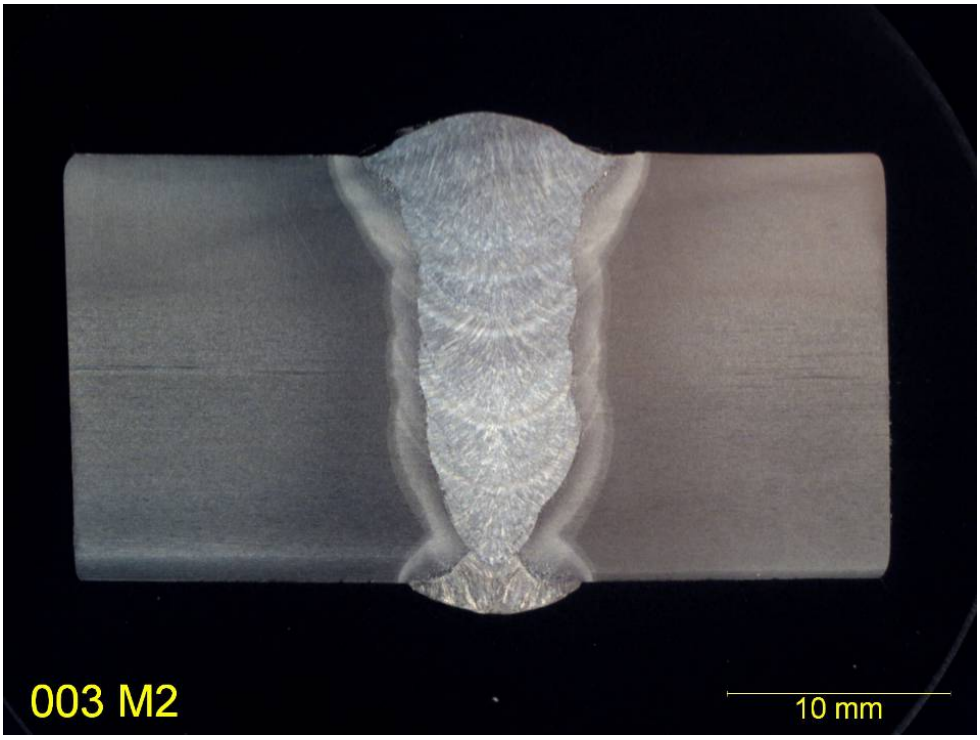

Figure 75. Photo-macrograph Showing Cross-section of Weld A3

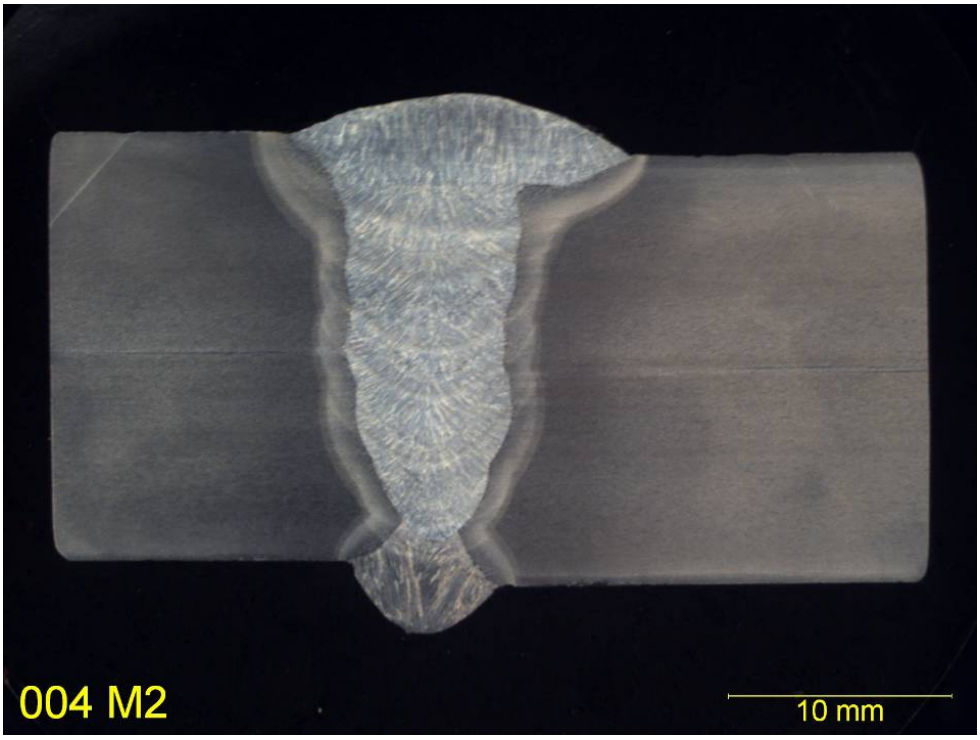

Figure 76. Photo-macrograph Showing Cross-section of Weld A4

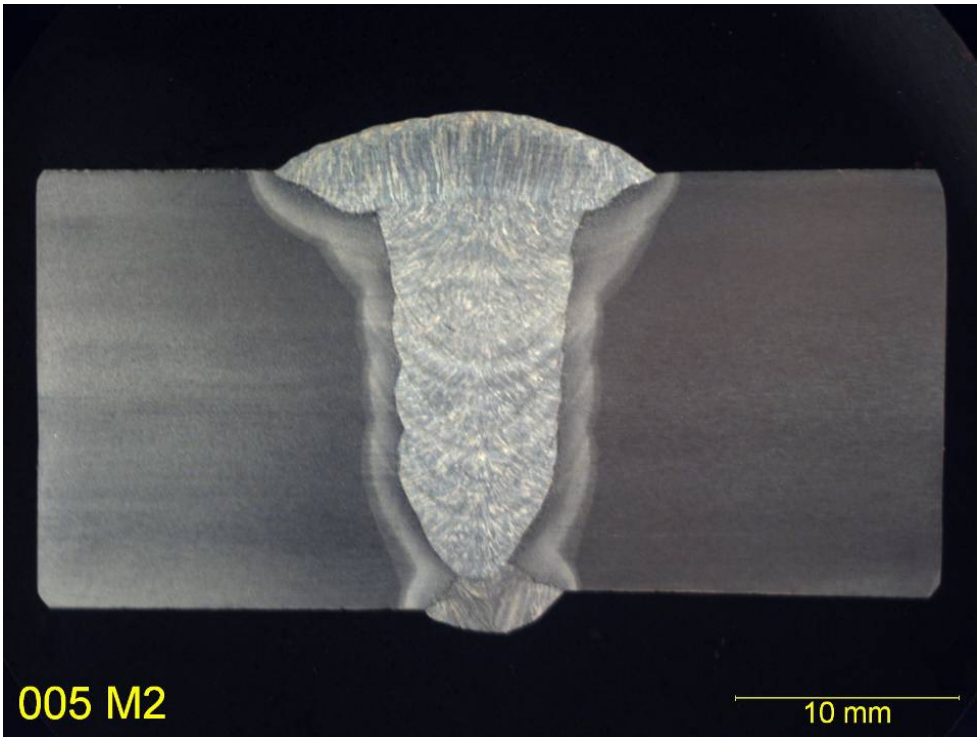

Figure 77. Photo-macrograph Showing Cross-section of Weld B5

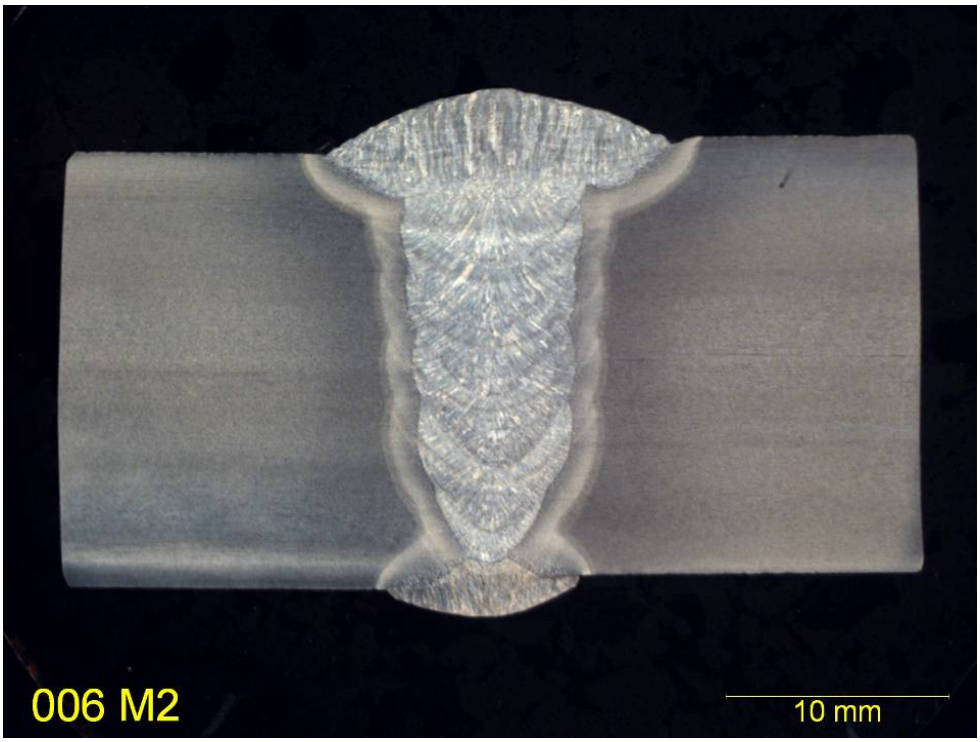

Figure 78. Photo-macrograph Showing Cross-section of Weld B6

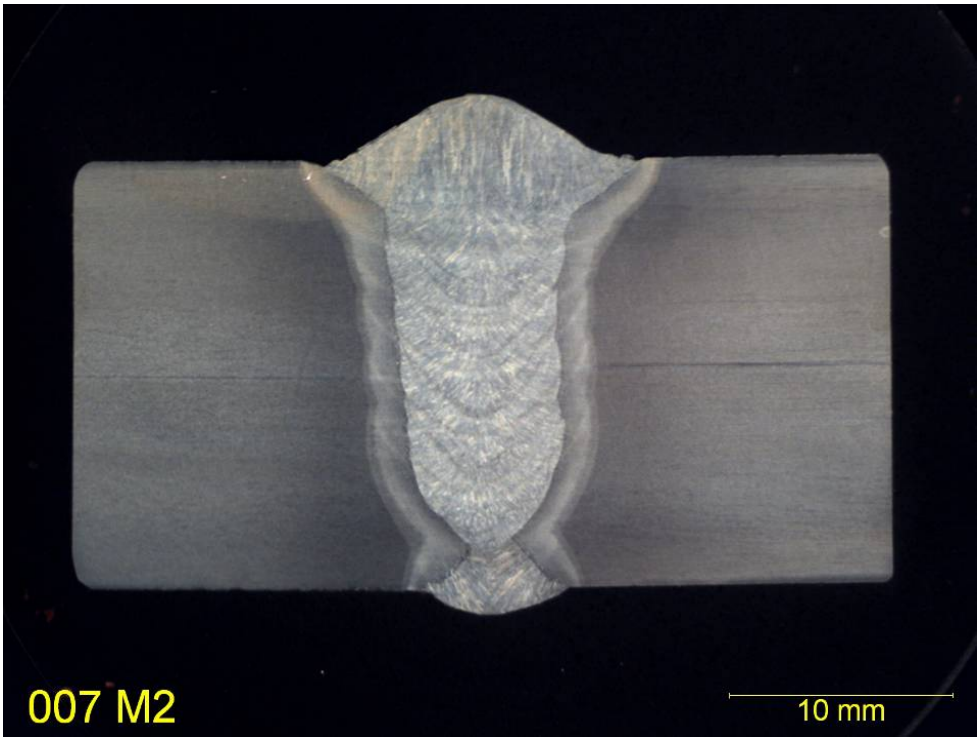

Figure 79. Photo-macrograph Showing Cross-section of Weld B7

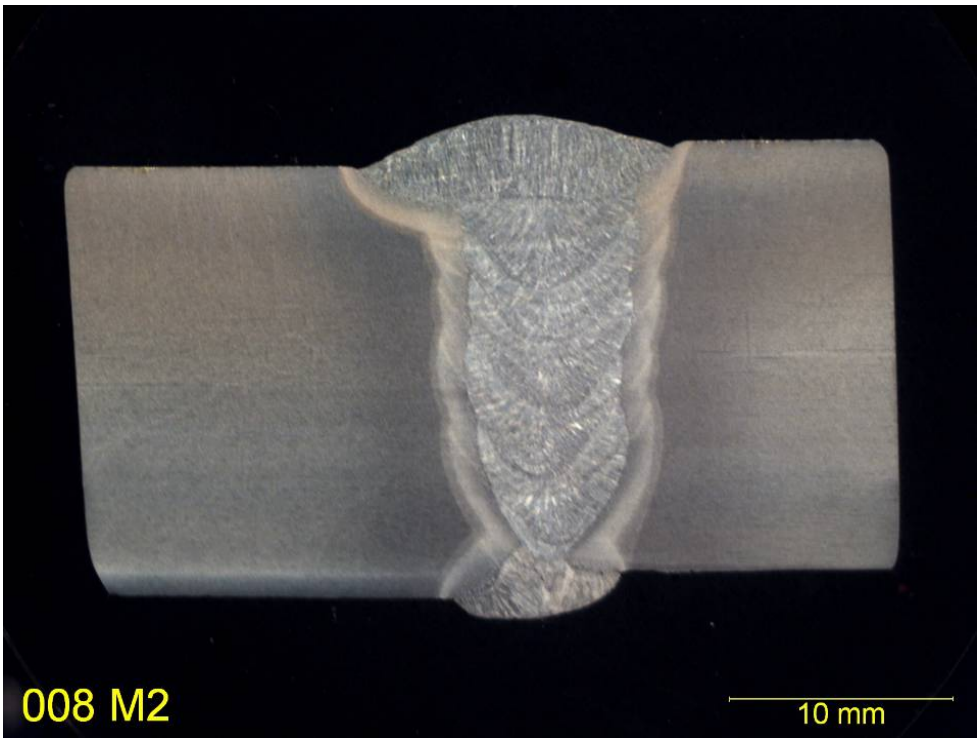

Figure 80. Photo-macrograph Showing Cross-section of Weld B8

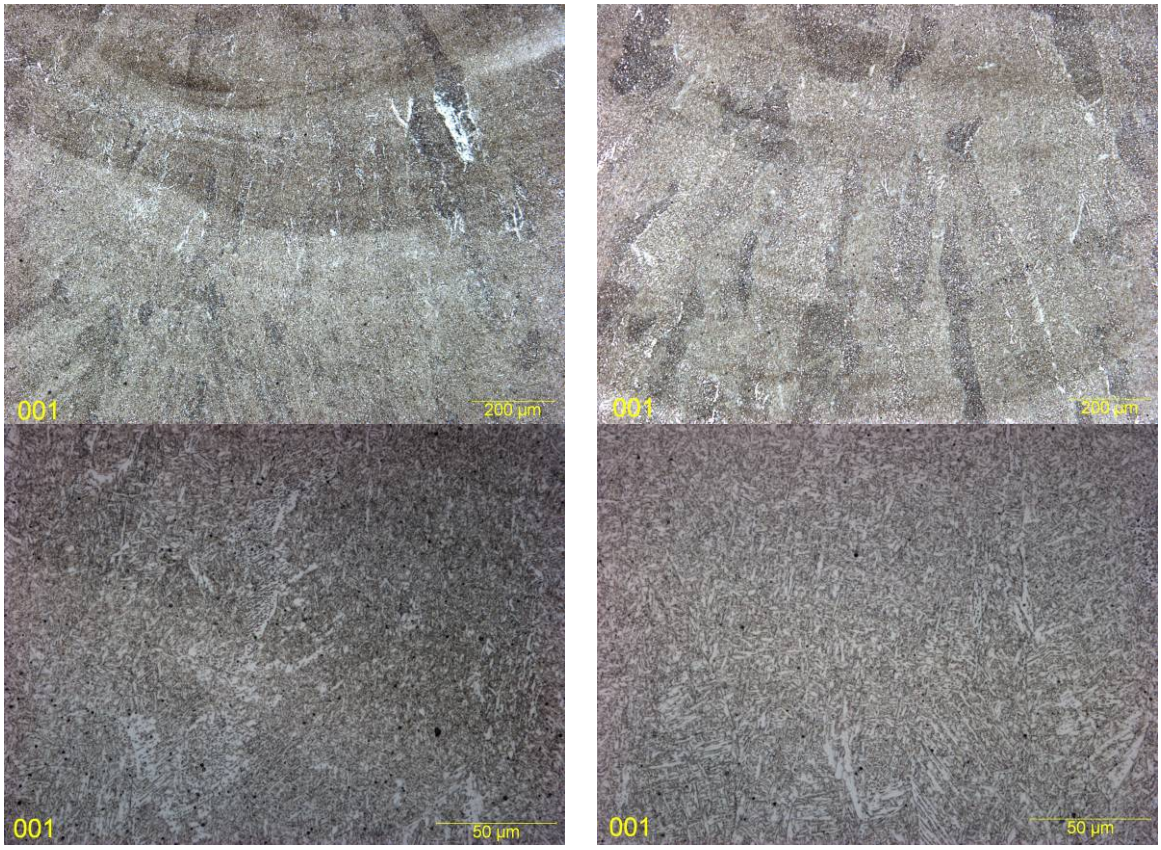

Near I.D. Near O.D.

Figure 81. Photo-micrographs Taken from Weld A1

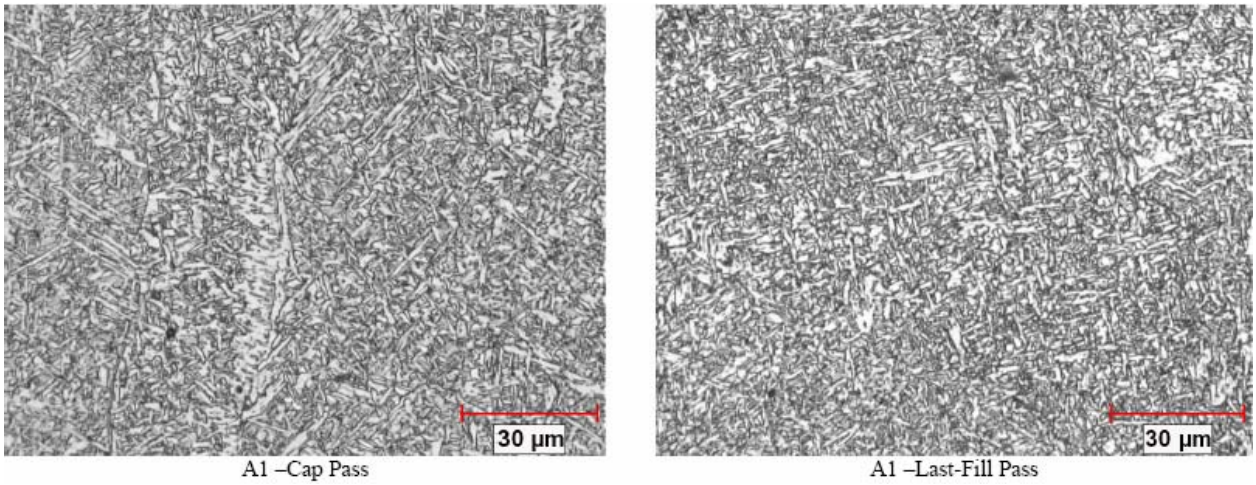

A1 –Cap Pass A1 –Last-Fill Pass

Figure 82. Photo-micrographs of Weld A1 Taken at CANMET-MTL

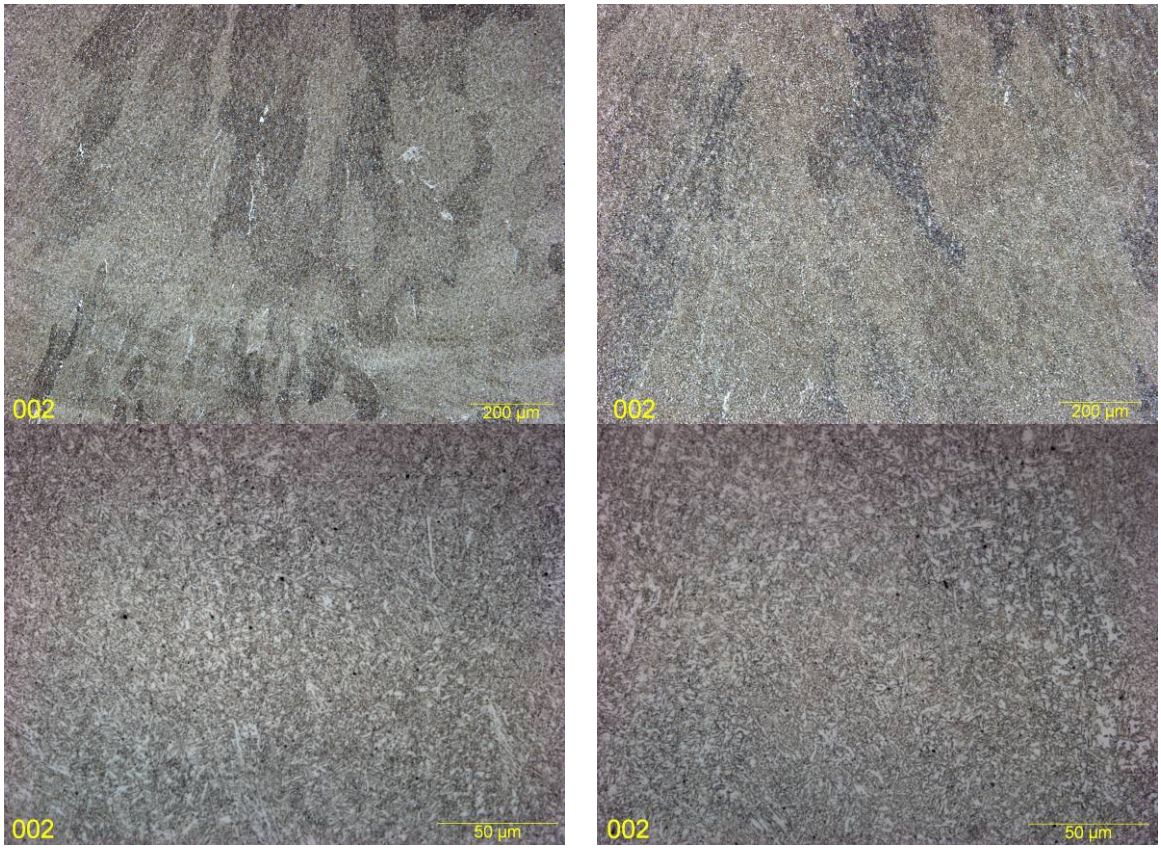

Near I. D. Near O. D.

Figure 83. Photo-micrographs Taken from Weld A2

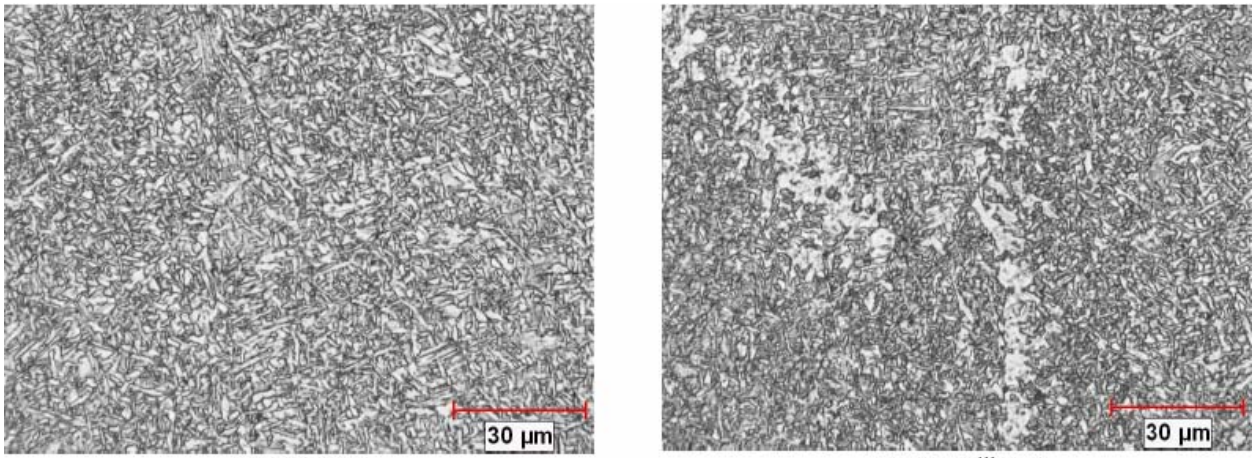

A2 –Cap Pass A2 –Last-Fill Pass

Figure 84. Photo-micrographs of Weld A2 Taken at CANMET-MTL

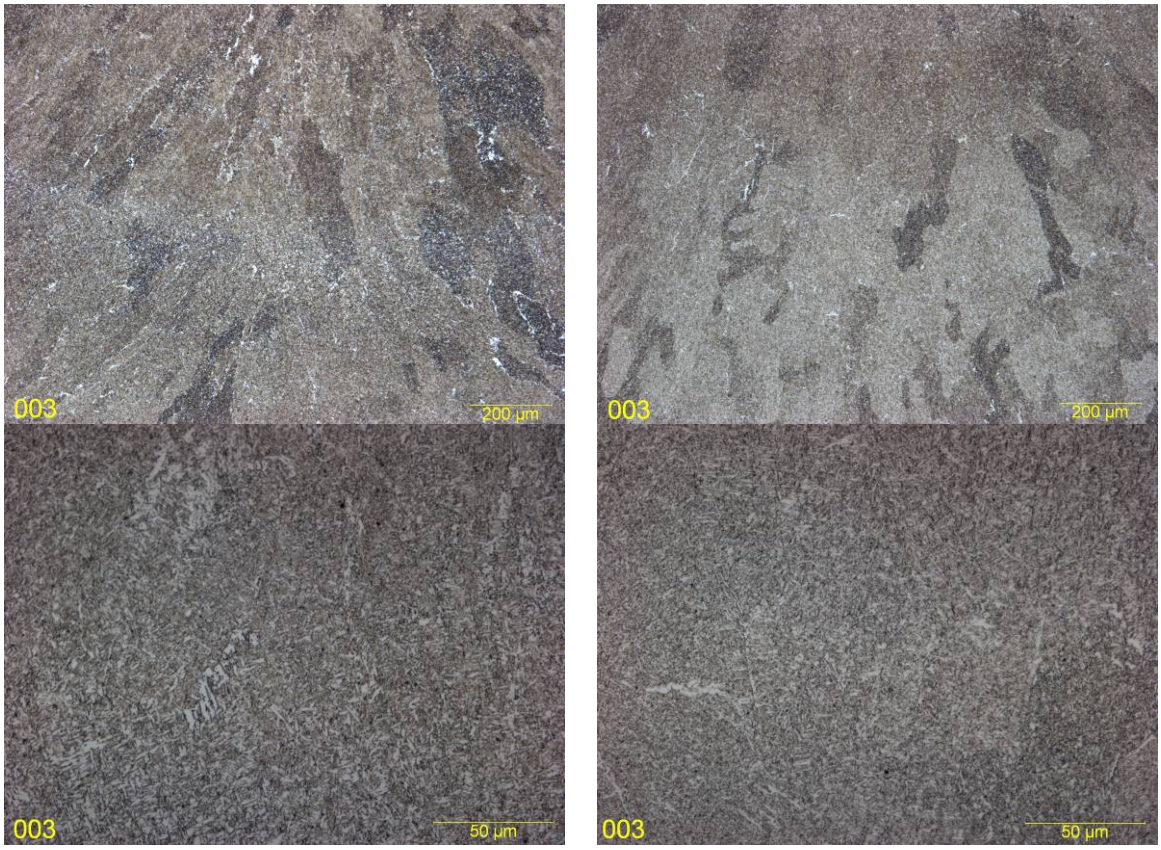

Near I.D. Near O.D.

Figure 85. Photo-micrographs Taken from Weld A3

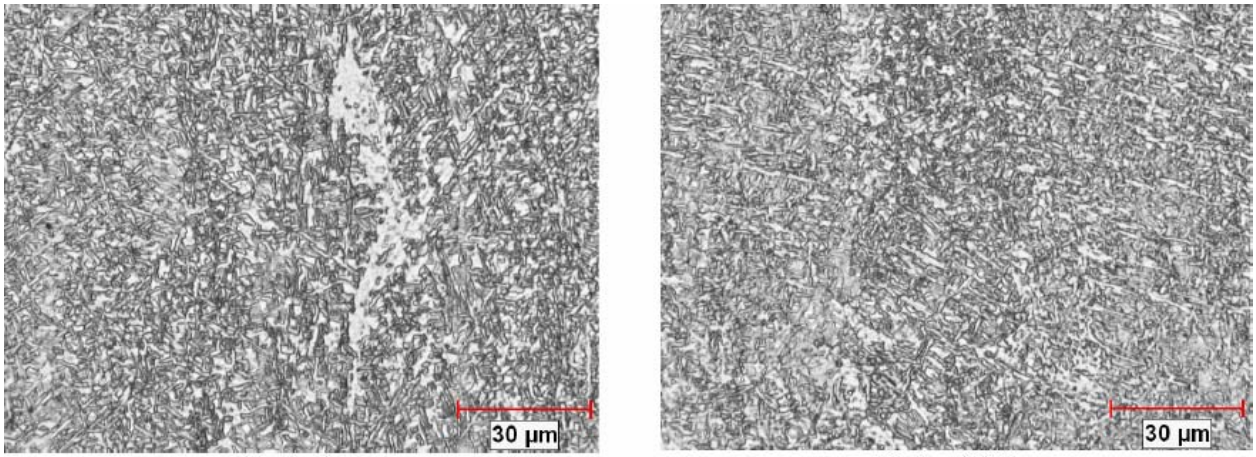

A3 –Cap Pass A3 –Last-Fill Pass

Figure 86. Photo-micrographs of Weld A3 Taken at CANMET-MTL

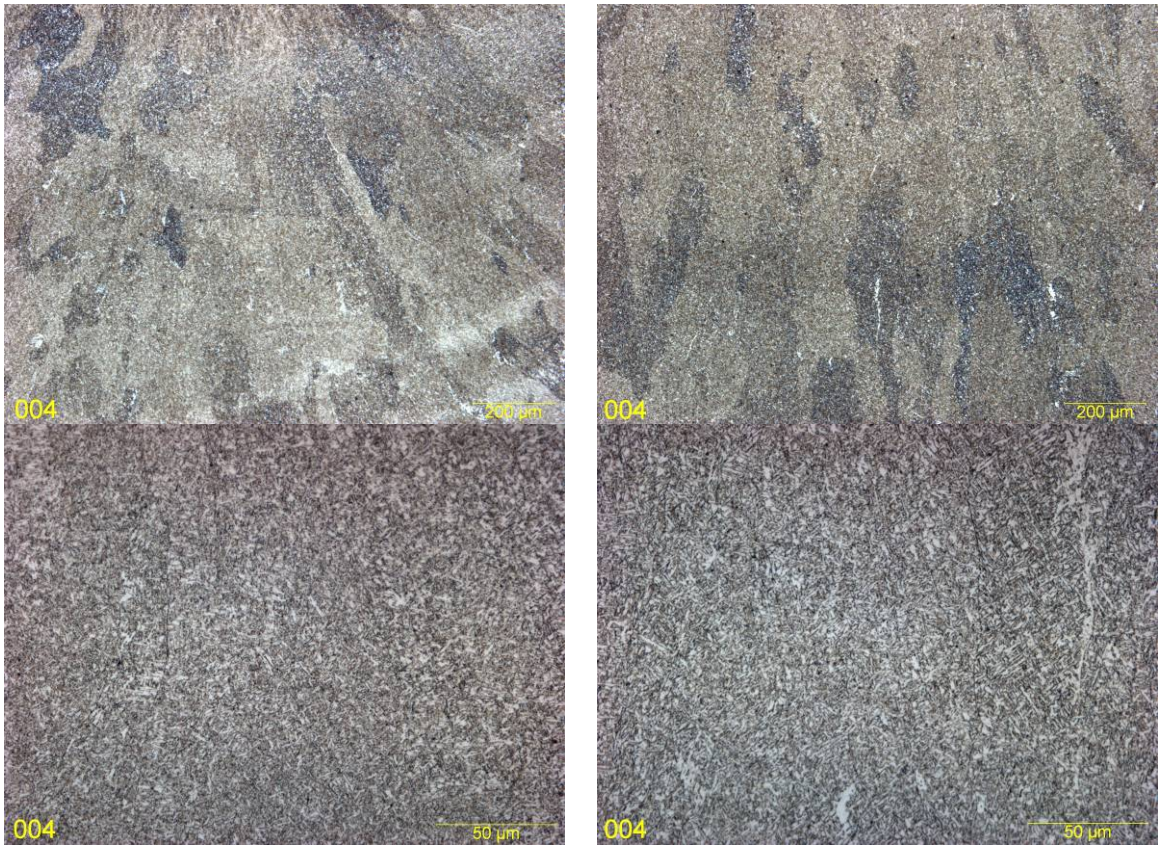

Near I. D. Near O. D.

Figure 87. Photo-micrographs Taken from Weld A4

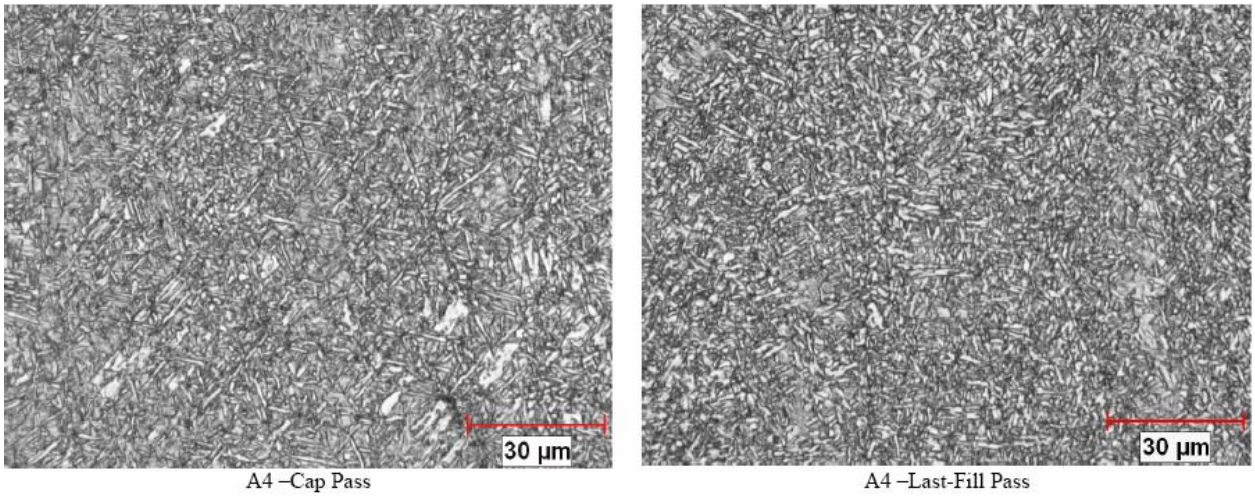

A4 –Cap Pass A4 –Last-Fill Pass

Figure 88. Photo-micrographs of Weld A4 Taken at CANMET-MTL

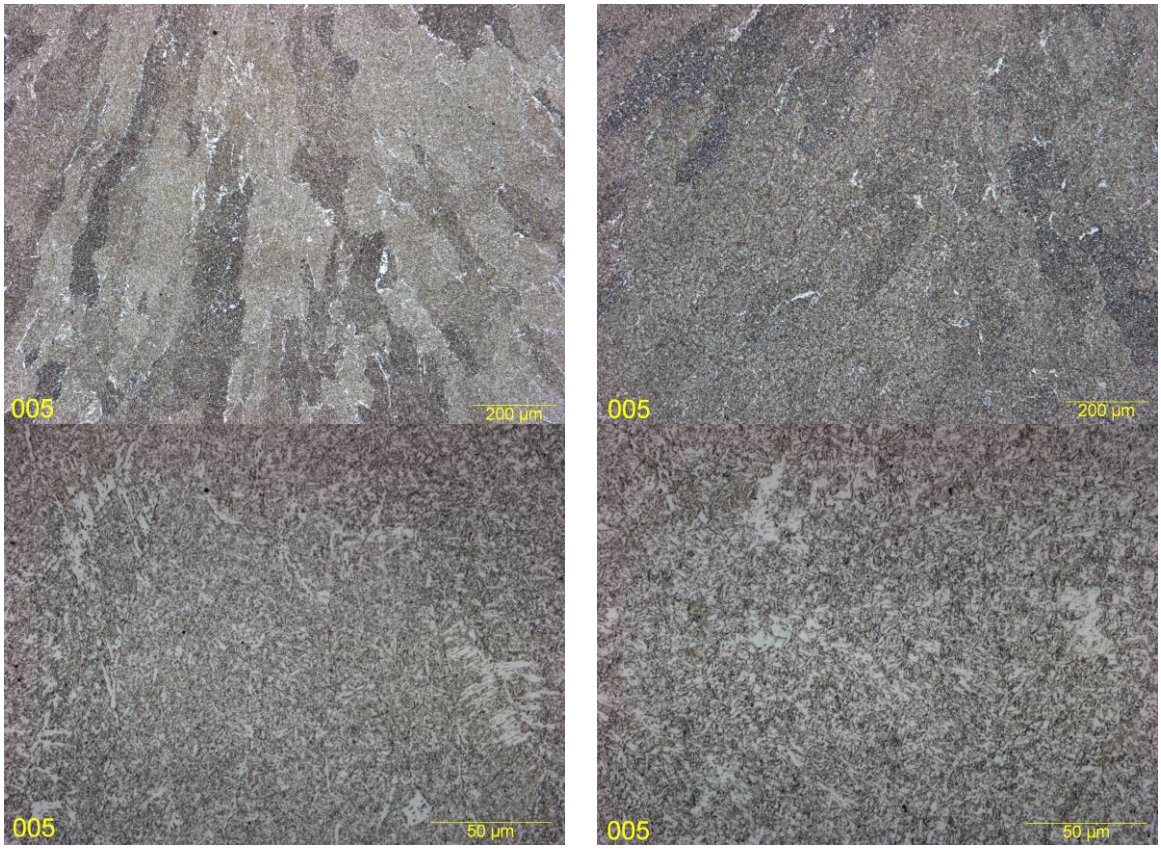

Near I.D. Near O.D.

Figure 89. Photo-micrographs Taken from Weld B5

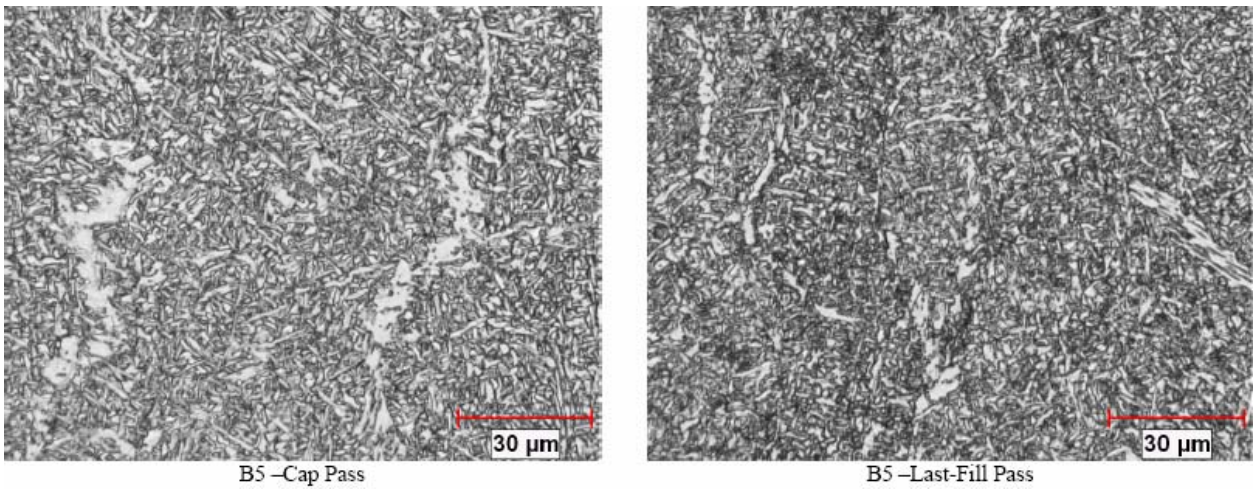

B5 –Cap Pass B5 –Last-Fill Pass

Figure 90. Photo-micrographs of Weld B5 Taken at CANMET-MTL

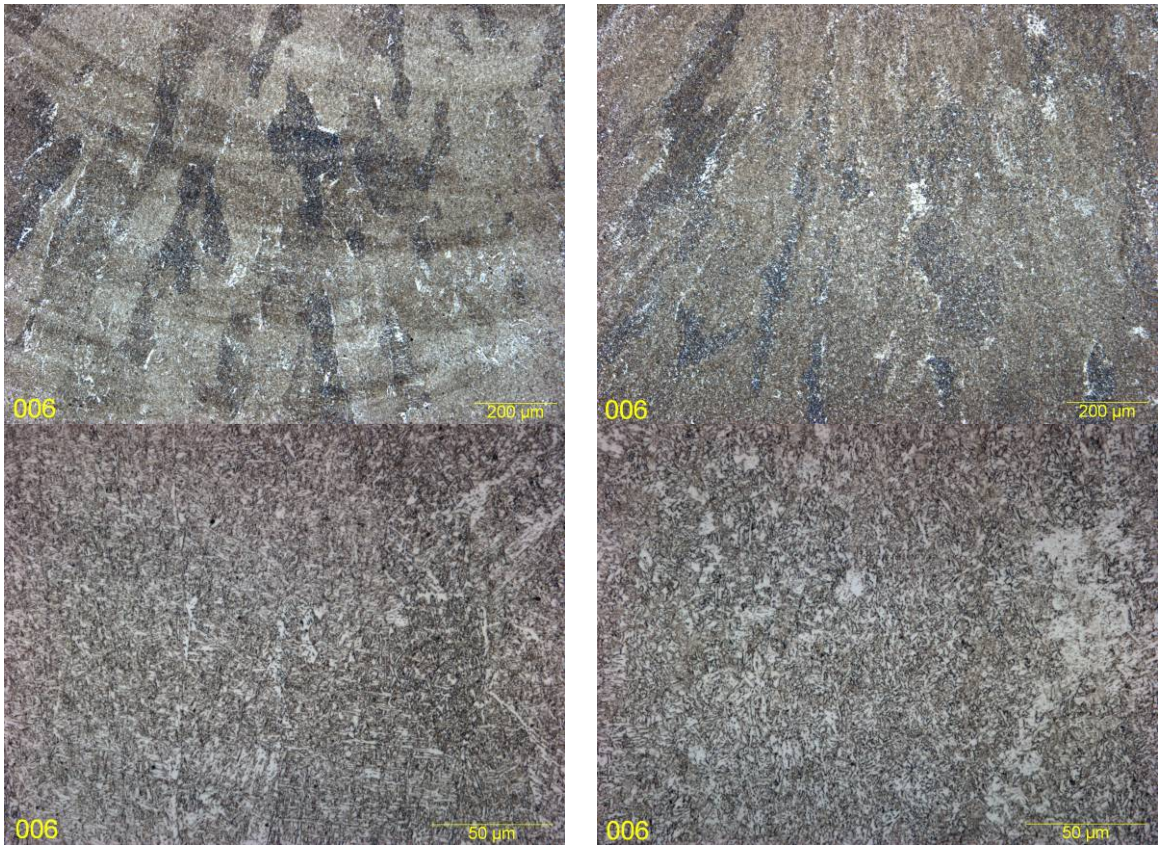

Near I.D. Near O.D.

Figure 91. Photo-micrographs Taken from Weld B6

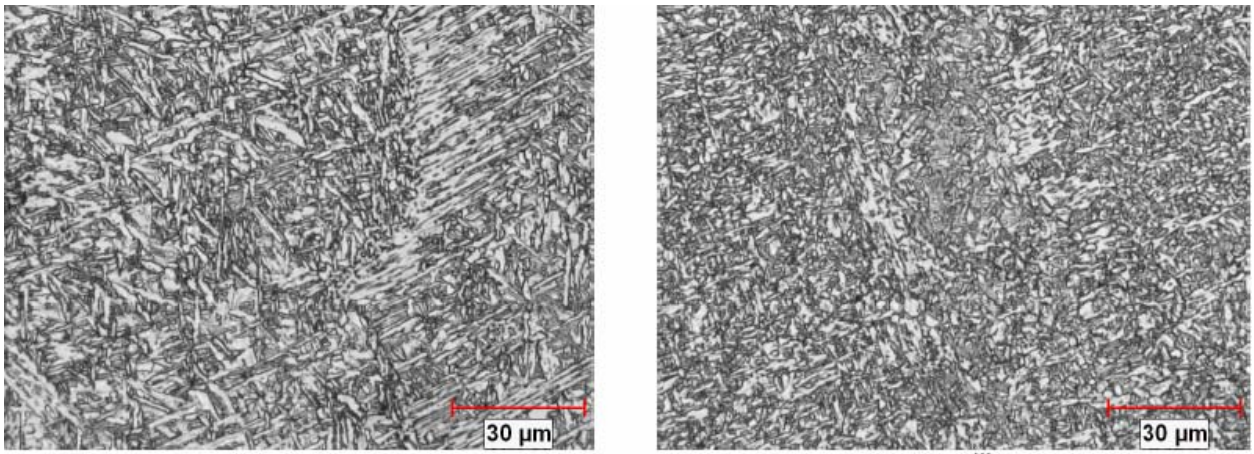

Figure 92. Photo-micrographs of Weld B6 Taken at CANMET-MTL

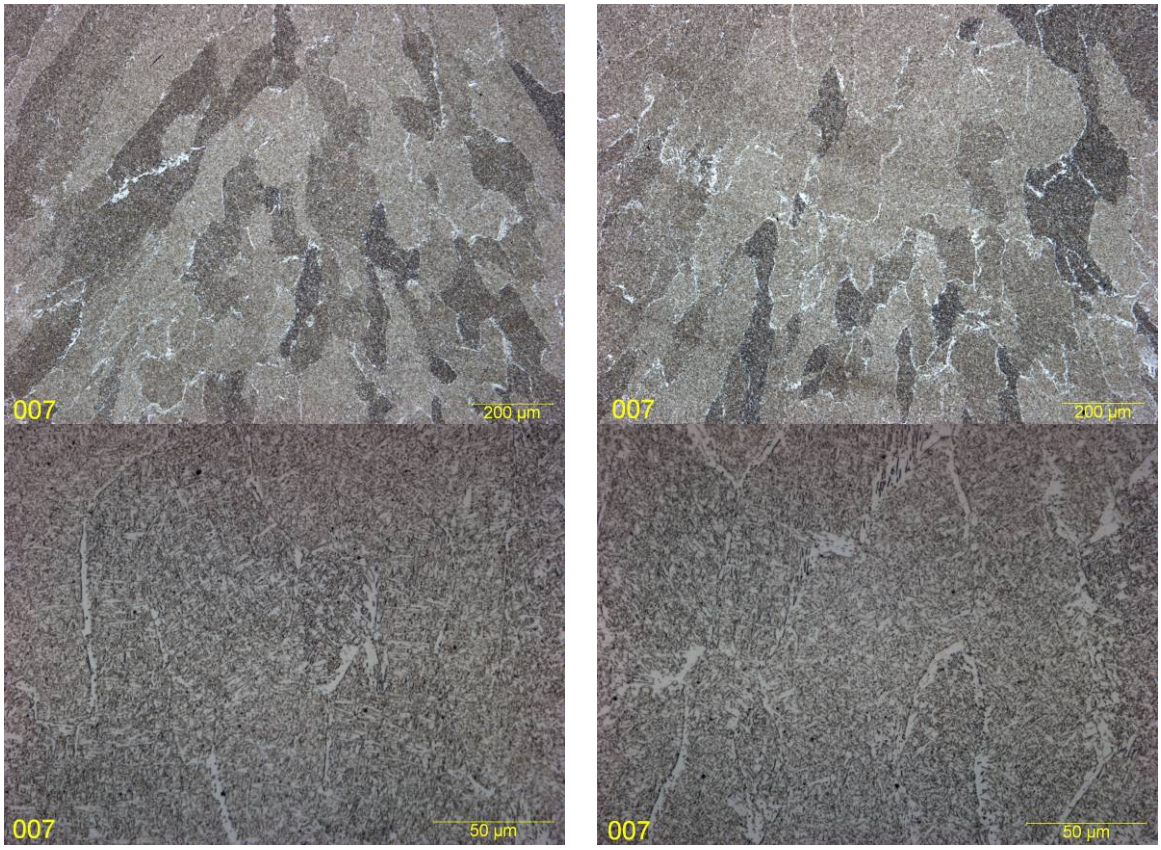

Near I. D. Near O. D.

Figure 93. Photo-micrographs Taken from Weld B7

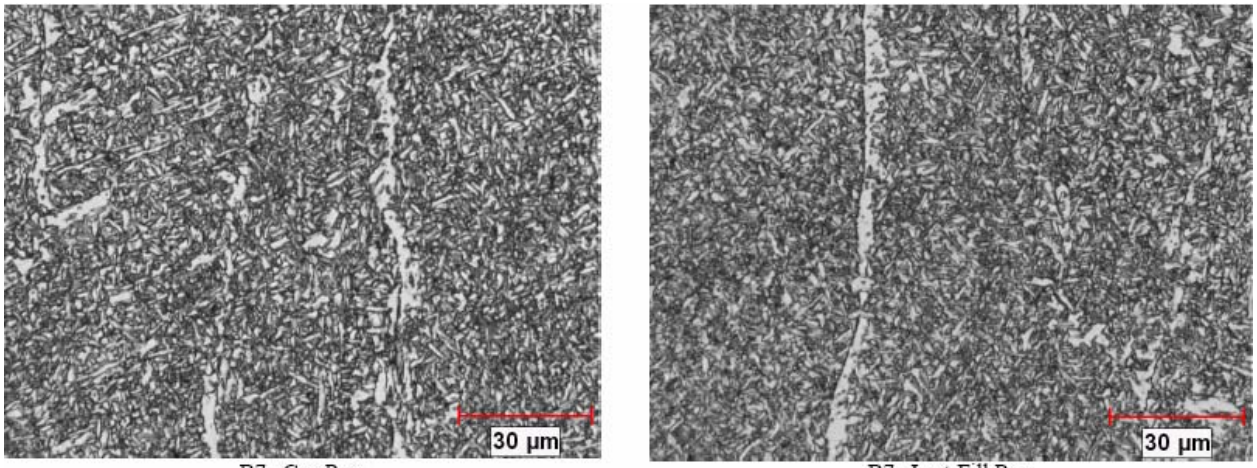

B7 –Cap Pass B7 –Last-Fill Pass

Figure 94. Photo-micrographs of Weld B7 Taken at CANMET-MTL

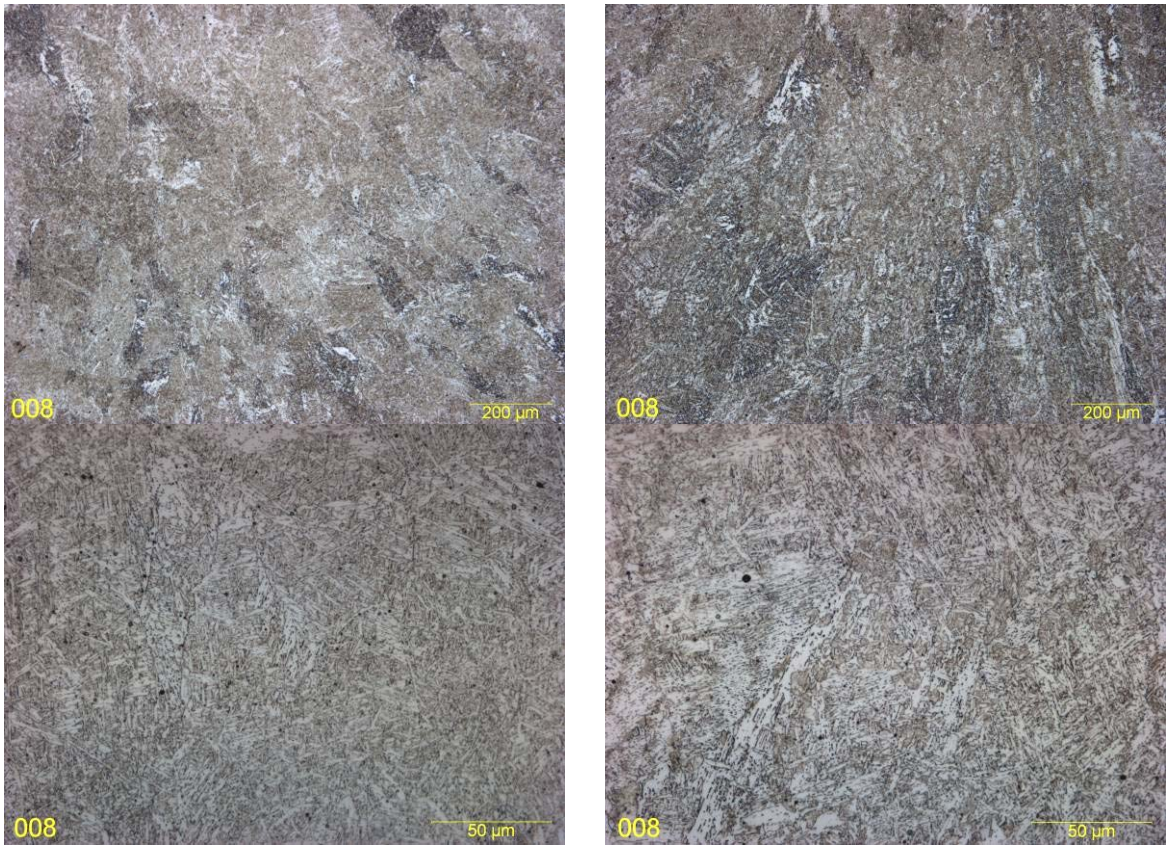

Near I. D. Near O. D.

Figure 95. Photo-micrographs Taken from Weld B8

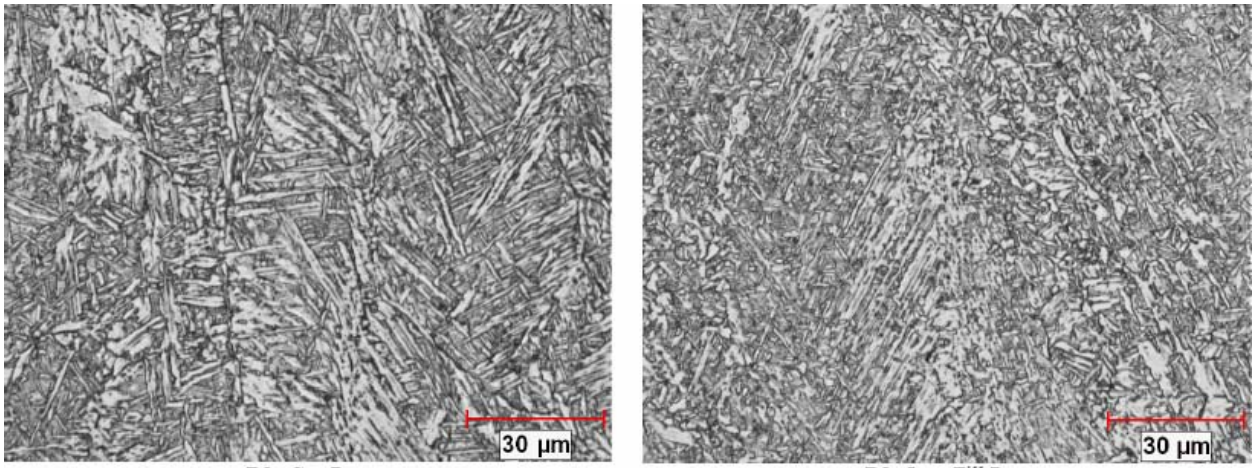

B8 –Cap Pass B8 –Last-Fill Pass

Figure 96. Photo-micrographs of Weld B8 Taken at CANMET-MTL

9.0 Appendices

Appendix A

Title: Task 1 Report: Review of X80 and X100 Pipeline Welding

This report has been provided to the DoT (PHMSA Research and Development) by EWI. It is impractical to reproduce it here due to its size. It can be obtained by the reader from EWI (Contact: Sue Fiore at 614-688-5057 or sfiore@ewi.org) or DoT (Contact: Frank Licari at 202-366-5162 or frank.licari@dot.gov)

Appendix B

Title: Task 2 Report: Development of Best Practice Welding Guidelines for X80 Pipelines

Text = This report has been provided to the DoT (PHMSA Research and Development) by EWI. It is impractical to reproduce it here due to its size. It can be obtained by the reader from EWI (Contact: Sue Fiore at 614-688-5057 or sfiore@ewi.org) or DoT (Contact: Frank Licari at 202-366-5162 or frank.licari@dot.gov)

Appendix C

Title: Welding Procedures for Metal-cored Consumables (CRC-Evans)

This report has the details of the welding procedure development undertaken by CRC-Evans (Houston, TX) using the metal-cored consumables produced under this project by Miller/Hobart. It is impractical to reproduce it here due to its size but will be provided to DoT separately. It can be obtained by the reader from EWI (Contact: Sue Fiore at 614-688-5057 or sfiore@ewi.org) or DoT (Contact: Frank Licari at 202-366-5162 or frank.licari@dot.gov)